Venkata Viswanadh Edara, Transcriptome and functional profiles of R/G-HIV+ human astrocytes: Implications for shock or lock therapies in the brain. Doctor of Philosophy (Biomedical Sciences), December 2019, 88 pp., 6 tables, 16 figures, bibliography, 165 titles.

Abstract

A significant number of people living with human immunodeficiency virus (HIV) suffer from HIV-associated neurocognitive disorders (HAND). Many previous studies investigating HIV in astrocytes as a heterogenous population have established the relevance of astrocytes to HIV-associated neuropathogenesis. However, these studies were unable to differentiate the state of infection, *i.e.* active or restricted, or to evaluate how this affects astrocyte biology. In this study a pseudotyped doubly labelled fluorescent reporter R/G-HIV-1 was used to identify and enrich restricted and active populations of HIV+ astrocytes based on the viral promoter activity. Here we report, the majority of human astrocytes restricted R/G-HIV-1 gene expression early during infection and were resistant to reactivation by vorinostat and interleukin-1β. However, actively infected astrocytes were inducible, leading to increased expression of viral proteins upon reactivation. R/G-HIV-1 infection also significantly decreased cell proliferation and glutamate clearance ability of astrocytes, which may contribute to excitotoxicity. Moreover, transcriptome analyses to compare gene expression patterns of astrocytes harboring active *vs* restricted long terminal repeats revealed that the gene expression patterns were similar, and the active population demonstrated more widespread and robust changes. Our data suggest that harboring the HIV genome profoundly alters astrocyte biology and strategies that keep the virus latent (*e.g.* Block

and Lock), or those that reactivate the latent virus (*e.g.* Shock and Kill) may be detrimental to astrocyte function and possibly augment their deleterious contributions to HAND.

Transcriptome and functional profiles of R/G-HIV+ human astrocytes: Implications for shock or lock therapies in the brain

Venkata Viswanadh Edara, M.S.

APPROVED:

_____

Dr. Kathleen Borgmann, Ph.D., Major Professor

_____

Dr. Rance Berg, Ph.D., Co-Major Professor

_____

Dr. Raghu Krishnamoorthy, Ph.D., Committee Member

_____

Dr. Porunelloor Mathew, Ph.D., Committee Member

_____

Dr. Shaohua Yang, Ph.D., Committee Member

_____

Dr. Rita Patterson, Ph.D., University Member

_____

Dr. Johnny He, Ph.D., Chair, Department of Microbiology, Immunology and Genetics

_____

Dr. Michael Mathis, Ph.D., Dean, Graduate School of Biomedical Sciences

Transcriptome and functional profiles of R/G-HIV+ human astrocytes: Implications for shock or lock therapies in the brain.

DISSERTATION

Presented to the Graduate Council of the

Graduate School of Biomedical Sciences at the

University of North Texas Health Science Center at Fort Worth

in Partial Fulfillment of the Requirements

For the Degree of

DOCTOR OF PHILOSOPHY

BIOMEDICAL SCIENCES

By:

Venkata Viswanadh Edara, M.S.

Fort Worth, TX

December 2019

ACKNOWLEDGEMENTS

Gurur Brahma, Grurvishnu: Gurudevo Maheswara: (Guru/teacher is the guide to your ultimate liberation). Dr. Kathleen Borgmann, Dr. Anuja Ghorpade, and Dr. Rance Berg, I sincerely thank all of you for being my guru/teacher. I take an immense pleasure in thanking all of you for your constant support, mentorship, and guidance throughout my professional and personal life. Each one of you taught me so many things that I will carry forever with me. My sincere gratitude goes to my committee Dr. Raghu Krishnamoorthy, Dr. Yang Shaohua, Dr. Porunelloor Mathew and my university member Dr. Rita Patterson for their encouragement, guidance and constructive criticism.

Through the past few years my lab family has been have been a blessing to me. Lin, Lili, Lisa, Chai, Shruthi, Satomi, Brian, Naomi, Shannon and Jessica, Thanks a lot for tolerating and taking care of me all the time. Thank you all! Special thanks go to Satomi and Lin for always processing the tissues and providing astrocytes.

My dear friends, Busola and Frank! Thanks a lot for making me socially less awkward. You've always been the supporting shoulder. I would cherish our friendship forever.

The Department of Cell Biology, Microbiology and Immunology and the Graduate School of Biomedical Sciences at UNTHSC, thanks for supporting me financially and academically in achieving my degree.

To Dr. Venkateswara Rao Namburu and Mrs. Lakshmi Namburu, thanks for taking care of me and treating me like your own child. Thanks for always being there for me. I will be forever in debt to you.

Finally, to my parents amma (mom) and nanna (dad) I cannot thank you enough for all the sacrifice you made to provide a perfect life for me. You always wanted the best for me. You are the reason for what and where I am today. With my due respect, I dedicate this work to both of you.

LIST OF PUBLICATIONS

Venkata Viswanadh Edara, Anuja Ghorpade, and Kathleen Borgmann. Insights into the gene expression profiles of active and restricted R/G-HIV+ human astrocytes: Implications for shock or lock therapies in the brain. *Journal of Virology*. 2020. In press. doi: 10.1128/JVI.01563-19.

Yang You, Kathleen Borgmann, **Venkata Viswanadh Edara**, Satomi Stacy, Anuja Ghorpade, Tsuneya Ikezu. Activated human astrocyte-derived extracellular vesicles modulate neuronal uptake, differentiation and firing. *Journal of Extracellular Vesicles*. 2020. 9(1):1706801. doi: 10.1080/20013078.2019.1706801

TABLE OF CONTENTS

ABBREVIATIONS

AAN	American academy of neurology
Aβ	Amyloid beta
AD	Alzheimer's Disease
AEG	Astrocyte elevated gene
AIDS	Acquired immune deficiency syndrome
ANI	Asymptomatic neurocognitive impairment
AP	Activator protein
ART	Antiretroviral therapy
BBB	Blood brain barrier
BIO	2′,3′-6-bromoindirubin-3′-oxime
BrdU	5-bromo-2-deoxyuridine
cAMP	Cyclic adenosine monophosphate
CCR	C-C chemokine receptor
CNS	Central nervous system
CSF	Cerebrospinal fluid
DAPI	4', 6-diamidino-2-phenylindole
EAAT2	Excitatory amino acid transporter 2
FACS	Fluorescence activated cell sorting
GAPDH	Glyceraldehyde phosphate dehydrogenase

GFAP	Glial fibrillary acidic protein
GFP	green fluorescence protein
GSK3	Glycogen synthase kinase-3
gp	Glycoprotein
HAD	HIV-associated dementia
HAND	HIV-associated neurocognitive disorders
HDACi	Histone deacetylase inhibitor
HIV	Human immunodeficiency virus
HIVE	HIV encephalitis
IFN	Interferon
IL	Interleukin
iNOS	Inducible -nitric oxide synthase
IP	IFN-γ induced protein
IPA	Ingenuity Pathway Analysis
JAK	Janus kinase
LEF	Lymphoid enhancer factor
LRA	Latency reactivating agent
LTR	Long terminal repeat
MAP	Molecular activity prediction
MAPK	Mitogen activated protein family of kinases
MMP	Matrix metalloproteinases
MND	Minor neurocognitive disorder
MS	Multiple sclerosis

MTT	3-(4,5-dimethylthiazol-2-yl)-2,5-diphenyltetrazolium bromide
Nef	Negative regulatory factor
NO	Nitric oxide
NF-κB	Nuclear factor kappa-light-chain-enhancer of activated B cells
Nrf2	Nuclear factor erythroid 2–related factor 2
PBMCs	Peripheral blood mononuclear cells
PD	Parkinson Disease
PG	Prostaglandins
PLWH	People living with HIV-1
PK	Protein kinase
R/G-HIV-1	Red/Green-Human Immunodeficiency Virus-1
RTA	Reverse transcriptase activity
STAT	Signal transducer and activator of transcription
Tat	HIV-1 transactivator of transcription
TNF	Tumor necrosis factor
TCF	T-cell factor
VSVG	Vesicular stomatitis virus glycoprotein
Vpr	HIV-1 viral protein R
Wnt	Wingless type ligand

LIST OF TABLES

LIST OF FIGURES

CHAPTER 1

INTRODUCTION

1.1 Societal burden of HIV:

Human immunodeficiency virus (HIV) attacks the immune system by gradually infecting and depleting the body's immune cells. This leads to a state of immune deficiency making people living with HIV (PLWH) susceptible to opportunistic infections, resulting in acquired immunodeficiency syndrome (AIDS). The two major types of HIV, HIV-1 and HIV-2 both can lead to AIDS. However, they are different from each other. Both HIV-1 and HIV-2 were further divided into groups and subtypes or strains. HIV-1 is the most common type and is responsible for the HIV epidemic. Whereas, HIV-2 occurs in a much smaller population of approximately 0.01% of all HIV cases and those are primarily people from west Africa (1). Despite significant declines in HIV/AIDS-related mortality, an estimated 770,000 people died from HIV-related illnesses in 2018, and approximately 1.7 million new cases of HIV were also diagnosed. Since the beginning of the HIV epidemic, 78 million people have become infected with HIV, and nearly half, *e.g.* 37.9 million, are living with HIV world-wide. Of which, an estimated 1.7 million are children under the age of 15. The vast majority PLWH are in sub-Saharan Africa, where new HIV infections decreased by 35% between 2000 and 2015 and AIDS-related deaths decreased by 24%. Simultaneously, access to antiretroviral therapy (ART) increased significantly. At the end of 2017, there were approximately 1.2 million PLWH in the United States (US), and 1 in 7 were unaware of their status. Most of the PLWH in the US were clustered in the south. There were 15,807 deaths among PLWH in the year of 2016 (2, 3). The federal government dedicated $ 34.8 billion to HIV/AIDS for the 2019 fiscal year. Of this, 7 % was spent on research.

1.2 HIV-1 infection and reservoirs:

HIV-1 transmission usually occurs through the exposure of mucosal surface to the virus. In the mucosal tissue, the virus comes in to contact with either CD4 T cells, Langerhans cells or

submucosal dendritic cells. From there, HIV-1 disseminates into the draining lymph nodes. Then the infection rapidly expands to gut-associated lymphoid tissue, and finally systemic dissemination of the virus occurs (4). When HIV-1 infects a particular cell, it leads to either active replication of the virus (productive infection) or remains dormant after integrating and becomes part of the cellular genome (latent infection). The term latent infection or latency is usually defined as a non-productive state of infection of a pool of cells that are transcriptionally silent but retain the capacity to produce viral particles upon reactivation (5). HIV-1 infection can be controlled by optimal ART regimen, but it is not possible to achieve sterile cure. This is due to integration of HIV into the host genome and persist as latent infection in different anatomical sites of human body. CD4 T cells are the major targets for HIV-1 infection. Other immune cells of myeloid origin are also implicated as reservoirs and targets of infection. Activated T cells are the preferential targets for productive HIV-1 infection. However, their lifespan is short due to viral cytopathy (6). During their life cycle, some effector T cells will become long lived memory T cells. Infected effector CD4 T cells that transform into memory T cells become viral reservoirs. Out of various types of CD4 memory T cells, central memory T cells are the best characterized reservoirs for latent HIV-1 (7).

Once the viral particles and infected cells become systemic, the infection spreads across the multiple anatomical sites of the body. HIV-1 infected cells can be found in the brain, lungs, kidneys, liver, adipose tissue, gastrointestinal tract, male and female genitourinary systems and bone marrow. During active infection, lymphoid tissues are the most important sites for viral replication. However, the contribution of all these anatomical sites as latent reservoirs is still debatable (8, 9).

The definition of latency varies as it includes cells that harbor both replication competent and replication incompetent viral genome. The latter are also considered as reservoirs because they

can become replication competent by either mutations or recombinant events. Moreover, they can harbor open reading frames for viral proteins that could have toxic effects (10).

Lymphoid reservoirs of HIV-1 are well characterized, whereas brain reservoirs are difficult to study. The only available samples to understand the disease while the patients are alive is cerebrospinal fluid (CSF). Presence of divergent strains in CSF in high number compared to the blood indicate that there is compartmentalization of brain reservoirs (11). Presence of viral proteins such as Tat and p24 along with viral RNA in the CSF also proves CNS as a potential viral reservoir.

1.3 CNS HIV-1 infection:

HIV-1 enters the central nervous system (CNS) early during infection *via* infected monocytes, a phenomenon known as the trojan horse hypothesis. Another mechanism of entry is, the inflammatory cytokines, such as tumor necrosis factor-α (TNF-α) from the periphery, disrupt the blood brain barrier (BBB) facilitating entry of cell free HIV-1 into the CNS where it infects resident microglia and macrophages. Not only pro-inflammatory cytokines from periphery have an effect on the BBB, overexpression of the envelope glycoprotein 120 (gp120) in a form that circulates in plasma also altered BBB integrity in mice (12). This suggests that cell free virus or viral envelope proteins may disrupt BBB during viremic phase of the infection. HIV-1 CNS infection is persistent, and the brain serves as a sanctuary for the ongoing infection since the majority of antiretroviral drugs have low CNS penetration index. Neurons are not susceptible to HIV-1 infection. The susceptible major neural cell types are macrophages, microglia and astrocytes (13, 14). HIV-1 resides and replicates in both macrophages and microglia that are productively infected. HIV-1 infection of astrocytes is controversial and will be discussed in detail below. However, up to 19% of astrocytes isolated from autopsy brain tissue tested positive for

integrated HIV-1 viral genomes (15). These cell types are long lived with turn-over rates from months to years. The low penetration index of ART into the CNS and longer life spans of these cell types support long term expression of viral particles, and these infected cells also serve as HIV-1 reservoirs. Multiple studies have also shown the presence of viral RNA and viral proteins in the CSF suggesting that CNS acts as a reservoir for HIV-1 (16). We know that HIV-1 invades brain soon after infection. HIV-1 infection was shown in astrocytes, perivascular macrophages and microglia. Therefore, a clear sterilization cure for HIV-1 is not possible without addressing both productive and latent infection in the CNS. Presence of different set of target cells and unique immunological selection pressures in the brain allow HIV-1 to evolve and persist in the CNS (15).

1.4 HAND:

The introduction of antiretroviral therapy ART in the mid 1990s significantly increased the lifespan of PLWH. However, these people suffer from various comorbidities such as hypertension, diabetes, and hyperlipidemia. Another major manifestation of prolonged HIV-1 infection is HIV-associated neurocognitive disorders (HAND) (17, 18). HAND were commonly observed in infected individuals since the beginning of the HIV/AIDS epidemic. Changes in the brain structure were observed within 100 days of infection even before seroconversion (19). HAND refers to a group of neurocognitive dysfunctions associated with HIV-1 infection. Approximately 30-70% of PLWH suffer from HAND (20, 21). These conditions range from asymptomatic neurological impairment to disabling dementia. In 1991 the American Academy of Neurology (AAN) defined two levels of neurological manifestations of HIV-1 infection, a severe form called HIV-associated dementia (HAD) and minor cognitive motor disorder. After the introduction of the combined ART therapy in 1996 the incidence of the most common and severe form, HAD, declined from

approximately 16% to less than 5%. However, the incidence of milder forms of the disease increased to 30-70% with the increased life expectancy of PLWH (22). With the changes in the incidence of various forms of the neurocognitive complications, the AAN refined the diagnosis criteria for HAND in 2007. The newer criteria were revised into three categories named as asymptomatic neurocognitive impairment (ANI), mild neurocognitive disorder (MND) and HAD. Clinically these three are collectively referred to as HAND. The criteria used to distinguish these three variants of HAND are presented in Table 1.1. Today, the milder forms of HAND, MND and ANI, together account for 60-70% of all HAND (23). Also, those with an ANI diagnosis were two to six times more likely to develop a more severe form of HAND, such as mild neurocognitive disorder (MND) or HAD (24).

Table 1. 1 Classification of HAND

HAND type*	Diagnostic criteria	Functional status	Prevalence
Asymptomatic neurocognitive impairment (ANI)	Impairment in ≥ 2 neurocognitive domains (≥1 SD)[#]	Does not interfere with daily functioning	30 %
Mild neurocognitive disorder (MND)	Impairment in ≥ 2 neurocognitive domains (≥ 1 SD) [#]	Mild to moderate interference in daily functioning	20-30 %
HIV-associated dementia (HAD)	Marked (≥ 2 SD) impairment in ≥ 2 neurocognitive domains[#]	Marked interference in daily functioning	2-8 %
* Cannot be explained by other comorbidities, [#] Minimum of five domains measured, standard deviation (SD)			
Neurocognitive domains: attention-information processing, language, abstraction-executive, complex perceptual motor skills, memory including learning and recall, and simple motor skills or sensory perceptual abilities. Adapted from (25)			

HIV-associated neuropathogenesis is a consolidated response of multiple types of cells as depicted in **figure 1.1**. It is a combination of intracellular and intercellular interactions, and

alterations of normal cell function. Upon infection, macrophages and microglia release various neurotoxic viral proteins such as gp120, transactivator of transcription (Tat), negative regulatory factor (Nef) and viral protein R (Vpr). Along with viral proteins, they also secrete various proinflammatory cytokines such as interleukin (IL)-1β, TNF-α, and matrix metalloproteinases. These neurotoxic viral proteins and inflammatory mediators act on various types of cell in the CNS, resulting in further upregulation of cytokines, chemokines and endothelial adhesion molecules that facilitate chemotaxis and attachment of immune cells of peripheral origin such as CD4 T cells, CD8+ T cells and monocytes into the CNS. At the same time, uninfected macrophages and microglia are responsive to viral proteins such as gp120 and cytokines secreted by infected glia and astrocytes (14, 26, 27). Neurotoxic proteins expressed by activated microglia include excitatory amino acids and related substances such as quinolinate, cysteine and other amine compounds. These excitatory amino acids can directly lead to apoptosis of neurons (28, 29). Other candidate neurotoxins secreted by macrophages and microglia include nitric oxide, platelet activating factor, arachidonic acid metabolites (prostaglandins), IL-1β, TNF-α, interferon (IFN) alpha and beta and IL-6 (30).

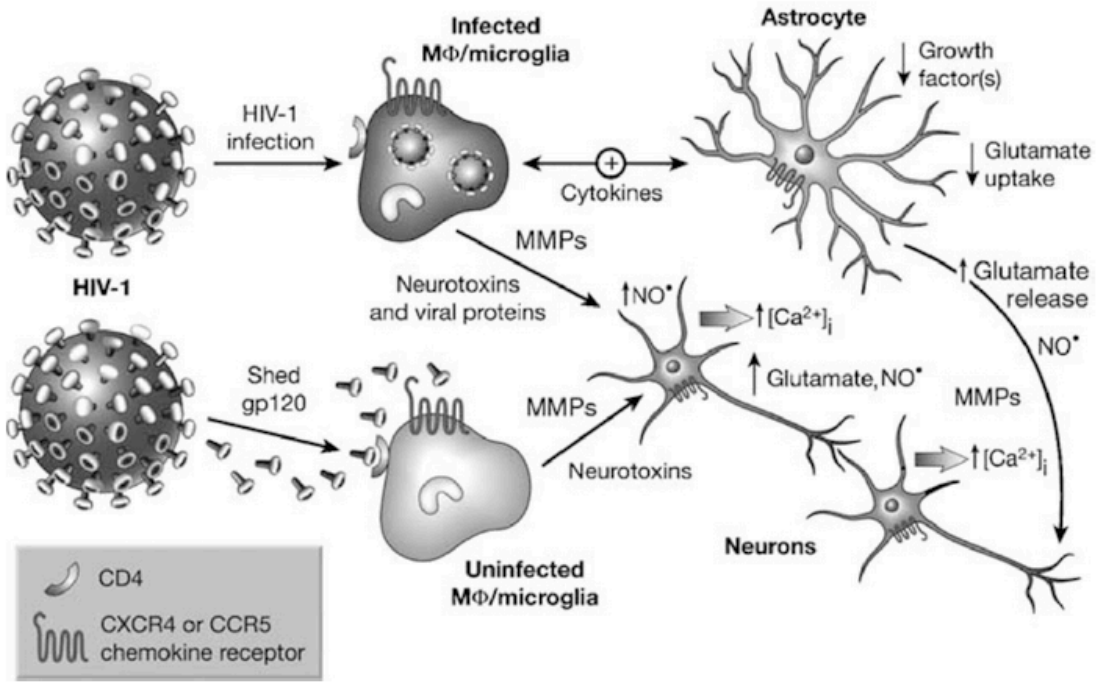

Figure 1.1 Current model for HIV-1-mediated neuropathogenesis in the CNS (adapted from Kaul *et al*., cell death and differentiation, 2005) (31).

HIV-infected macrophages and microglial cells secrete neurotoxic viral proteins gp120, Tat, Nef and Vpr, and cytokines that trigger astrocyte activation. This results in further dysregulation of astrocyte functions. Astrocytes are restrictively infected and are capable of secreting viral proteins. Elevated extracellular glutamate levels and reactive oxygen species cause aberrant synaptodendritic pruning, excitotoxicity and oxidative damage in the neurons. Proinflammatory cytokines expressed by astrocytes and vascular endothelial cells further activate microglia and macrophages leading to increased production of chemokines and cytokines that contribute to neuronal injury.

1.5 Astrocytes in HAND pathogenesis:

1.5.1 Morphology and functions of astrocytes:

Astrocytes are the most numerous and diverse glial cells in the CNS. Astrocytes in the brain are as heterogenous as neurons. Different types of astrocytes are found in different regions of the brain that exert different physiological properties. Based on their location and morphology astrocytes are mainly classified into two categories. Protoplasmic astrocytes are present in the grey matter. These cells have several branching processes that form tripartite synapses and end feet that cover the tight junctions of blood vessels. The other type, fibrous astrocytes, are found in the white matter. Fibrous astrocytes have elongated unbranched cylindrical processes that align with myelinated fibers (32, 33). Astrocytes are one of the most abundant cell types in the CNS. In some regions of the brain, the number of astrocytes outweighs the number of neurons and *vice versa*. Astroglia perform a wide variety of functions in the CNS, including providing structural support, maintenance of ion-balance and BBB integrity, synaptic regulation, immune modulation, energy source to neurons, uptake and recycling of neurotransmitters, enhancement of myelination by oligodendrocytes and many more. Even though astrocytes do not conduct action potential across their processes, they exhibit changes in intracellular calcium, representing a form of astrocyte excitability (34).

Astrocyte are a key part of the neurovascular unit. Astrocyte foot processes make extensive contact with blood vessels that aid in formation of BBB, thereby regulating the movement of ions, molecules, and cells between the neural cells and the blood. Additionally astrocytes communicate between each other through gap junctions and it has been suggested that the astrocytic mechanisms that regulate the vasoconstriction and vasodilation are transmitted through these inter-astroglial gap junctions (35). Their endfeet also play a major role in the movement of CSF from periarterial space into the brain parenchyma. This process is facilitated by the water channels aquaporin-4 (AQP4) that are abundantly expressed on the astrocytic endfeet that ensheathe the brain

vasculature. This influx of CSF into the brain parenchyma causes the flux of interstitial fluid towards the perivenous space from where it drains out of the brain through the cervical lymphatic system. This rapid fluid flux with interchange of CSF and interstitial fluid is termed as glymphatic system based on its similarity to the peripheral lymphatic system, and on the important role of the of the glial AQP4 channels in the fluid transport (36).

Astrocytes are also known to secrete different mediators such as prostaglandins, nitric oxide and arachidonic acid that regulate local blood flow in the CNS (37). Another key function of astrocytes is to uptake excessive glutamate from neuronal synapses and to prevent excitotoxicity. Upon uptake astrocytes convert glutamate to glutamine and provide precursors to neurons for neurotransmitter synthesis (38). Astrocytes act as immune modulators in CNS. They respond to various pathogens as well as inflammatory cytokines by upregulating expression of various cytokines and chemokines, while simultaneously altering their morphology and physiological functions. This process is called reactive astrogliosis (39).

1.5.2 Reactive astrogliosis:

Reactive astrogliosis is a finely graduated continuum of changes that occur in context-dependent manners regulated by specific signaling events. These changes range from alterations in reversible gene expression to long-lasting scar formation with rearrangement of tissue structure. Recently, it has become widely accepted that astrogliosis is a hallmark of several neuroinflammatory diseases. The changes that occur during reactive astrogliosis can alter astrocyte function. This could be beneficial or detrimental to the CNS health and homeostasis. Several intercellular signaling mediators act as molecular triggers of astrogliosis. These include a wide variety of cytokines secreted by other cell types in the CNS, innate immune mediators such as lipopolysaccharide and toll like receptor (TLR) ligands and reactive oxygen species. It is also

known that various intercellular signaling pathways associated with cAMP, nuclear factor (NF)-κB, signal transducer and activator of transcription (STAT) 3 and Nrf2 are also implicated in regulating different aspects of astrogliosis, including glial fibrillary acidic protein upregulation, secretion of pro- and anti-inflammatory cytokines and cell proliferation. During the process of astrogliosis, astrocytes contribute to the CNS disease mechanism through potential loss of normal functions or gain of detrimental effects (39).

1.5.3 Astrocyte HIV-1 infection:

Astrocytes lack expression of the conventional CD4 receptor, which mediates the fusion and entry of HIV-1 virus with target cells. This major resistance factor makes astrocytes unsusceptible to conventional HIV-1 infection. However, astrocytes express both coreceptors C-C chemokine receptor type 5 (CCR5) and C-X-C chemokine receptor type 4 (CXCR4) that mediate fusion of the virion with the target cell. It was shown that HIV-1 can infect CD4 negative cells *via* these coreceptors and other unconventional mechanisms. Nonetheless, the infection rates are quite low (40, 41). HIV-1 infection of astrocytes most likely occurs by endocytosis or cell-to-cell contact with infected cells, rather than by cell free virus (42-46). Being a major structural part of the brain vasculature astrocyte end feet are in constant contact with the extravagating immune cells which could potentially make them susceptible for HIV-1 infection. *In vitro* astrocytes are susceptible to HIV infection. Yet, it is inefficient, and few cells become persistently infected, approximately 0.5% (47-49). Astrocytes also actively resist HIV infection by constraining viral RNA processing or translation and preferentially expressing viral regulatory proteins over structural proteins, which disrupts virion assembly (50-52). While HIV+ astrocytes produce several neurotoxic viral proteins such as Tat, gp120, Vpr and Nef, viral productivity in terms of infectious viral particles and viral protein expression is low (53-58). This is why astrocyte HIV-1 infection is called restricted

infection. *Ex vivo* studies provide evidence that up to 7-19 % of astrocytes had integrated HIV-1 genomes (15). Immunological studies looking for viral proteins in astrocytes in *ex vivo* brain tissues have been hampered by restricted/latent infection (false negatives) and uptake/transfer of viral proteins from other cells (false positives). None the less, the consensus of the scientific community is that at least some human astrocytes are restrictively infected by HIV. An infection rate of even 1% would correlate to 0.4 – 1.3 billion HIV+ astrocytes in a human brain, which could have widespread consequences on neuronal survival, BBB permeability and neuroinflammation.

1.5.4 Role of Wnt/β-catenin in astrocyte HIV-1 infection:

Wingless type ligand (Wnt)/β-catenin is a highly conserved signaling pathway involved in processes such as embryogenesis, development and adult multi-organ homeostasis. This pathway plays a crucial role in cellular events such as cell proliferation, differentiation, migration, survival and apoptosis (59). Aberrations or mutations in this pathway are implicated in numerous cancers (59). Wnt/β-catenin signaling is robust in astrocytes, and expression of its downstream transcriptional effectors T-cell factor/lymphoid enhancer factor (TCF/LEF) family members was previously shown in progenitor-derived astrocytes (60). The Wnt/β-catenin pathways have been shown to restrict the HIV life cycle in target cell types, including peripheral blood mononuclear cells and astrocytes. Four TCF-4 binding sites were found in HIV-1 promoter region close to transcription initiation site. The association between TCF-4, β-catenin and a nuclear matrix binding protein SMAR-1 on one of these sites is known to pull the DNA away from the transcription machinery (60, 61). Upregulation of Wnt/β-catenin signaling is evident in several neuroinflammatory diseases such as Parkinson's disease, cerebral ischemia, Alzheimer's disease, Huntington's disease, as well as, HAND (62-64).

During CNS HIV-1 infection microglia- and macrophage-derived IL-1β and TNF-α also induce NF-κB signaling in astrocytes (65). NF-κB acts as a central regulator of innate and adaptive immune responses, cell proliferation, and apoptosis in various cell types (66). Inflammatory cytokines such as C-X-C motif chemokine ligand (CXCL) 8, C-C motif chemokine ligand (CCL) 2, CCL3, IFN-γ and IL-6 production is upregulated by astrocytes in response to macrophage-derived IL-1β and TNF-α during HIV-1 CNS infection (67). These key astrocyte derived cytokines recruit neutrophils and monocytes to the CNS and exacerbate HIV-1-associated inflammation. Astrocytes are the predominant source for IL-6 in the CNS, and its levels are low under physiological conditions. In the CNS, IL-6 acts as both a neurotropic and neurotoxic cytokine depending on the cellular context. Elevated IL-6 levels were found during several neurological disorders including injury, viral and bacterial meningitis, multiple sclerosis, Alzheimer's disease and HIV-associated dementia (68). Previously, Ma *et al.* have shown that in chondrocytes, β-catenin negatively regulates NF-κB-mediated IL-6 expression (69).

Crosstalk between Wnt/β-catenin and NF-κB signaling during inflammation has been extensively studied in peripheral cells (70). However, little is known about its contributions to the neuroinflammatory responses of astrocytes.

1.5.5 Astrocyte-mediated HAND pathogenesis:

Even though astrocytes make little or no virus under normal conditions, they express neurotoxic viral proteins such as Tat, gp120, Vpr and Nef (71, 72). Exposure to gp120 induces apoptosis in astrocytes and upregulates expression of neuroinflammatory cytokines (73). As an activating transcription factor of the viral genome, Tat also upregulates expression of various cytokines, chemokines, prostaglandins, reactive oxygen species and cell adhesion molecules (74). HIV-1 Nef is known to upregulate astroglial production of CXCL10, which recruits monocytes

and T cells to the CNS and to chronic neuroinflammation (72). In addition, astrocytes are highly sensitive to the proinflammatory cytokines secreted by infected macrophages and microglia, including IL-1β and TNF-α. Upon activation by both of these proinflammatory cytokines, astrocytes express large amounts of IL-6, CXCL8 and CCL2. Both CXCL8 and CCL2 are known to recruit neutrophils and monocytes respectively to the site of inflammation.

Astrocyte excitatory amino acid transporter 2 (EAAT2) is the primary glutamate transporter expressed on astrocytes and helps in the uptake of excessive glutamate from neuronal synapses to prevent excitotoxicity. Astrocytes are highly sensitive to IL-1β-mediated activation as they possess an IL-1β autocrine loop. IL-1β and TNF-α are known to downregulate astrocyte EAAT2 expression resulting in excitotoxicity (75). Viral protein Tat also decreases cell surface expression of EAAT2.

HIV-1-infected astrocytes can transmit toxic signals to uninfected cells *via* gap junctions, leading to cell death (76). As astrocytes are in close contact with neurons and capable of sensing neuronal activity, impairment of all these astrocyte functions can lead to neuronal dysfunction or injury. These mechanisms could be, increased extracellular potassium inducing depolarization of neuronal membrane, glutamate excitotoxicity, increased intracellular concentration of Ca^{2+} in neurons and finally neurotoxicity exerted by astrocyte derived inflammatory cytokines (77).

1.6 Therapies for HIV-1 cure:

Despite effective ART, PLWH suffer from several comorbidities such as HAND as discussed above, and to suppress viremia, patients need to follow the strict antiviral regimen. This is why achieving a sterile/functional cure has become a priority in the HIV field of research. Several attempts have been made towards achieving a functional cure, and only few people were cured from HIV-1 (78). In all these cases long term HIV-1 remission was achieved by allogenic

hematopoietic stem-cell transplantation from a donor with a homozygous mutation in the HIV-1 coreceptor CCR5 (CCR5 Δ32/Δ32) to treat their cancer. However, this strategy is not feasible to cure HIV-1 in millions of PLWH across the world.

The current strategies to eliminate viral reservoirs can be classified into three main categories. 1) Shock and Kill – Reactivating latently infected cells to make them susceptible to killing by the immune system, while concurrently preventing new infection with ART. 2) Block and Lock – Inducing epigenetic changes or chromatin structure alterations to render provirus *completely* silent, forcing cells into a functional cure. And 3) Use of genetic engineering tools either to make cells resistant to the infection or excise/truncate the provirus from infected cells (10).

Shock and kill strategy is one of the widely used strategies to cure HIV-1 infection. There are approximately 15 clinical trials currently assessing various classes of latency reactivating agents (LRA). So far, no one LRA has successfully reduced the size of viral reservoirs, indicating that this one strategy is not sufficient in and of itself. LRAs will need to be combined with immune therapy or vaccinations that induce high affinity neutralizing antibodies to help effector-mediated cell death. Increased expression of inhibitory cell surface markers, like programmed cell death protein-1 (PD-1) / cytotoxic t-lymphocyte associated protein 4 (CTLA4), is a biomarker for viral infection and is a marker for T cell exhaustion and anergy. Blocking these inhibitory surface molecules with antibodies may increase ability of the immune cells (CD4 and CD8 T cells) to protect against viral infection (79).

The most recent strategy block and lock aims to suppress the viral transcription and keeps the virus silent till the infected cells die. HIV-1-Tat activates viral transcription by binding to Tat-TAR element on the viral genome. Limited Tat activity leads to limited transcription of viral

genome and potential establishment of latency. Some studies used small molecules such as didehydro-cortistatin A that inhibit Tat to show delayed viral rebound in T cells isolated from aviremic patients when combined with treatment interruption. However, there is a greater need to explore multiple other mechanisms to keep the virus completely silent (80).

The other alternative and promising cure therapy is using gene editing technology such as cluster interspaced short palindromic repeats/CRISPR associated protein 9 (CRISPR/Cas9) or transcription activator-like effector nucleases (TALEN)/Zinc fingers. These gene editing strategies could be applied in various forms. First, designing and delivering guide RNA against HIV-1 sequence will potentially excise the viral genome or renders it silent. Secondly, these techniques could also be used to induce mutations at Tat-TAR binding sites preventing transactivation of the viral genome by Tat. Finally, the widely used approach is to mutate the CCR5 coreceptor during HIV-1 infection. The famous Berlin patient who was successfully cured of HIV-1 is because of receiving hematopoietic stem cell transplantation with CCR5Δ32 homologous allele during his cancer treatment. However, phase one and two clinical trials of gene editing strategies targeting CCR5 were not successful (81-83) and may have unintended consequences.

A common feature in all these approaches is the challenge posed by the CNS reservoirs. Presence of the BBB and the type of cells infected are different than the conventional T cell reservoirs. Moreover, the brain cannot survive long term inflammation, which can lead to permanent neuronal damage.

1.7 Objectives and specific aims:

Once HIV-1 infects a cell, its viral genome integrates into the host genetic material. This persistent nature is why we failed to generate a HIV cure in the four decades since it was identified as the cause of AIDS. ART effectively suppresses peripheral viremia, it struggles to eliminate latent viral

reservoirs distributed across several anatomical sites in the human body of which the CNS remains a challenging sanctuary. HIV-1 CNS infection often leads to neurological impairment including cognitive and motor dysfunction collectively called as HAND. Despite the fact that ART significantly increased the lifespan of PLWH and decreased the incidence of the most severe form of HAND, mild to moderate neurocognitive impairment still persists in 30 to 50% of PLWH (20, 84).

As one of the most abundant cell types in the CNS, healthy astrocytes perform an array of important functions in maintaining homeostasis ranging from physical and metabolic support to other cells, uptake and regulation of neurotransmitters such as glutamate, maintaining BBB integrity, synaptogenesis, immune surveillance, and promoting neuronal survival by secreting neurotrophic factors. In this context, astrocytes directly and indirectly potentiate HAND pathogenesis during HIV-1 CNS infection. Direct expression of viral proteins by astrocytes can result in neurotoxicity (85, 86), while impaired astrocyte function, such as impaired neurotransmitter clearance leading to excitotoxicity, or amplification of the neuroinflammatory response in the CNS, would indirectly contribute to neuronal dysfunction or death. This type of reactive astrocytes, *i.e.* astrogliosis, is evident during several neurocognitive disorders including HAND (87, 88).

Despite all the progress toward understanding altered astrocyte function contributing to HIV neuropathogenesis, little is known about how HIV-1 latency affects their function. The contribution of astrocytes harboring HIV-1 on the CNS and development of neurological disease remain highly debated topics (89). Astrocytes harboring HIV-1 genome can be reactivated by pharmacological LRAs such as vorinostat, a classic histone deacetylase inhibitor (HDACi), as well as inflammatory cytokines such as TNF-α, and IL-1β (56, 90-92). However, the effects of ART

and eradication strategies on astrocyte function are not well understood. Therefore, understanding the effects of integrated HIV virus on astrocyte function is critical to future therapeutic options for restoring or preserving CNS function in PLWH.

Here our goal is to decipher the consequences of HIV-1 integration in human astrocytes and how viral long terminal repeat (LTR) activity affected the functional responses of HIV+ astrocytes. We further hoped to identify targetable surface biomarkers of HIV+ astrocytes that could facilitate viral reservoir eradication. Thus we **hypothesize that astrocyte HIV-1 proviral reservoirs alter their function in conjunction with unique gene expression patterns that could serve as biomarkers for HIV-1 infection.**

To address our hypothesis, we used a double fluorescent labelled HIV-1 reporter virus, red/green-HIV-1 (R/G-HIV-1) (93) that can distinguish the transcriptional state of the viral promoter and allows the isolation of HIV+ astrocyte populations with active (R+/G+, yellow) and silent/restricted (R+/G-, red) viral promoters.

Specific Aim 1: To investigate how harboring HIV-1 provirus contributes to astrocyte dysfunction and HAND pathogenesis.

Specific Aim 2: To identify targetable surface biomarkers for HIV-1 latency in human astrocytes that can potentially aid in the eradication of viral reservoirs.

To address our specific aims, **first** we optimized the vesicular stomatitis virus glycoprotein (VSVG)-pseudotyped R/G-HIV-1 infection using both WT and integrase deficient (D116A) mutant in multiple human astrocyte donors. The R/G-HIV-1 construct was previously characterized in various T cell lines and primary human CD4 T cells (93). To investigate the viral promoter activity in astrocytes post infection and integration, endogenous fluorescence reporter-based flow analysis was performed. The integration of the viral genome into the astrocyte genome

was also confirmed by Alu-gag PCR. Few studies have shown the detrimental outcomes of changes in gene expression of HIV-1-infected astrocytes towards understanding the role of astrocytes in HAND pathogenesis (94, 95). However, none of these studies was able to isolate the type of infection and its effects on the gene expression and function of astrocytes during inflammation and reactivation. Thus, we hypothesized HIV-1 infection of astrocytes significantly changes their gene expression along with their function and reactivation would exacerbate the dysregulation of the CNS homeostasis. So, **next** to determine the changes in gene expression and functions we isolated both active and restrictively infected R/G-HIV-1+ astrocytes by fluorescence activated cell sorting (FACS).

Simultaneously, to compare and contrast the altered canonical and biological function pathways among active and restrictively infected astrocytes we used Ingenuity Pathway Analysis (IPA) to analyze the gene expression data. "Shock and Kill" therapy that reactivate latent reservoirs for clearance by cytotoxic immune cells will also be challenging since HIV+ astrocytes may be inducible to LRAs leading to augmented production of viral proteins. Therefore, it is important to identify biomarkers to target HIV+ astrocytes in the CNS without reactivating. IPA biomarker analysis also facilitated the analysis of surface biomarkers based on the RNA sequencing data. **Finally**, to determine the phenotypic similarities between our *in vitro* R/G-HIV-1 infection model in primary human astrocytes and *in vivo* samples from multiple brain regions of HIV-1-infected individuals we performed comparison analysis using IPA.

Taken together, the studies within this dissertation will prove highly significant as they delineate the outcomes of astrocytes harboring either active or restricted viral promoters. We discuss how these studies provide new context and direction to understanding astrocyte-associated neuropathogenesis during HAND. These findings have significant implications that may guide

therapeutic interventions to promote astrocyte health and alleviate HIV-associated neurocognitive impairment.

1.8 Importance:

More than 37 million people are living with HIV-1 worldwide, and despite antiretroviral therapy 50-70% of the PLWH suffer from mild to moderative neurocognitive disorders. HIV-1 reservoirs in the CNS are challenging to address due to low penetration of antiretroviral drugs, lack of resident T cells, and permanent integration of provirus into neural cells such as microglia and astrocytes. Several studies have shown astrocyte dysfunction during HIV-1 infection. However, little is known about how HIV-1 latency affects their function. The significance of our research is in identifying that the majority of HIV+ astrocytes remained latent and were resistant to reactivation. Further, simply harboring the HIV genome profoundly altered astrocyte biology, resulting in a proinflammatory phenotype and functional changes. In this context, therapeutic strategies to reactivate or silence astrocyte HIV reservoirs, without excising proviral DNA, will likely lead to detrimental neuropathological outcomes during HIV CNS infection.

CHAPTER 2

MATERIALS AND METHODS

PORTIONS FORMATTED AND PUBLISHED AS:

Insights into the Gene Expression Profiles of Active and Restricted Red/Green-HIV^{+} Human Astrocytes: Implications for Shock or Lock Therapies in the Brain

Journal of Virology. 2020. February 28. e01563-19

https://jvi.asm.org/content/94/6/e01563-19.long

2.1 Cell culture:

Human astrocytes were isolated from brain tissues recovered from first- and early second-trimester conceptual tissue as described previously (96). Tissue samples were obtained from the Birth Defects Research Laboratory at the University of Washington in Seattle in full compliance with the ethical guidelines of the National Institutes of Health (NIH), Universities of Washington and North Texas Health Science Center. Isolated astrocytes were cultured in 1:1 v/v DMEM:F12 medium containing 10% fetal bovine serum (catalogue no. PS-FB1 lot no. 27C1171, Peak Serum, Wellington, CO) (catalogue no. F-05000-D, lot no. F12C18D1 Atlas Biologicals, Fort Collins, CO), penicillin-streptomycin-neomycin 50 U - 50 μg/ml -100 μg/ml (PSN) (catalogue no. P4083, Sigma Aldrich, St. Louis, MO) and Amphotericin B 2.5 μg/ml (Catalogue no. A2942, Sigma Aldrich).

2.2 Transfection of astrocytes:

Human astrocytes were transfected either with no siRNA (mock), or scrambled non-targeting siRNA (siCon, Dharmacon), or siRNA specific to β-catenin (siβ-catenin) using the Amaxa^{TM} P3 primary cell 96-well nucleofector kit (Lonza, Walkersville, MD, USA). Briefly, 1.6 million astrocytes were suspended in 20 μl nucleofector solution containing no si RNA or siCon or siβ-catenin (200 nM) and transfected using a Nucleofector/Shuttle (Lonza) device. Transfected cells were supplemented with media and incubated for 20 min at 37°C prior to plating. Cell were then cultured and allowed to recover for 48 h prior to experimental use.

2.3 Constructs:

Red/Green-HIV-1-WT or D116A were obtained from NIH AIDS Reagent Program (#12427 and #12428, respectively) (Fig 2.1A). The constructs were designed by Dr. Ivan Sadowski's group at University of British Columbia in Vancouver, British Columbia, Canada (93). Briefly, the R/G-

HIV-1 clone consist of two fluorescent markers to identify both silent (red) and productive HIV-1 infection (green/yellow) (Fig 2.1B). The green fluorescent protein (eGFP) protein was placed in gag region flanked by matrix and capsid. The expression of gag-eGFP upon integration is under the control of HIV-1 LTR. The second reporter mCherry fluorescent protein replaced viral *Nef*. The expression of mCherry is under an individual CMV promoter, which is constitutively expressed and allows detection of integrated virus irrespective of the transcriptional state of the HIV-1 LTR promoter. The presence of two individual fluorescent reporters allow quantitative detection and fluorescence activated cell sorting (FACS) of cells with active (mCherry+/eGFP+ or R+/G+) and silent (mCherry+/eGFP- or R+/G-) viral promoter (Fig 2.1B). Another variant of R/G-HIV-1 (D116A), a catalytically defective integrase mutant, was used as infection control.

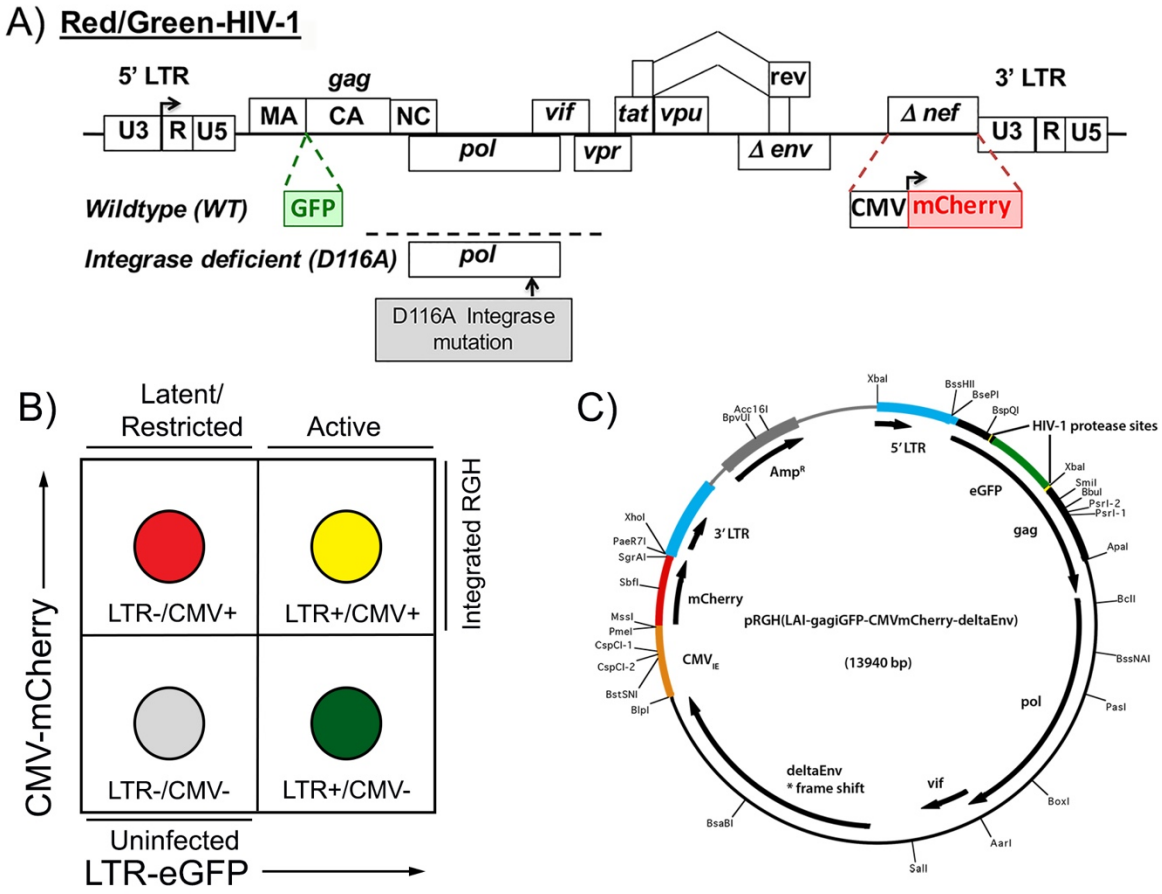

Figure 2. 1 Red/Green-HIV-1 Model.

(A) Schematic representation of the R/G-HIV-1-WT/D116A constructs. (B) Schematic depiction of R/G-HIV-1 infected astrocyte population detected by FACS analysis. (C) Plasmid map of R/G-HIV-1-WT construct used for pseudotyping and mapping of RNA sequencing reads.

2.4 Pseudotyping R/G-HIV-1-WT/D116A:

Human embryonic kidney (HEK) 293 cells were plated at 50% confluency in T75 tissue culture flasks. Then co-transfected with pRGH-WT/D116A and pHEF-VSVG (p-human elongation-factor 1 alpha promoter driven vesicular stomatitis virus glycoprotein) at 10:1 ratio by calcium phosphate ($CaPO_4$) precipitation according to the manufacturer's instructions (Clonetech Laboratories, Inc., Mountain View, CA). Briefly, plasmid DNA (3 μg/1X10^6 cells) and 2M calcium solution were added to sterile water (solution A). Then equivalent volume of 2X HEPES [4-(2-hydroxyethyl)-1-piperazineetanesulfonic acid] solution (solution B) was slowly added to solution A, gently vortexed and incubated for 5 to 15 minutes. Then 2 ml of the precipitate was slowly added to the culture flask under sterile conditions and incubated overnight at 37^{o}C and 5% CO_2. Then calcium phosphate containing medium was removed; cells were washed with PBS; fresh culture medium was added and cultured at 37^{o}C and 5% CO_2. Cell culture supernatants were harvested 48 hours post-transfection, clarified to remove cellular debris by centrifuging at 3000 g for ten minutes and stored at -80^{o}C.

2.5 Reverse transcriptase activity assay:

To measure reverse transcriptase activity, 10 μl of viral stock was lysed with 10 μl of dissociation buffer [100 mM of Tris-HCl pH 7.9, 300 mM KCl, 10 mM dithiothreitol (DTT), 0.1% NP-40] in

a round bottom well plate and incubated at 37°C and 5% CO_2 for 15 minutes. 25 µl reaction buffer [50 mM of Tris-HCl pH 7.9, 150 mM KCl, 5 mM DTT, 0.05% NP-40, 15 mM $MgCl_2$, 5 µl of 1 mg/ml poly (A) x $(dT)_{15}$ (Roche, Indianapolis, IN), and 1 µCi /ml of [^{3}H] thymidine 5'-triphosphate tetrasodium salt (PerkinElmer, Inc., Waltham, MA)] was added to the mixture and incubated for 18 – 24 hours at 37°C and 5% CO_2. Fifteen minutes before harvesting the reverse transcribed cDNA was precipitated by adding 50 µl of ice cold 10% trichloroacetic acid (TCA) to each well. Precipitated DNA was transferred onto a filter plate (MultiScreen 96 well harvest plates, catalog no. MAHFB1H60, Millipore, Burlington, MA) with the help of FilterMate Harvester (PerkinElmer, Inc.). Then the filter plate was washed extensively with 5% TCA and dehydrated with 95% ethanol. The filter plate was counted for ^{3}H-incorporation using MicroBeta^2 scintillation counter (PerkinElmer, Inc). Counts per minute (CPM) was used to quantify the reverse transcriptase activity as a measure of viral concentration.

2.6 Spinoculation of primary human astrocytes:

Primary human astrocytes were seeded in either T-75 tissue culture flasks ($10X10^6$ cells/flask, catalog no. 130190, Thermo Fisher, Waltham, MA) or six well plates ($2X10^6$ cells/well) and allowed to recover overnight. VSVG-pseudotyped R/G-HIV-1-WT/D116A equivalent to 35,000 CPM RT activity/ml was added to the cultures along with polybrene (8 µg/ml) (catalog no. TR-1003-G, Sigma) in a final volume of 13 ml/T75 flask or 3 ml/well on a six well plate. Flasks or plates were centrifuged at 600 g in a bench top centrifuge model ST40R using the swing bucket rotor # 75003180 and plate rack # 75003617 (Thermo Fisher Sorvall) at room temperature for two hours and incubated overnight at 37°C and 5% CO_2. Next day unbound viral particles were removed by multiple PBS washes, and the cells were cultured in fresh medium.

2.7 Flow analysis and fluorescence activated cell sorting (FACS):

R/G-HIV-1-WT/D116A-infected astrocytes were trypsinized and harvested from tissue culture plates at specified time points, and flow data were acquired using BD LSR II flow cytometer (BD, Franklin Lakes, NJ) and analyzed by FlowJo software (FlowJo LLC, Ashland, OR). R/G-HIV-1-WT/D116A-infected astrocytes were maintained in culture with regular passaging. Two weeks post-infection cells were harvested by trypsinization, washed with PBS, filtered through a 70 μM filter and resuspended in FACS buffer (1% FBS in PBS) ($10X10^6$ cells/ml). Cells were sorted using Sony SH800 cell sorter (Sony Biotechnology, San Jose, CA).

2.8 Immunocytochemistry:

Sorted human astrocytes were plated in 48 well tissue culture plates at $1X10^5$ cells/well and allowed to recover for at least 24 hours. Cells were washed multiple times with PBS and fixed with 4% paraformaldehyde in PBS for 15 minutes at room temperature to preserve red and green fluorescence. Cells were blocked with blocking buffer (2% BSA and 0.1% Triton X-100 in PBS) for one hour and probed overnight with primary antibody against HIV-1 p24 (produced in mouse, 1:200, monoclonal, clone Kal-1, catalog no. M0587, Dako, Denmark). Then cells were washed three times with PBS and labelled with anti-mouse secondary antibody Cy5 (1:500, Thermo Fisher) for two hours. Images were taken at 20x magnification using Eclipse Ti-300 and processed by NIS-Element BR 3.2 software (Nikon Instruments, Inc., Melville, NY).

2.9 Alu-gag PCR:

Integration of R/G-HIV-1 was assessed as previously described (97). Briefly, chromosomal DNA was isolated from astrocytes and 8e5 cells using DNeasy Blood and Tissue kit (Qiagen, Germany) as per the manufacturer's procedures. The first PCR was carried out using Phusion High-Fidelity PCR kit (catalog no. F553S, Thermo Fisher) with an Alu-sequence-specific sense primer, Alu-HIV (5'-TCC CAG CTA CTC GGG AGG CTG AGG-3'), and an antisense primer made to the R/G-HIV-1 sequence (5'-CCT GCG TCG AGA GAG CTC CTC TGG-3') with an input DNA of 10 ng in 50 µl reaction. The cycling conditions included an initial denaturation step (95^{o}C) for three minutes followed by 25 cycles of denaturation (95^{o}C for 30 seconds), annealing/extension (72^{o}C for five minutes) and then a final extension (72^{o}C for ten minutes). Then the first PCR product was diluted 10 fold and subjected to another PCR for measuring R/U5 DNA using sense primer M667 (5'-GGC TAA CTA GGG AAC CCA CTG C-3'), antisense AA55 (5'-CTG CTA GAG ATT TTC CAC ACT GAC-3'), and subsequently second PCR product was then run on a 1% agarose gel and visualized using ethidium bromide (EtBr) on FluorochemQ gel imaging station (ProteinSimple, SanJose, CA). 1 kb marker was used (catalog no. SM0311, Thermo Fisher) to compare size of the PCR product.

2.10 Real time gene expression analysis:

RNA was isolated using Trizol reagent (Thermo Fisher Scientific, Waltham, MA) as previously described (96) followed by DNA digestion and precipitation. A Nanodrop fluorospectrometer (Thermo Fisher Scientific) was used to assess RNA purity and to quantify total RNA levels. Then transcripts were made into cDNA as per the manufacturer's instructions (High Capacity cDNA Reverse Transcription Kit, catalogue no. 4368814, Thermo Fisher). Tat gene expression was quantified by TaqMan Fast Virus 1-Step Master Mix (catalogue no. 4444432, Applied Biosystems,

Foster City, CA) in 20 µl reactions, using StepOnePlus Real-Time PCR system according to the manufacturer's protocols (Thermo Fisher). Primers used for Tat detection were 5' GGAAGCATCCAGGAAGTCAG 3' and 5' GGAGGTGGGTTGCTTTGATA 3' with 5' CCTCCTCAAGGCAGTCAGAC 3' used as probe. GAPDH (Thermo Fisher) was used as an internal control. Expression levels of β-catenin, LEF-1, and GAPDH were measured by real-time polymerase chain reaction (PCR) using Taqman® gene expression assays and the StepOnePlus detection system (Thermo Fisher Scientific). The 20 µl reactions were carried out at 60°C for three minutes, 95°C for three minutes, followed by 40 cycles of 95°C for 15 seconds and 60°C for one minute in 96-well optical RT^2-PCR plate (Thermo Fisher). Transcripts were quantified by the comparative ΔΔCT method and represented as fold change to R/G-HIV-1-WT-infected untreated control.

Table 2. 1 Gene expression assay target:

Target	Assay number (Thermo Fisher)	Dye
Glyceraldehyde 3-phosphate dehydrogenase (GAPDH)	4310884E	(VIC/TAMRA)
β-catenin	Hs00355049_m1	(FAM/MGB)
Lymphoid enhancement factor LEF-1	Hs01547250_m1	(FAM/MGB)
Interluekin-6 (IL-6)	Hs00985639_m1	(FAM/MGB)

2.11 Protein isolation, identification and analysis:

Cytoplasmic and nuclear lysates were isolated using a nuclear and cytoplasmic extraction kit according to the manufacturer's methods (NE-PER, Thermo Fisher Scientific). Protein concentrations were determined by the BCA protein assay kit (Thermo Fisher Scientific) according to manufacturer's instructions. The levels of specific proteins were determined by the WES

capillary protein detection system (ProteinSimple) according to manufacturer's directions. 0.4 mg/ml protein was loaded into WES capillaries. columns were probed with antibodies for Lamin A/C (mouse, cat: NBP-19324, Novus Biologicals, Littleton, CO lot:41815; WES 1:50), β-catenin, NFkB, GAPDH.

2.12 Glutamate clearance assay:

Sorted astrocytes were plated in triplicates in 96-well tissue culture plates at a density of 7.5×10^4 cells/well and allowed to recover for 24 hours. Subsequently cells were treated with either IL-1β (20 ng/ml) or vorinostat (1 μM) alone or in combination for another 24 hours at 37°C and 5% CO_2. Glutamate (400 μM) dissolved in phenol red free astrocyte medium was added into each well post treatment. Glutamate clearance was measured at 24 hours post-glutamate addition according to the manufacturer's protocols (Amplex Red Glutamic Acid/Glutamate Oxidase Assay Kit, Thermo Fisher). Glutamate clearance was normalized to relative cell size of different astrocyte populations measured by flow analysis. Briefly; flow cytometry standard (FCS) file for each astrocyte culture was analyzed in FlowJo to calculate both the geometric mean of area under the curve of forward scatter and fold changes to D116A as the experimental control. These fold changes were then used to normalize glutamate clearance levels prior to calculating fold changes to the untreated D116A control.

2.13 Measures of cell viability:

Metabolic activity of astrocytes was measured by 3-(4,5-dimethylthiazol-2-yl)-2,5-diphenyl tetrazolium bromide (MTT) assay as previously described (98). Briefly 0.25% MTT was added to astrocytes and incubated for 20 to 45 minutes at 37°C. Then MTT solution was removed, and crystals were dissolved in dimethyl sulfoxide (DMSO) for 15 minutes with gentle agitation.

Absorbance was assayed at 490 nm in a SpectraMax M5 microplate reader (Molecular Devices, Sunnyvale, CA).

2.14 Quantification of HIV-1 viral protein and pro-inflammatory cytokines by ELISA:

Cell culture supernatants were collected at specified timepoints after treatments and used to quantify HIV-1 viral protein p24 (catalogue no. 5421, HIV-1 p24 antigen capture assay, ABL, Inc., Rockville, MD), and proinflammatory cytokines CXCL8, CCL2, and IL-6 (catalogue no. D8000C, DCP00, and D6050 respectively, Quantikine ELISA Kits, R&D Systems, Minneapolis, MN) were assayed as per the manufacturer's instructions and normalized to MTT levels as mentioned earlier.

2.15 BrdU incorporation assay:

Sorted astrocytes were plated in triplicates in 96 well tissue culture plates at 5×10^4 cells/well and allowed to recover overnight. Then cells were treated with either with IL-1β (20 ng/ml) or vorinostat (1 μM) alone or in combination 24 hours. BrdU was added halfway through the treatments and incorporation was measured using BrdU Cell Proliferation Assay Kit (catalogue no. 6813, Cell Signaling Technology, Inc, Danvers, MA) as per the manufacturer's instructions. Data were normalized to R/G-HIV-1-D116A-infected untreated control.

2.16 RNA isolation and sequencing:

RNA was isolated using Trizol reagent as previously mentioned above. Samples were run on the Agilent 4200 TapeStation System (Agilent, Santa Clara, CA) to determine level of degradation thus ensuring only high-quality RNA was used (RIN Score 8 or higher). The Qubit 4 Fluorometer

(Thermo Fisher) was used to determine the concentration prior to staring library prep. Four μg of total DNAse treated RNA were then prepared with the TruSeq Stranded mRNA Library Prep Kit (Illumina, San Diego, CA). Poly (A) RNA was purified and fragmented before strand specific cDNA synthesis. cDNA was then A-tailed, and indexed adapters were ligated. After adapter ligation, samples were PCR amplified and purified with AMPure XP beads (Beckman Coulter, Brea, CA), then validated again on the Agilent 4200 TapeStation System. Before being normalized and pooled, samples were quantified by Qubit and later run on the Illumina NextSeq 500 using NextSeq 500/550 V2 sequencing reagent kit (Illumina).

2.17 Bioinformatics analysis:

Basic bioinformatics analysis of gene expression raw data was performed at The McDermott Center Bioinformatics Lab, UT Southwestern Medical Center, Dallas, Texas. Briefly the samples were sequenced using Illumina NextSeq 500 with the read configuration as 75bp, single end. Fastq files were checked for quality using fastqc (v0.11.2) (99) and fastq_screen (v0.4.4) (100) and were quality trimmed using fastq-mcf (ea-utils/v1.1.2-806) (101). Trimmed fastq files were mapped to hg19 (UCSC version from igenomes) using Tophat (102). Duplicates were marked using picard-tools (v1.127 https://broadinstitute.github.io/picard/). Read counts were generated using featureCounts (103), and the differential expression analysis was performed using edgeR (104).

2.18 Quantification of R/G-HIV-1 transcripts:

Raw demultiplexed Illumina RNAseq reads were quality trimmed using Trimmomatic v. 0.36 with the following options: LEADING:20 TRAILING:20 MINLEN:35 AVGQUAL:20 (105). The BWA MEM algorithm v.0.7.17 (106) was used with default settings, to map quality trimmed reads to the pRGH-WT HIV-1 molecular clone map and sequence file available on

www.aidsreagent.org, and reads were sorted using SAMtools (107). Counts were generated for reads based on the plasmid map feature list (NIH-AIDS Reagent Program, ARP) (Fig 2.1C). Raw expression counts were normalized by combining the R/G-HIV counts to the total human reference counts using the trimmed mean of M-values (TMM) normalization method in edgeR (104, 108).

2.19 IPA analysis:

Bioinformatics analysis was performed to analyze differentially expressed genes from uninfected, R/G-HIV-1 D116A-infected R-/G-, R/G-HIV-1-WT-infected R+/G- and R+/G+ samples from three different astrocyte donors as mentioned above. Outcomes from gene expression analysis were uploaded into Qiagen Bioinformatics' IPA system (version 01-14) for core analysis, comparison analysis, biomarker analysis and analysis match. Cutoff values used to run the IPA were fold change either ≤ -2 or ≥ 2, and false discovery rate (FDR) ≤ 0.05.

2.20 Statistical analysis:

Statistical analyses were performed using GraphPad Prism 8.3.1 (GraphPad software, San Diego, CA). All numerical data were taken as mean ± SEM. All data were analyzed using student t-test, a one-way, or a two-way ANOVA with Tukey or Fisher's least significant difference post-hoc tests for pair-wise comparisons. Differences were considered statistically significant with $p \leq 0.05$.

CHAPTER 3

GENE EXPRESSION PROFILES OF ACTIVE AND RESTRICTED R/G-HIV+ HUMAN ASTROCYTES

PORTIONS FORMATTED AND PUBLISHED AS:

Insights into the Gene Expression Profiles of Active and Restricted Red/Green-HIV^{+} Human Astrocytes: Implications for Shock or Lock Therapies in the Brain

Journal of Virology. 2020. February 28. e01563-19

https://jvi.asm.org/content/94/6/e01563-19.long

3.1 Most HIV+ human astrocytes restrict the viral LTR promoter:

The R/G-HIV-1 construct (Fig 3.1A) was previously characterized in primary human CD4 T-cells where latent populations with silent HIV LTRs were identified (93). In primary human astrocytes R/G-HIV-1 infection resulted in more red cells (R+/G-) compared to yellow cells (R+/G+) indicating the majority of the infected astrocytes restricted HIV LTR activity. These distinct populations appeared 48 – 72 hours post-infection, and the percentage of red cells (66.7%) was two-fold higher than that of yellow cells (33.3%) (Fig 3.1B). Therefore, R/G-HIV-1 promoter activity in human astrocytes was established early during R/G-HIV-1 infection. Further the proportions of R+/G- and R+/G+ cells remained steady through 21 days post-infection, despite declines in the overall infection rate (data not shown). While the proportion of red and yellow cells varied among 30 biologically independent astrocyte cultures, ranging between 41.6% to 88.7% R+/G- (red) and 11.2% to 58.3% R+/G+ (yellow) of infected cells 14 days post-infection (Fig 3.1B), all together a significant majority of HIV+ astrocytes were R+/G- (67.95% ***$p < 0.001$) as identified by this model.

To isolate these populations, HIV+ astrocytes were separated by FACS based on the gating strategies shown for uninfected cells, R/G-HIV-1 D116A-infected R-/G- cells, and R/G-HIV-1-WT-infected R+/G- (red) and R+/G+ (yellow) cells (Fig 3.1C). The purity of the sorted populations was greater than 90% when tested by flow cytometry (Fig 3.1D). The absence of yellow cells coupled with very low percentage of red cells, due to transient expression of mCherry in R/G-HIV-1-D116A-infected cells, confirmed that HIV+ reporter expression depends on integration of proviral DNA into the astrocyte genome (Fig 3.1C). Alu-gag nested PCR also established integration of proviral DNA in R/G-HIV-1-WT-infected astrocytes (Fig 3.1E). When sorted populations were visualized microscopically, R+/G- astrocytes did not express the LTR driven

eGFP reporter or the viral protein p24 (Fig 3.1F), whereas R+/G+ astrocytes expressed both eGFP and the viral protein p24 (Fig 3.1G). Therefore, a clear distinction exists in this reporter model facilitating enrichment of the resultant HIV+ astrocyte populations.

Figure 3. 1 Astrocyte R/G-HIV-1 infection was predominantly silent/restricted.

*(A) Schematic representation of the R/G-HIV-1-WT/D116A constructs. (B) Time kinetics of R/G-HIV-1 LTR activity in astrocytes was quantified by flowcytometry. Graph is representative of the mean +/- SEM of three individual astrocyte donors in triplicate determination. PI indicates post-infection. Astrocytes were infected with R/G-HIV-1-WT, cultured for two weeks and analyzed by flow cytometry. Graph is representative of 30 individual astrocyte donors. Whiskers on the box plot indicate range of minimum to maximum (*** $p < 0.001$ when compared to R+/G- population). Astrocytes were infected with R/G-HIV-1-WT/D116A and sorted 14 days post-infection. (C) Plots show the gating strategy used for sorting uninfected R-/G-, D116A-infected R-/G-, and R/G-HIV-1-WT infected R+/G- and R+/G+ astrocytes. Graphs are representative of data from multiple donors. (D) R/G-HIV-1-WT-infected astrocytes were sorted to a purity of greater than 90%. Graphs show flow analysis of R/G-HIV-1-WT-infected astrocytes prior to sorting, and purity of individual cell populations R+/G- and R+/G+ post-sorting. Data shown are representative of two individual astrocyte donors. (E) Genomic DNA isolated from R/G-HIV-1-infected, sorted astrocytes and the 8e5 cell line, which harbors a single HIV-1 proviral genome per cell were analyzed to evaluate integrated R/G-HIV-1 by Alu-gag nested PCR. Data are representative of two individual astrocyte donors. R/G-HIV-1-WT-infected astrocytes were sorted seven days post infection and probed for HIV-1 viral protein p24. (F) Visually R+/G- astrocytes were p24 negative, and R+/G+ astrocytes were p24 positive (G). Fluorescent microscopy images (X 20) shown here are representative of three astrocyte donors.*

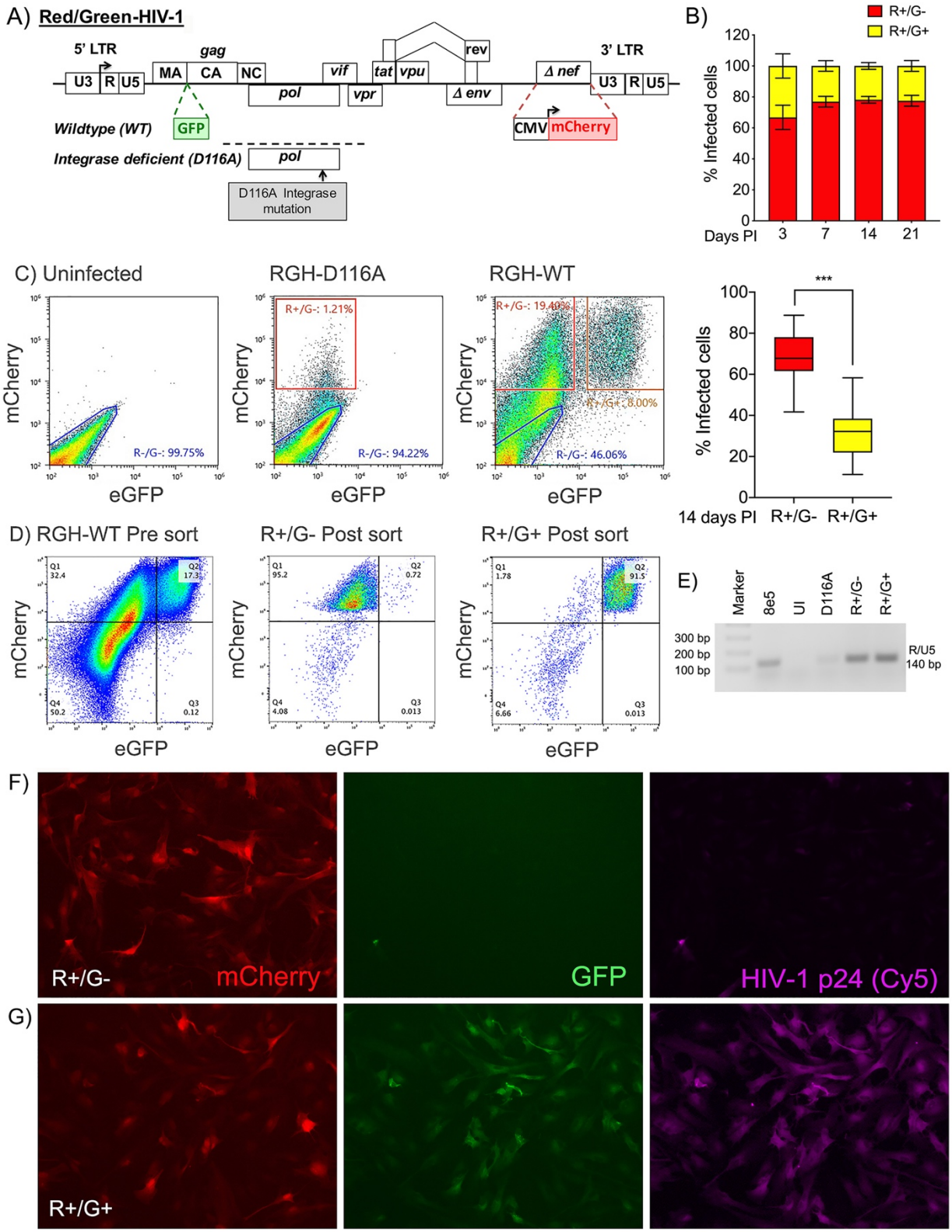
A) Red/Green-HIV-1
5' LTR
gag
rev
3' LTR
U3 R U5
MA CA NC
vif
tat vpu
Δ nef
U3 R U5
pol
vpr
Δ env
Wildtype (WT)
GFP
CMV mCherry
Integrase deficient (D116A)
pol
D116A Integrase mutation
B)
R+/G-
R+/G+
% Infected cells
Days PI
3
7
14
21
C) Uninfected
RGH-D116A
RGH-WT
mCherry
eGFP
R-/G-: 99.75%
R+/G-: 1.21%
R-/G-: 94.22%
R+/G-: 19.40%
R+/G+: 8.00%
R-/G-: 46.06%
***
% Infected cells
14 days PI
R+/G-
R+/G+
D) RGH-WT Pre sort
R+/G- Post sort
R+/G+ Post sort
Q1 32.4
Q2 17.3
Q4 50.2
Q3 0.12
Q1 95.2
Q2 0.72
Q4 4.08
Q3 0.013
Q1 1.78
Q2 91.5
Q4 6.66
Q3 0.013
E)
Marker
8e5
UI
D116A
R+/G-
R+/G+
300 bp
200 bp
100 bp
R/U5
140 bp
F)
R+/G-
mCherry
GFP
HIV-1 p24 (Cy5)
G)
R+/G+

3.2 R+/G- astrocytes resisted reactivation by vorinostat and IL-1β:

Since the majority of R/G-HIV-1-infected astrocytes reported silent LTRs, we wanted to determine if this population could be reactivated by HIV-relevant neuroinflammation or a classic LRA. HIV+ monocytes and microglia secrete the pro-inflammatory cytokine IL-1β, which upregulates several known HIV LTR activating factors including protein kinase C (PKC), activation protein 1 (AP1), NF-κB and nuclear factor of activated T-cells (NFAT) (109). Further, astrocytes have a sensitive IL-1β autocrine loop that induces a reactive phenotype (110). In this context, IL-1β was chosen as a prototypical activator and an endogenous LRA for these studies. The classic HDACi vorinostat was used as a pharmacological LRA. To determine if the HIV-1 LTR is susceptible to reactivation in human astrocytes, cells were infected with R/G-HIV-1. Two weeks post infection, unsorted HIV+ cultures were treated with either IL-1β (20 ng/ml) or vorinostat (1 μM) alone and in combination for 24 hours followed by flow cytometry analysis (Fig 3.2A, B, C, and D). Surprisingly, neither the percentage of red *vs* yellow cells, nor the mean MFI of GFP (data not shown) were not affected by vorinostat or IL-1β, when normalized to the untreated HIV+ population (Fig 3.2E). Interestingly, the total number of infected cells declined with IL-1β treatment alone and in combination with vorinostat; however, the changes were not significant.

As reactivation was not detected by fluorescent reporters of the R/G-HIV-1 construct, the effects of vorinostat or IL-1β on viral gene expression were also evaluated by measuring viral mRNA and protein expression. Two weeks post-infection HIV+ cultures were treated with LRAs as described above. While IL-1β did not alter Tat mRNA levels, vorinostat increased Tat mRNA by 75% (Fig 3.2F, *$p < 0.05$). Dual treatment induced significantly higher Tat mRNA expression than untreated HIV+ astrocytes (*$p < 0.05$) but did not have a synergistic effect compared to

vorinostat alone. To measure HIV-1 LTR reactivation by LRAs at translational level, late viral protein p24 expression was measured by ELISA in cell supernatants collected 24 hours post-LRA treatment. Here, vorinostat increased p24 expression by 50% (Fig 3.2G, *p <0.05), and IL-1β and vorinostat cotreatment synergistically increased p24 levels (***p <0.001). Since these measures were inconsistent with R/G-HIV model reporter results, we wanted to determine, which population whether the silent LTR (red) or active LTR (yellow), was driving the changes in viral protein expression.

R/G-HIV-1-infected astrocytes were sorted and treated with vorinostat and IL-1β for 24 hours as described above. HIV p24 levels in sorted red HIV+ astrocytes were minimal as compared to that of yellow HIV+ astrocytes, which were 15-fold higher (Fig 3.2H, **p <0.01). Moreover, red astrocytes were resistant to reactivation. Treatment with either IL-1β or vorinostat alone or in combination failed to increase p24 levels of red HIV+ astrocytes to the basal levels of untreated yellow cells. However, yellow HIV+ astrocytes were sensitive to vorinostat, and HIV p24 levels were significantly higher compared to untreated yellow astrocytes ($$ p <0.01, $$$ p <0.001). In this context, the changes in viral gene expression measured in unsorted HIV+ astrocytes were likely the result of activating yellow populations, rather than inducing red cells to take on a yellow phenotype. Thus, the viral gene expression measures match the R/G-HIV reporters.

Next, we wanted to determine if harboring HIV and reactivation affect a key anti-excitotoxicity function of astrocytes, glutamate clearance. Glutamate clearance was measured in D116A-infected R-/G-, WT-infected R+/G- and R+/G+ populations 24 hours post-LRA treatment (Fig 2I). Glutamate clearance capacity was significantly diminished in yellow astrocytes compared to the D116A infection control (^^ p <0.01) and WT-infected red populations (**p <0.01). IL-1β treatment significantly decreased glutamate clearance regardless of R/G-HIV-1 promoter activity,

while vorinostat showed no effect. Red HIV+ astrocytes appeared to be more sensitive to IL-1β-mediated decreases in glutamate clearance capacity (-50%) than yellow HIV+ astrocytes (-30%) compared to their respective untreated controls. This could be because their glutamate clearance abilities were already severely impaired by harboring the provirus as well as significant viral protein expression. Together these studies demonstrated that the majority of HIV+ astrocytes reported as harboring silent viral promoters were resistant to reactivation by vorinostat and/or IL-1β. However, astrocytes with active viral promoters were susceptible to activation by vorinostat. Finally, harboring active viral promoter also significantly reduced the glutamate clearance ability of these astrocytes, which was exacerbated by IL-1β treatment.

Figure 3. 2 Restrictively infected astrocytes were resistant to reactivation.

Human astrocytes were infected with R/G-HIV-1-WT in T-75 tissue culture flasks. Two weeks post-infection cells were treated with either IL-1β (20 ng/ml) or vorinostat (1 μM) alone or in combination for 24 hours. Cells were harvested, and fluorescence reporter activity was measured by flow analysis (A, B, C, D). Histograms are representative of seven donors. (E) Quantitative flow data were normalized to the total untreated R/G-HIV-1-WT population. (F) In parallel HIV-1, Tat levels were evaluated by real-time PCR. Graph is cumulative of three experiments in individual astrocyte donors. (G) Supernatants were collected 24 hours post-treatment and assayed for HIV-1 viral protein p24. Graph is cumulative of seven individual astrocyte donors ($p < 0.05$ and *** $p < 0.001$ when the treatments were compared to untreated control). (H) Red or yellow populations of astrocytes were sorted two weeks post infection, plated and allowed to recover for 24 hours. Cells were then treated as described above and assayed for HIV-1 viral protein p24. Data are representative of three individual astrocyte donors. (I) Glutamate (400 μM) was then added to the treated cells. Supernatants were collected 24 hours*

*after addition of glutamate, and clearance was measured. Graph shows normalized clearance levels in three separate astrocyte donors. Grey colored bars indicate D116A-infected R-/G- population, red and yellow colored bars indicate R+/G- and R+/G+ populations of astrocytes, respectively. Data represent mean ± SEM with triplicate determinations for each donor (*** $p < 0.001$ when the treatments were compared to untreated R+/G- population, ## $p < 0.01$, ### $p < 0.001$ when bars were compared to their respective treatments in R+/G- population, $$ $p < 0.01$, $$$ $p < 0.001$ when bars were compared to untreated R+/G+ population and ^^ $p < 0.01$, ^^^ $p < 0.001$ when bars were compared to D116A-infected R-/G- population).*

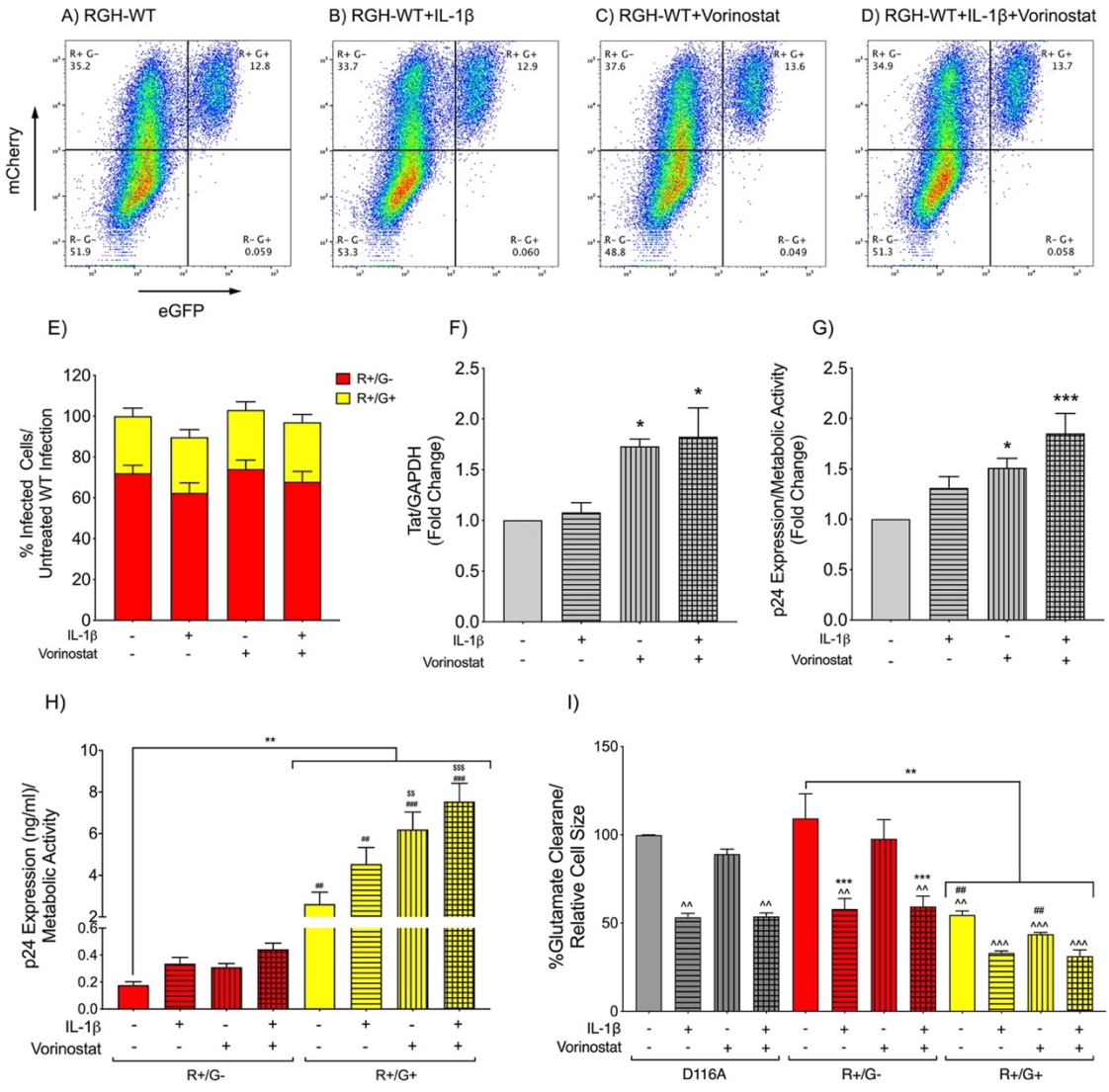

3.3 Gene expression profiles of astrocytes with silent and active R/G-HIV+ reporters:

Exposure to HIV-1 caused changes in gene expression in astrocytes that contribute to neuropathogenesis. In order to determine how harboring the provirus alters transcriptome, human astrocytes were infected with R/G-HIV-1-WT or the integrase deficient clone R/G-HIV-1-D116A. Two weeks post-infection, uninfected, D116A-infected R-/G-, WT-infected R+/G- (red), and R+/G+ (yellow) cells were sorted. RNA was isolated, and RNA-seq was performed. The transcriptome data of sorted populations from three independent experiments were visualized as minus-over-average (MA) plots (Fig 3.3A, B, and C). Comparisons between uninfected and the infection control (D116A) astrocytes showed no significant differences in their gene expression profiles. Thus, D116A-infected R-/G- astrocytes were used to calculate gene expression fold changes and subsequent comparisons. Both red and yellow HIV+ astrocyte gene expression profiles were significantly different from that of D116A-infected cells (Fig 3.3B and C, respectively). A heatmap (Fig 3.3D) of the top 100 differentially expressed genes from the D116A *vs* R+/G+ comparison highlighted the similarities between D116A-infected cells and uninfected astrocytes, and between red and yellow HIV+ across three donor astrocyte cultures.

Along with the human transcriptome, HIV-associated genes were also mapped to the R/G-HIV-1 reference genome and relative counts of HIV-1 transcripts expression among red and yellow cells from the three astrocyte donors were plot as a heatmap (Fig 3.3E). The transcription of HIV-associated genes was silent or significantly restricted in the R+/G- population compared to the R+/G+ population, but not completely silenced. Normalized levels of most HIV-associated transcripts were repressed by approximately 90% in R+/G- astrocytes as compared to R+/G+ astrocytes and were not statistically different than D116A-infected controls. We were unable to ascertain what proportion of R+/G- cells had silenced LTR versus restricted LTR activity.

Expression of the R/G-HIV 5' and 3' UTR/LTRs was undetectable in both the red and yellow astrocyte transcriptomes, suggesting that neither population was expressing full length HIV RNA for virion generation.

Differentially expressed genes that were at least two-fold up or down with a false discovery rate (modified p value) of ≤ 0.05 were used to plot Venn diagrams for comparisons between D116A and red (R+/G-) or yellow (R+/G+) populations (Fig 3.3F and G). Among a total of 163 upregulated genes, only six were unique to the red (R+/G-) population (Fig 3.3H), while 101 were unique to the yellow (R+/G+) population, and 56 were common to both. Among 520 downregulated genes, one was unique to the red population (Fig 3.3H); 333 were unique to the yellow population, and 186 were common to both. Thus, gene expression profile of the red population was mostly encompassed within that of yellow population. IPA's core analysis was used to analyze the gene expression data. Comparison analysis of canonical pathways (Fig 3.3I) altered in both red and yellow populations indicated enrichment of typical antiviral responses such as interferon signaling, death receptor signaling, and activation of interferon regulatory factor (IRF) by cytosolic pattern recognition receptors. However, yellow cells showed additional enrichment of canonical pathways including inducible nitric oxide synthase (iNOS) signaling, role of pattern recognition receptors in recognition of bacteria and viruses, role of retinoic acid-inducible gene-1 (RIG1) like receptors in antiviral innate immunity, interleukin-1 (IL-1) signaling, macrophage migration inhibitory factor (MIF) regulation of innate immunity, TNF receptor-2 signaling, and induction of apoptosis by HIV-1. Downregulation of canonical pathways was also similar across HIV+ astrocyte populations including cell cycle regulation, chromosomal replication, and DNA damage responses. The similarities between disease and biological functions of red and yellow populations were profound and included upregulation of antimicrobial response,

antiviral response, apoptosis and necrosis, and downregulation of biological functions such as cell survival, cell viability, viral infection, replication of viruses, replication of RNA virus, and replication of viral replicon (Fig 3J). Together these data indicated that simply harboring the HIV provirus induces an infected phenotype, regardless of R/G-HIV-1 LTR activity, which could have profound implications on astrocyte function and associated neurotoxicity.

Interferon signaling (Fig 3.4A) was the most upregulated canonical pathway in both populations. IFN-β1, IRF1, and 9, interferon-induced transmembrane protein (IFITM) 1, and 3, 2'- 5'- oligoadenylate synthetase 1 (OAS1), and STAT1 were the key upregulated proteins among this pathway. IPA's MAP tool predicted the activation of antiviral response and inhibition of replication of RNA virus mechanisms up on activation of interferon signaling pathway (Fig 3.4B). The upregulation of interferon signaling in both populations was also confirmed by measuring the mRNA levels of key transcription factor STAT1 in both population by real-time PCR (Fig 3.4C). Data show a near three-fold increase in the mRNA levels of STAT1 in both red and yellow astrocytes (* $p \leq 0.05$).

Figure 3. 3 Differential gene expression of R/G-HIV-1-infected astrocytes.

RNA sequencing data were analyzed by edgeR program. MA plots for (A) uninfected vs D116A, (B) D116A vs R+/G-, and (C) D116A vs R+/G+. (D) The top 100 differentially expressed genes among all four populations were presented as a heat map (blue color indicates downregulation, and red color indicates upregulation) in three astrocyte donors D1, D2 and D3. (E) Quality trimmed and TMM normalized RNA sequencing reads were mapped to the R/G-HIV-1 reference sequence. A heat map shows relative expression of HIV transcripts across the same populations and astrocyte donors. (F) Upregulated and (G) downregulated genes compared to D116A among R+/G- and R+/G+ populations were plotted as Venn diagrams where red: genes unique to R+/G-

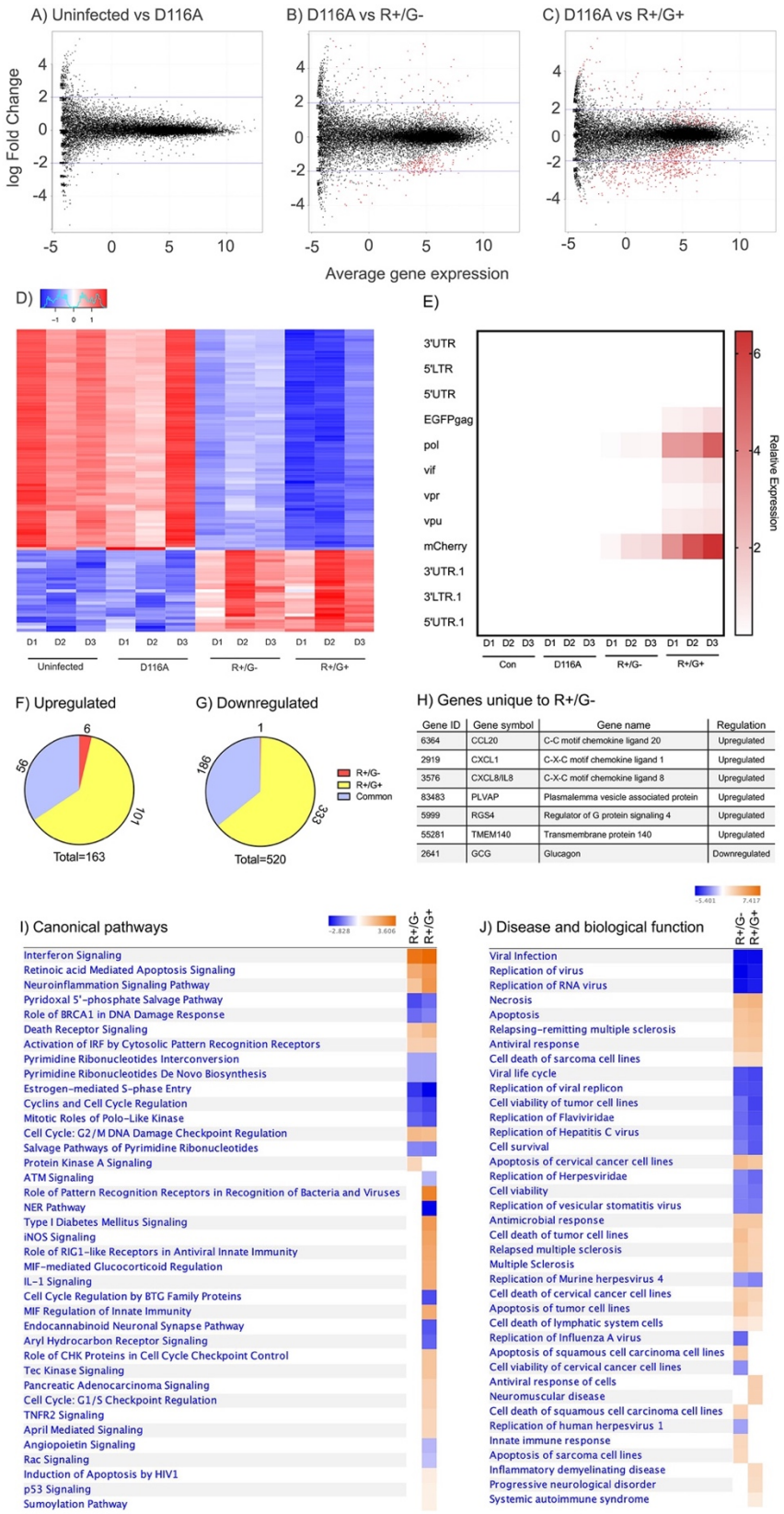

, yellow: genes unique to R+/G+, and blue: genes common to both populations. (H) Differentially expressed genes unique to R+/G- astrocytes. Expression ratios were analyzed using IPA core analysis tool. Further, comparison analyses show heat maps depicting changes in Z-scores for selected (I) canonical pathways, and (J) disease and biological function. Blue and orange represent negative and positive Z-scores, respectively, indicating that the biological process was respectively increased or decreased based on the transcripts from each category.

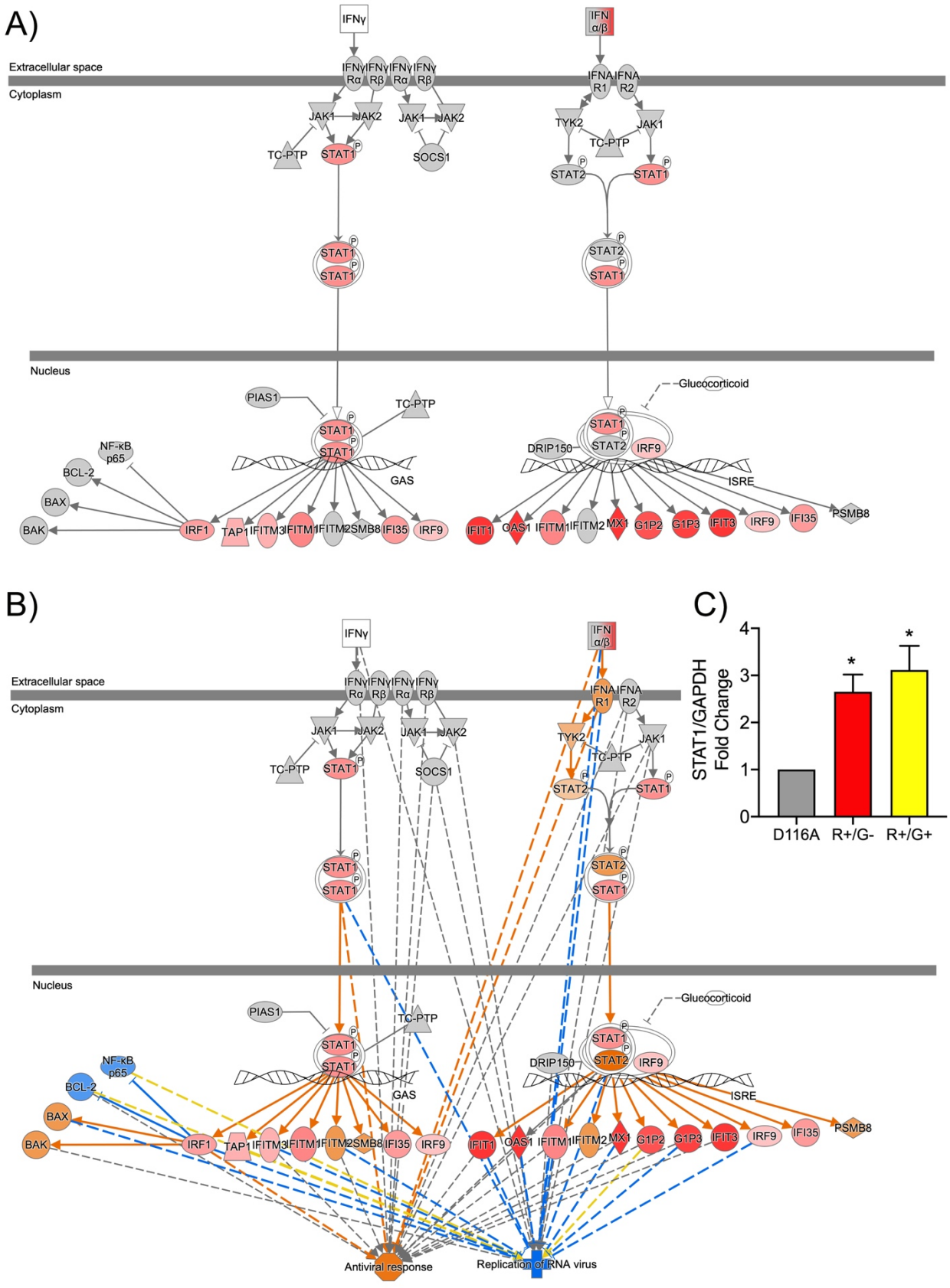
A)
IFNγ
IFN α/β
Extracellular space
Cytoplasm
IFNγ Rα
IFNγ Rβ
IFNγ Rα
IFNγ Rβ
IFNA R1
IFNA R2
JAK1
JAK2
JAK1
JAK2
TYK2
JAK1
TC-PTP
STAT1
SOCS1
TC-PTP
STAT2
STAT1
STAT1
STAT1
STAT2
STAT1
Nucleus
PIAS1
TC-PTP
Glucocorticoid
STAT1
STAT1
STAT1
STAT1
STAT2
IRF9
DRIP150
NF-κB p65
BCL-2
GAS
ISRE
BAX
BAK
IRF1
TAP1
IFITM3
IFITM1
IFITM2
SMB8
IFI35
IRF9
IFIT1
OAS1
IFITM1
IFITM2
MX1
G1P2
G1P3
IFIT3
IRF9
IFI35
PSMB8
B)
IFNγ
IFN α/β
Extracellular space
Cytoplasm
IFNγ Rα
IFNγ Rβ
IFNγ Rα
IFNγ Rβ
IFNA R1
IFNA R2
JAK1
JAK2
JAK1
JAK2
TYK2
JAK1
TC-PTP
STAT1
SOCS1
TC-PTP
STAT2
STAT1
STAT1
STAT1
STAT2
STAT1
Nucleus
PIAS1
TC-PTP
Glucocorticoid
STAT1
STAT1
STAT1
STAT1
STAT2
IRF9
DRIP150
NF-κB p65
BCL-2
GAS
ISRE
BAX
BAK
IRF1
TAP1
IFITM3
IFITM1
IFITM2
SMB8
IFI35
IRF9
IFIT1
OAS1
IFITM1
IFITM2
MX1
G1P2
G1P3
IFIT3
IRF9
IFI35
PSMB8
Antiviral response
Replication of RNA virus
C)
STAT1/GAPDH Fold Change
0
1
2
3
4
*
*
D116A
R+/G-
R+/G+

Figure 3. 4 Upregulation of interferon signaling pathways.

(A) Pathway image from IPA core analysis illustrating gene expression associated with interferon signaling. (B) Molecular activity prediction (MAP) tool indicates the potential outcomes of activating the interferon signaling. The color intensity indicates the degree of upregulation (red). Predicted activation (orange), inhibition (blue), and unknown association (yellow) were also shown. Grey color indicates molecules that were present in the dataset but did not pass the cut off values of false discovery rate ≤ 0.05 (FDR) and Log_2 fold change (FC) either ≥ 1 or ≤ -1. (C) Individual populations (red and yellow) were sorted, and STAT1 gene expression was measured by real-time PCR two weeks post infection. Data display mean fold changes with +/- standard error of mean (SEM) compared to D116A-infected cells. Data are cumulative of three individual astrocyte donors. Statistical analyses were performed using one-way ANOVA with Tukey's post hoc-test for multiple comparisons ($p < 0.05$).*

3.4 Both active and restricted R/G-HIV-1 infection upregulated neuroinflammatory signaling pathways in astrocytes:

Neuroinflammatory signaling (Fig 3.5A) was one of the most upregulated pathways among both red and yellow populations. HIV-1 infection is known to induce secretion of inflammatory cytokines by astrocytes. Our gene expression data also demonstrated the upregulation of different cytokines by R/G-HIV-1-infected astrocytes. Along with the cytokines, transmembrane receptors, kinases, and transcriptional regulators were also present among the genes with increased abundance (Table 3.1). CCL5, CXCL10, IL-6, and IFN-β1 were key upregulated cytokines in both populations. Transmembrane receptors included Fas cell surface death receptor (FAS), major histocompatibility complex class 1, B and C (HLA-B, and C), intracellular adhesion molecule 1

(ICAM1), and TLR3. IRF7, NFATC2, NF-κB1-2 and STAT1 were among the upstream regulators or transcription regulators known to potentially drive the expression of inflammatory cytokines. The IPA MAP function predicted these cytokines would recruit T-cells and activate microglia. Even though all these transcripts were upregulated in both populations, the fold changes in astrocytes with active viral promoters (yellow cells) were higher compared to those of astrocytes with silent/restricted viral promoters (red cells).

In order to verify the sequencing studies, we did confirmation studies by measuring mRNA levels of ICAM1 (Fig 3.5B) and CCL2 (Fig 3.5C) by real-time PCR in sorted populations. ICAM1 and CCL2 mRNA levels were significantly elevated in both red and yellow astrocytes (*** $p \leq 0.001$). Culture supernatants from these populations were also assayed to quantify CCL5 by ELISA (Fig 3.5D). Data indicate that red HIV+ astrocytes had comparable CCL5 levels to D116A control cells, and yellow astrocytes expressed significantly higher CCL5 levels compared to other populations (* $p \leq 0.05$). From these observations it is evident that harboring R/G-HIV-1 provirus activated neuroinflammatory signaling pathways in human astrocytes, and these pathways were more prominent in populations with active HIV LTRs.

Figure 3. 5 Molecular activity prediction (MAP) tool indicates neuroinflammatory outcomes.

(A) Pathway image from IPA core analysis illustrating genes associated with neuroinflammatory signaling. MAP tool indicates the potential outcomes of neuroinflammatory cytokines being upregulated. The color intensity indicates the degree of upregulation (red) or downregulation (green) within the pathway and predicted activation (orange) or inhibition (blue) is also shown. Grey color indicates molecules that were present in the dataset but did not pass the cut off values of FDR ≤0.05, and Log_2FC of either ≥1 or ≤-1 for significantly changed transcripts. Human astrocytes were infected with R/G-HIV-1-WT/D116A; individual populations (red and

yellow) were sorted. Gene expression of ICAM1 (B) and CCL2 (C) were measured by real-time PCR 14 days post-infection. (D) In parallel, culture supernatants were assayed for CCL5 by ELISA and normalized to MTT activity. Data are representative of three individual astrocyte donors. Statistical analyses were performed using one-way ANOVA with Tukey's post hoc-test for multiple comparisons ($p < 0.05$, *** $p < 0.001$ when the samples were compared to D116A control).*

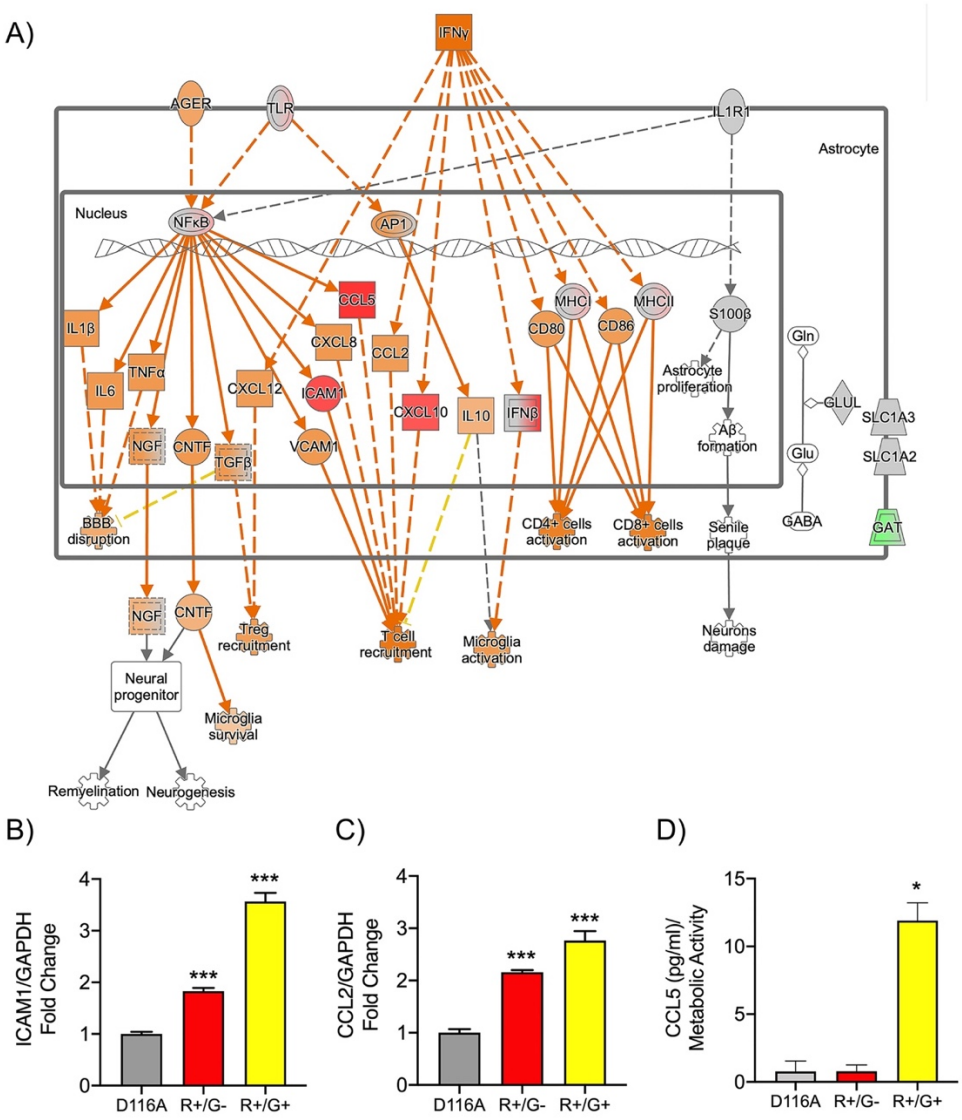

3.5 R/G-HIV-1 infection reduced DNA replication and cell proliferation in human astrocytes:

Several genes involved in cell cycle regulation were downregulated in both populations (Fig 3.6A). Common key regulators of S, G2, and M phases of cell cycle, including the kinases, cyclin dependent kinase1 (CDK1), cyclin (CCN) A2, CCNB1, B2, CCNE2 and transcriptional regulators, such as E2F transcription factor (E2F) 1, 2, and 8, were decreased with R/G-HIV-1 infection, which predicted cell cycle arrest during S-phase. Simultaneously comparison analysis of differentially expressed genes from red and yellow HIV+ astrocytes indicated downregulation of cell cycle control of chromosomal replication pathway (Fig 3.6B). Fold changes of the downregulated genes were higher among yellow astrocytes compared to those of red. Commonly downregulated transcripts included various key kinases and enzymes (Table 3.2) that regulate chromosomal replication such as DNA topoisomerase II alpha (TOP 2A), DNA primase subunit 1 (PRIM1), different subunits of DNA polymerase [(alpha, delta, and epsilon) (POLA1, 2, POLD1, POLE)], mini-chromosome maintenance complex component (MCM) 2, 4, 5, 6, 7, and 8, cell division cycle (CDC) 6, 7, and 45, and CDK1, which together would inhibit DNA replication.

Corroborating with sequencing data and MAP predictions, cell proliferation in R/G-HIV-1-infected astrocytes was significantly reduced compared to that of D116A controls when measured by BrdU incorporation assay (Fig 3.6C). Yellow astrocytes were most affected with a 70% reduction in cell proliferation. Reactivation with vorinostat also decreased cell proliferation of human astrocytes irrespective of the population; however, this effect was more evident in astrocytes harboring HIV-1 compared to D116A control cells. IL-1β activation did not alter proliferation rates significantly in either populations compared to their respective controls. Overall

the data suggest that HIV-1 infection broadly suppressed genes involved in cell cycle regulation, which affected functional outcomes.

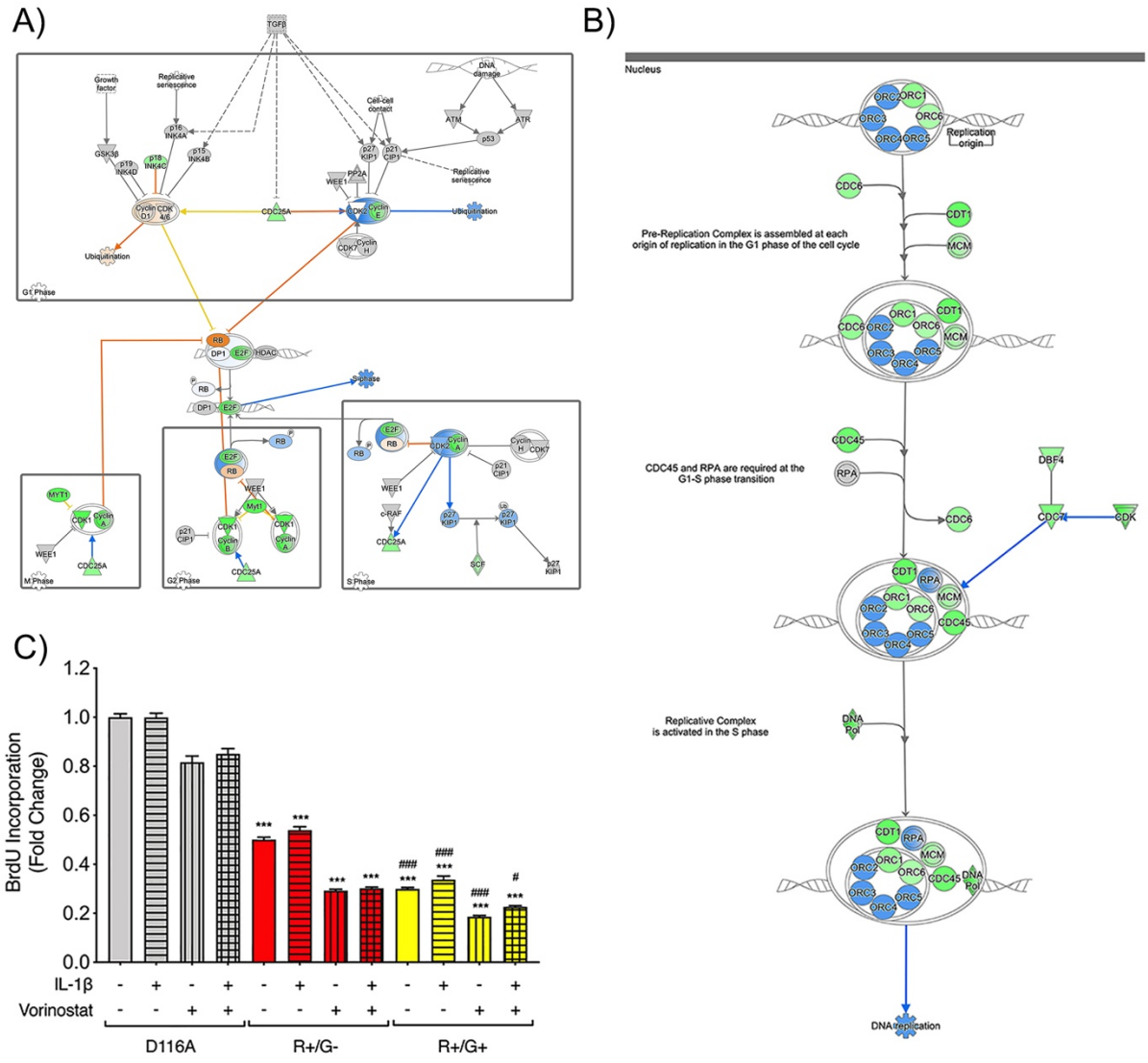

Figure 3. 6 R/G-HIV-1 infection inhibited astrocyte proliferation.

(A) Pathway images from IPA core analysis illustrating genes associated with cell cycle regulation phases in the R+/G+ population. (B) Pathway image from IPA core analysis illustrating genes associated with cell cycle control of chromosomal replication. The color intensity indicates the degree of upregulation (red) or downregulation (green) within the pathway, correspondingly predicted activation (orange) or inhibition (blue) is also shown. Grey color indicates molecules

that were present in the dataset but did not pass the cut off values of FDR ≤ 0.05 and Log_2FC of either ≥ 1 or ≤ -1. (C) Individual populations of astrocytes were sorted two weeks post infection, plated and allowed to recover overnight. Cells were then treated with either IL-1β (20 ng/ml) or vorinostat (1 μM) alone or in combination for 24 hours. BrdU was added 12 hours post-treatment, and incorporation was measured at 24 hours by BrdU incorporation assay. Graph is representative of three individual astrocyte donors. Statistical analyses were performed using two-way ANOVA with Tukey's post hoc-test for multiple comparisons ($p < 0.05$, ** $p < 0.01$, *** $p < 0.001$ when the treatments were compared to respective treatments in D116A control, and $^{\#} p < 0.05$, $^{\#\#} p < 0.01$, $^{\#\#\#} p < 0.001$ when bars were compared to their respective treatments in R+/G- population).*

3.6 Extracellular targetable biomarkers specific for latent/restricted *vs* actively infected astrocytes were not identified:

In an attempt to identify astrocyte specific biomarkers of HIV infection, a list of differentially upregulated genes predicted to be located on the plasma membrane was compiled. These transcripts included ion channels, enzymes and transmembrane receptors (Tables 3.3 and 3.4). While several cell surface transcripts were significantly upregulated during R/G-HIV-1 infection, no astrocyte specific cell surface markers were identified among R+/G- and R+/G+ populations. Biomarker analysis also indicated overlap between both populations of R/G-HIV+ astrocytes. Seven of eight cell surface transcripts upregulated in R+/G- astrocytes were also present in R+/G+ cells. These included bone marrow stromal cell antigen 2 (BST2), IFITM1-3, ICAM1, lymphocyte antigen 6 family membrane E (LY6E), phospholipid scramblase 1 (PLSCR1), and HLA-C (Table 3.3 and 3.4). However, these proteins are expressed by various cell types

throughout the brain and body and thus are unlikely to serve as targetable biomarkers for elimination of HIV+ astrocytes or therapeutic intervention to regulate their function.

3.7 R/G-HIV-1-infected astrocyte transcriptomes were phenotypically comparable to brain gene expression array data from neurocognitively impaired (NCI) HIV-1-infected individuals:

Using analysis match feature of IPA, the gene expression signatures of R/G-HIV-1-infected astrocytes with transcriptome data were matched with National NeuroAIDS Tissue Consortium (NNTC) brain gene expression array data (111, 112). The NNTC datasets were collected from various regions (corpus callosum, white matter, neocortex, and neostriatum) of HIV-1-infected individuals classified post-mortem into three different subject categories: HIV-1-infected individuals without substantial NCI, HIV-1-infected subjects with substantial NCI without HIV encephalitis (HIVE), and HIV-1-infected subjects with substantial NCI and HIVE. This analysis indicated broad similarities between our R/G-HIV-1-infected astrocyte transcriptomes and *ex vivo* brain gene expression array data. Although there were fewer similarities between the HIV+ astrocytes and subjects without substantial NCI's gene expression patterns, striking similarities were observed with the other two categories. The comparisons were made based on the altered canonical pathways and upstream regulators. Similar canonical pathways included, interferon signaling, neuroinflammatory signaling, role of pattern recognition receptors in recognition of bacteria and viruses, IL-1 signaling, iNOS signaling, type1 diabetes mellitus signaling, and retinoic acid-mediated apoptosis signaling (Fig 3.7A). Most of the similarities were seen in upregulated canonical pathways; however, comparisons between upstream regulators included both upregulated and downregulated transcripts. Key upstream regulators of pathways

involved innate immune responses, antiviral responses, inflammatory pathways, cell cycle regulation, protein kinase A signaling, and neuronal synapse pathways (Fig 3.7B). Overall this comparison analysis suggested that there were great phenotypic similarities between the transcriptome data from pure *in vitro* red and yellow HIV+ astrocyte cultures and *in vivo* samples from multiple brain regions.

Figure 3. 7 Gene expression patterns of R/G-HIV-1-infected astrocytes matched with HIV+ ex vivo brain gene expression array datasets.

IPA's analysis match illustrating comparisons of (A) canonical pathways, and (B) upstream regulators of R/G-HIV-1-infected astrocyte dataset to other HIV-1 CNS infection datasets in the IPA knowledge base. Blue and orange represent negative and positive Z-scores, respectively, indicating that the biological process or the upstream regulator is increased or decreased based on the transcripts from each category. Data set descriptions: NCI and HIVE; HIV-1-infected individuals with substantial neurocognitive impairment and HIV encephalopathy, NCI and no HIVE; HIV-1-infected individuals with substantial NCI and without HIVE, HIV+ and no NCI; HIV-1 infected individuals with no substantial NCI. CC- corpus callosum, WM- white matter, NS- neostriatum, and FC- frontal cortex are different locations of brain samples (111, 112).

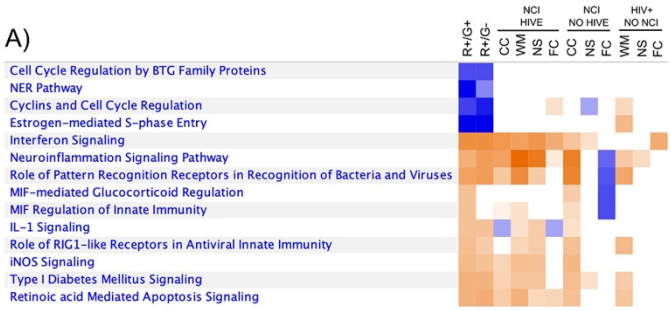
A)
R+/G+
R+/G-
NCI HIVE
NCI NO HIVE
HIV+ NO NCI
CC
WM
NS
FC
Cell Cycle Regulation by BTG Family Proteins
NER Pathway
Cyclins and Cell Cycle Regulation
Estrogen-mediated S-phase Entry
Interferon Signaling
Neuroinflammation Signaling Pathway
Role of Pattern Recognition Receptors in Recognition of Bacteria and Viruses
MIF-mediated Glucocorticoid Regulation
MIF Regulation of Innate Immunity
IL-1 Signaling
Role of RIG1-like Receptors in Antiviral Innate Immunity
iNOS Signaling
Type I Diabetes Mellitus Signaling
Retinoic acid Mediated Apoptosis Signaling

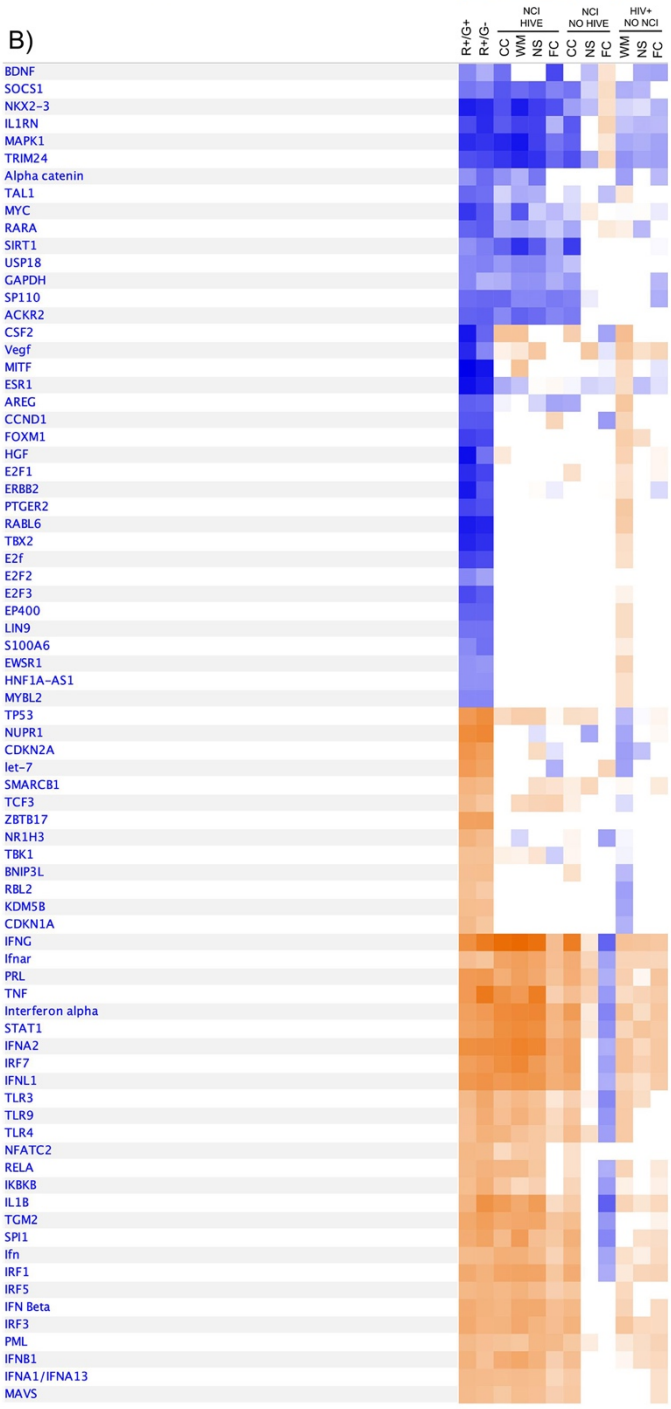
B)
R+/G+
R+/G-
NCI HIVE
NCI NO HIVE
HIV+ NO NCI
CC
WM
NS
FC
BDNF
SOCS1
NKX2-3
IL1RN
MAPK1
TRIM24
Alpha catenin
TAL1
MYC
RARA
SIRT1
USP18
GAPDH
SP110
ACKR2
CSF2
Vegf
MITF
ESR1
AREG
CCND1
FOXM1
HGF
E2F1
ERBB2
PTGER2
RABL6
TBX2
E2f
E2F2
E2F3
EP400
LIN9
S100A6
EWSR1
HNF1A-AS1
MYBL2
TP53
NUPR1
CDKN2A
let-7
SMARCB1
TCF3
ZBTB17
NR1H3
TBK1
BNIP3L
RBL2
KDM5B
CDKN1A
IFNG
Ifnar
PRL
TNF
Interferon alpha
STAT1
IFNA2
IRF7
IFNL1
TLR3
TLR9
TLR4
NFATC2
RELA
IKBKB
IL1B
TGM2
SPI1
Ifn
IRF1
IRF5
IFN Beta
IRF3
PML
IFNB1
IFNA1/IFNA13
MAVS

Table 3. 1 Genes altered in neuroinflammation signaling pathway.

		R+/G-			R+/G+					
Symbol	**Entrez Gene Name**	**Expr Log Ratio**	**Expr p-value**	**Expr False Discovery Rate (q-value)**	**Expr Log Ratio**	**Expr p-value**	**Expr False Discovery Rate (q-value)**	**Location**	**Type(s)**	**Entrez Gene ID for Human**
BIRC3	baculoviral IAP repeat containing 3	1.422	0.000306	0.0297	2.257	2.31E-08	3.64E-06	Cytoplasm	enzyme	330
BIRC5	baculoviral IAP repeat containing 5	-1.883	2.4E-06	0.000633	-2.892	3.34E-12	1.41E-09	Cytoplasm	other	332
CALB2	calbindin 2	0.071	0.912	1	-2.43	0.000455	0.0174	Cytoplasm	other	794
CCL5	C-C motif chemokine ligand 5	2.937	1.19E-05	0.00237	4.823	1.4E-11	4.85E-09	Extracellular Space	cytokine	6352
CXCL10	C-X-C motif chemokine ligand 10	2.171	0.00527	0.257	3.18	8.07E-05	0.00419	Extracellular Space	cytokine	3627
FAS	Fas cell surface death receptor	0.528	0.0614	0.967	1.023	0.000317	0.0129	Plasma Membrane	transmembrane receptor	355
GAD2	glutamate decarboxylase 2	-0.796	0.256	1	-2.748	0.000231	0.0101	Cytoplasm	enzyme	2572
HLA-B	major histocompatibility complex, class I, B	1.244	0.00156	0.104	1.443	0.000259	0.011	Plasma Membrane	transmembrane receptor	3106
HLA-C	major histocompatibility complex, class I, C	1.133	0.000342	0.0319	1.332	2.77E-05	0.00171	Plasma Membrane	other	3107
HMOX1	heme oxygenase 1	1.113	0.00566	0.272	1.864	5.55E-06	0.000432	Cytoplasm	enzyme	3162
ICAM1	intercellular adhesion molecule 1	2.046	9.53E-09	1.06E-05	3.327	7.65E-19	5.39E-15	Plasma Membrane	transmembrane receptor	3383
IFNB1	interferon beta 1	3.601	0.0269	0.693	6.895	1.34E-06	0.000131	Extracellular Space	cytokine	3456
IRAK2	interleukin 1 receptor associated kinase 2	1.381	0.00147	0.099	1.659	0.00015	0.0071	Plasma Membrane	kinase	3656
IRF7	interferon regulatory factor 7	1.291	0.00653	0.3	1.649	0.000577	0.0213	Nucleus	transcription regulator	3665
MAPK15	mitogen-activated protein kinase 15	-1.307	0.0446	0.864	-2.192	0.00119	0.0375	Cytoplasm	kinase	225689
MMP9	matrix metallopeptidase 9	1.506	0.0148	0.505	2.137	0.000575	0.0213	Extracellular Space	peptidase	4318
NFATC2	nuclear factor of activated T cells 2	4.857	0.000342	0.0319	4.792	0.000393	0.0155	Nucleus	transcription regulator	4773
NFKB1	nuclear factor kappa B subunit 1	1.366	0.00399	0.211	1.68	0.00045	0.0173	Nucleus	transcription regulator	4790
NFKB2	nuclear factor kappa B subunit 2	0.948	0.00615	0.288	1.309	0.000174	0.00794	Nucleus	transcription regulator	4791
PLA2G4C	phospholipase A2 group IVC	0.884	0.0654	0.982	1.624	0.000845	0.0291	Plasma Membrane	enzyme	8605
SLC6A1	solute carrier family 6 member 1	-0.937	0.141	1	-2.106	0.00136	0.0414	Plasma Membrane	transporter	6529

STAT1	signal transducer and activator of transcription 1	1.905	4.66E-06	0.00105	2.099	5.34E-07	5.97E-05	Nucleus	transcriptio n regulator	6772
TLR3	toll like receptor 3	0.987	0.00955	0.385	1.506	9.08E-05	0.00454	Plasma Membrane	transmembr ane receptor	7098

Table 3. 2 Genes altered in cell cycle control of chromosomal replication pathway.

		R+/G-			R+/G+					
Symbol	**Entrez Gene Name**	**Expr Log Ratio**	**Expr p-value**	**Expr False Discovery Rate (q-value)**	**Expr Log Ratio**	**Expr p-value**	**Expr False Discovery Rate (q-value)**	**Location**	**Type(s)**	**Entrez Gene ID for Human**
CDC45	cell division cycle 45	-1.516	0.000422	0.0382	-2.336	1.39E-07	1.79E-05	Nucleus	other	8318
CDC6	cell division cycle 6	-1.22	0.00278	0.159	-1.719	3.31E-05	0.00198	Nucleus	other	990
CDC7	cell division cycle 7	-1.685	0.000016	0.00304	-2.02	3.25E-07	3.84E-05	Nucleus	kinase	8317
CDK1	cyclin dependent kinase 1	-1.75	2.93E-09	5.59E-06	-2.803	6.71E-20	1.42E-15	Nucleus	kinase	983
CDT1	chromatin licensing and DNA replication factor 1	-1.508	0.00177	0.114	-2.508	5.53E-07	6.11E-05	Nucleus	other	81620
DBF4	DBF4 zinc finger	-1.432	0.000226	0.0238	-1.635	2.86E-05	0.00175	Nucleus	kinase	10926
DNA2	DNA replication helicase/nuclease 2	-1.182	0.000714	0.0571	-1.593	6.65E-06	0.000502	Cytoplasm	enzyme	1763
MCM2	minichromosome maintenance complex component 2	-1.108	0.000533	0.0455	-1.575	1.14E-06	0.000115	Nucleus	enzyme	4171
MCM4	minichromosome maintenance complex component 4	-1.045	0.000326	0.0311	-1.395	1.98E-06	0.00018	Nucleus	enzyme	4173
MCM5	minichromosome maintenance complex component 5	-1.034	0.000435	0.0386	-1.379	3.32E-06	0.00028	Nucleus	enzyme	4174
MCM6	minichromosome maintenance complex component 6	-1.047	0.00014	0.0168	-1.186	0.000017	0.00113	Nucleus	enzyme	4175
MCM7	minichromosome maintenance complex component 7	-0.861	0.00354	0.193	-1.106	0.000194	0.00869	Nucleus	enzyme	4176
MCM8	minichromosome maintenance 8 homologous recombination repair factor	-1.009	0.00244	0.145	-1.332	7.29E-05	0.00385	Nucleus	enzyme	84515
ORC1	origin recognition complex subunit 1	-1.316	0.00561	0.27	-1.776	0.00023	0.0101	Nucleus	other	4998
ORC6	origin recognition complex subunit 6	-1.045	0.00451	0.23	-1.348	0.000281	0.0118	Nucleus	other	23594

POLA1	DNA polymerase alpha 1, catalytic subunit	-0.743	0.0118	0.437	-1.081	0.000276	0.0116	Nucleus	enzyme	5422
POLA2	DNA polymerase alpha 2, accessory subunit	-0.969	0.00653	0.3	-1.187	0.00092	0.0311	Nucleus	enzyme	23649
POLD1	DNA polymerase delta 1, catalytic subunit	-0.833	0.00715	0.32	-1.026	0.000968	0.0325	Nucleus	enzyme	5424
POLE	DNA polymerase epsilon, catalytic subunit	-0.997	0.000616	0.0514	-1.295	1.01E-05	0.000738	Nucleus	enzyme	5426
PRIM1	DNA primase subunit 1	-1.555	0.000661	0.0535	-1.968	2.19E-05	0.00141	Nucleus	enzyme	5557
TOP2A	DNA topoisomerase II alpha	-2.111	9.5E-09	1.06E-05	-3.07	9.87E-16	1.97E-12	Nucleus	enzyme	7153

Table 3. 3 Biomarker candidates of R+/G- astrocytes altered on cell surface.

Symbol	Entrez Gene Name	Location	Family	Expr Log Ratio	Expr p-value	Expr False Discovery Rate (q-value)
PLVAP	plasmalemma vesicle associated protein	Plasma Membrane	other	4.095	0.0000286	0.00468
BST2	bone marrow stromal cell antigen 2	Plasma Membrane	other	3.146	1.51E-13	8.51E-10
IFITM1	interferon induced transmembrane protein 1	Plasma Membrane	transmembrane receptor	2.127	9.97E-08	0.0000676
ICAM1	intercellular adhesion molecule 1	Plasma Membrane	transmembrane receptor	2.046	9.53E-09	0.0000106
LY6E	lymphocyte antigen 6 family member E	Plasma Membrane	other	1.637	0.00000311	0.000763
IFITM3	interferon induced transmembrane protein 3	Plasma Membrane	other	1.413	3.75E-07	0.000183
PLSCR1	phospholipid scramblase 1	Plasma Membrane	enzyme	1.353	0.000337	0.0319
HLA-C	major histocompatibility complex, class I, C	Plasma Membrane	other	1.133	0.000342	0.0319

Table 3. 4 Biomarker candidates of R+/G+ astrocytes altered on cell surface.

Symbol	Entrez Gene Name	Location	Family	Expr Log Ratio	Expr p-value	Expr False Discovery Rate (q-value)
P2RX2	purinergic receptor P2X 2	Plasma Membrane	ion channel	5.892	0.000304	0.0125

P2RY12	purinergic receptor P2Y12	Plasma Membrane	G-protein coupled receptor	5.725	0.0000576	0.00317
HTR2B	5-hydroxytryptamine receptor 2B	Plasma Membrane	G-protein coupled receptor	5.665	1.93E-08	0.00000314
CFTR	cystic fibrosis transmembrane conductance regulator	Plasma Membrane	ion channel	5.395	0.000189	0.0085
DSG1	desmoglein 1	Plasma Membrane	other	4.954	0.000599	0.0219
PTPRC	protein tyrosine phosphatase, receptor type C	Plasma Membrane	phosphatase	4.796	0.0000114	0.000805
CDH19	cadherin 19	Plasma Membrane	other	4.557	0.0000545	0.00301
ICAM4	intercellular adhesion molecule 4 (Landsteiner-Wiener blood group)	Plasma Membrane	other	4.062	1.24E-07	0.0000161
ANO9	anoctamin 9	Plasma Membrane	ion channel	3.515	0.000197	0.00876
ICAM1	intercellular adhesion molecule 1	Plasma Membrane	transmembrane receptor	3.327	7.65E-19	5.39E-15
PCDH15	protocadherin related 15	Plasma Membrane	other	2.999	0.000247	0.0106
RTP4	receptor transporter protein 4	Plasma Membrane	other	2.931	0.000287	0.012
SELE	selectin E	Plasma Membrane	transmembrane receptor	2.565	0.000929	0.0314
BST2	bone marrow stromal cell antigen 2	Plasma Membrane	other	2.545	9.08E-10	0.000000184
LAMP3	lysosomal associated membrane protein 3	Plasma Membrane	other	2.527	0.000106	0.00523
CDH18	cadherin 18	Plasma Membrane	other	2.3	0.00149	0.0443
IFITM1	interferon induced transmembrane protein 1	Plasma Membrane	transmembrane receptor	2.278	1.41E-08	0.00000232
ICOSLG	inducible T cell costimulator ligand	Plasma Membrane	other	2.058	0.000327	0.0132
ICAM5	intercellular adhesion molecule 5	Plasma Membrane	other	2.021	0.000151	0.0071
LY6E	lymphocyte antigen 6 family member E	Plasma Membrane	other	1.993	1.96E-08	0.00000316

TNFRSF9	TNF receptor superfamily member 9	Plasma Membrane	transmembrane receptor	1.943	0.00156	0.046
IRAK2	interleukin 1 receptor associated kinase 2	Plasma Membrane	kinase	1.659	0.00015	0.0071
PLA2G4C	phospholipase A2 group IVC	Plasma Membrane	enzyme	1.624	0.000845	0.0291
MGLL	monoglyceride lipase	Plasma Membrane	enzyme	1.512	0.00134	0.0409
TLR3	toll like receptor 3	Plasma Membrane	transmembrane receptor	1.506	0.0000908	0.00454
LYNX1	Ly6/neurotoxin 1	Plasma Membrane	transporter	1.466	0.000365	0.0146
IFITM3	interferon induced transmembrane protein 3	Plasma Membrane	other	1.457	1.69E-07	0.0000214
HLA-B	major histocompatibility complex, class I, B	Plasma Membrane	transmembrane receptor	1.443	0.000259	0.011
PLSCR1	phospholipid scramblase 1	Plasma Membrane	enzyme	1.431	0.000153	0.00717
SDK2	sidekick cell adhesion molecule 2	Plasma Membrane	other	1.372	0.000122	0.00591
HLA-C	major histocompatibility complex, class I, C	Plasma Membrane	other	1.332	0.0000277	0.00171
IFIT5	interferon induced protein with tetratricopeptide repeats 5	Plasma Membrane	other	1.323	0.0000691	0.00372
ABCA5	ATP binding cassette subfamily A member 5	Plasma Membrane	transporter	1.308	0.000394	0.0155
S1PR1	sphingosine-1-phosphate receptor 1	Plasma Membrane	G-protein coupled receptor	1.277	0.000227	0.00994
CGNL1	cingulin like 1	Plasma Membrane	other	1.255	0.0000788	0.00412
ITGA2	integrin subunit alpha 2	Plasma Membrane	transmembrane receptor	1.153	0.000246	0.0106
ANO5	anoctamin 5	Plasma Membrane	ion channel	1.076	0.000624	0.0226
SLC41A2	solute carrier family 41 member 2	Plasma Membrane	transporter	1.04	0.00137	0.0414
FAS	Fas cell surface death receptor	Plasma Membrane	transmembrane receptor	1.023	0.000317	0.0129

3.8 Summary:

Most of the previous studies were looking at the HIV-1-infected astrocytes as a homogenous population and were unable to differentiate the type of infection, whether it was an active or latent/restricted infection and how this affects astrocyte biology. In this study we used R/G-HIV-1 reporter construct that was previously characterized in primary human CD4 T-cells where the infection lead to majority of cells being latently infected. Similarly, in our studies in primary human astrocytes R/G-HIV-1 infection resulted in more red cells (R+/G-) that have minimal to no viral protein expression compared to yellow cells (R+/G+) indicating the majority of the infected astrocytes restricted HIV LTR activity. Reactivation studies indicated that R+/G- astrocytes resisted reactivation, whereas R+/G+ astrocytes were highly inducible to vorinostat alone and combination treatment by both IL-1β and vorinostat. Gene expression studies by RNA-sequencing demonstrated that despite harboring restricted or silent viral promoters, R+/G- astrocytes transcriptome was significantly altered, and it was similar to that of R+/G+ astrocytes. However, R+/G+ astrocytes have more heightened and broad changes to their transcriptome compared to R+/G- astrocytes. Typical antiviral responses and neuroinflammatory pathways such as interferon signaling, death receptor signaling, and activation of pattern recognition receptors were upregulated in both transcriptome profiles. Along with changes in gene expression, R/G-HIV-1-infected astrocytes also showed functional anomalies. Despite the activity of viral promoter, both populations of astrocytes have reduced cell proliferation capacities. Our studies also demonstrated that being actively infected, significantly decreased glutamate clearance capacity of human astrocytes, a key function that prevents excitotoxicity in the CNS. Finally, comparison analysis studies suggested that there were great phenotypic similarities between our transcriptome data

from pure *in vitro* red and yellow HIV+ astrocyte cultures and *in vivo* samples from multiple brain regions of neurocognitively impaired HIV-1-infected individuals.

CHAPTER 4

β-CATENIN-MEDIATED NEGATIVE REGULATION OF IL-6 EXPRESSION BY HUMAN ASTROCYTES DURING HIV-ASSOCIATED INFLAMMATION

HIV-1 infection of macrophages and microglia in the CNS leads to cellular activation and secretion of neurotoxic cytokines such as IL-1β and TNF-α (26, 113). These cytokines indirectly mediate their neurotoxic effects by activating astrocytes and play an important role in the further induction of neuronal injury and HAND pathogenesis.

NF-κB acts as a central regulator of innate and adaptive immune responses, cell proliferation, and apoptosis in various cell types (66). Several studies have shown upregulation of inflammatory cytokines such as CXCL8, CCL2, CCL3, IFN-γ and IL-6 production by astrocytes in response to macrophage-derived IL-1β and TNF-α during HIV-1 CNS infection (67). Crosstalk between Wnt/β-catenin and NF-κB signaling during inflammation has been extensively studied in peripheral cells (70). Previously, Ma *et al.* have shown that in chondrocytes, β-catenin negatively regulates NF-κB-mediated IL-6 expression (69). The Wnt/β-catenin pathways has been shown to restrict the HIV life cycle in target cell types, including PBMCs and astrocytes (60, 61); however, little is known about its contributions to the neuroinflammatory responses of astrocytes. In this study, we aim to decipher the regulation of NF-κB signaling by the Wnt/β-catenin pathway to better understand the mechanisms regulating astrocyte inflammatory response.

4.1. HAND-relevant stimuli induce Wnt/β-catenin and NF-κB signaling in astrocytes:

To investigate how HAND-relevant stimuli affect Wnt/β-catenin signaling during CNS HIV-1 infection, human astrocyte cultures were exposed to the pro-inflammatory cytokines IL-1β (20 ng/ml) and TNF-α (50 ng/ml) for eight hours either alone or in combination. As a key member of the pathway, β-catenin mRNA levels were analyzed by real-time PCR. Both IL-1β and TNF-α significantly increased β-catenin transcription (Fig 4.1A, $p < 0.001$). To further confirm activation of Wnt/β-catenin pathway, levels of LEF-1, a key transcription factor and downstream modulator

of the pathway, were also measured. LEF-1 mRNA levels were elevated by at least 80% regardless of treatment (Fig 4.1B, $p < 0.001$). These cytokines also increased the NF-κB transcription significantly (Fig 4.1C, $p < 0.001$). Together, these data show that HAND-relevant inflammatory stimuli induce LEF-1 and β-catenin expression, suggesting induction of β-catenin signaling in human astrocytes.

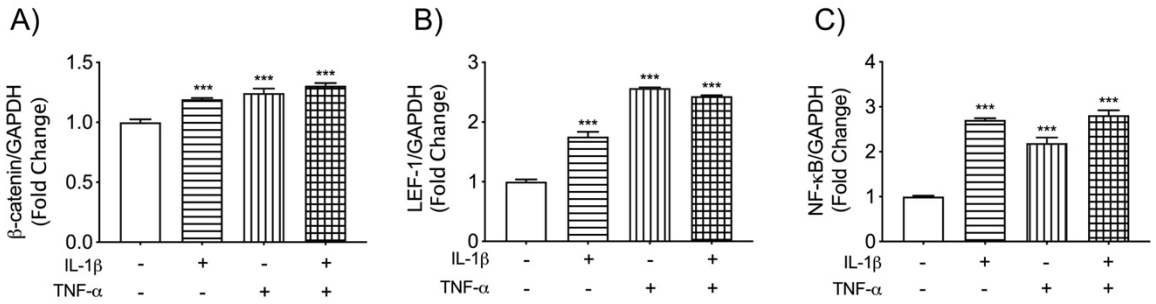

Figure 4. 1 HAND-relevant stimuli upregulated the canonical Wnt and NF-κB signaling in astrocytes.

Astrocytes were treated with HAND-relevant stimuli IL-1β (20 ng/ml) and TNF-α (50 ng/ml). Total RNA was isolated eight hours post-treatment, and ***(A)*** *β-catenin,* ***(B)*** *LEF-1, and* ***(C)*** *NF-κB mRNA levels were determined by real-time PCR. Glyceraldehyde 3-phosphate dehydrogenase (GAPDH) was used as a normalizing control, and bars are average mRNA fold changes to untreated controls with standard deviation (SD). Data are representative of three individual astrocyte donors. Statistical significance was determined by one-way ANOVA with Tukey's post hoc-test for multiple comparisons (***$p < 0.001$).*

β-catenin differentially regulates LEF-1 and NF-κB transcription during HAND-relevant stimuli:

To assess the crosstalk between Wnt/β-catenin and NF-κB signaling pathways, β-catenin was transiently knocked down in primary human astrocytes, and responses to HAND-relevant stimuli were tested. β-catenin specific siRNA decreased the mRNA levels of β-catenin approximately by 90% with and without HAND-relevant stimuli (Fig 4.2A) when compared to mock and siCon. β-catenin silencing also diminished IL-1β- and TNF-α-induced LEF-1 transcription. However, basal LEF-1 transcription was unchanged (Fig 4.2B). Also silencing β-catenin and LEF-1 did not affect NF-κB transcription (Fig 4.2C). Together, these data indicate that the Wnt/β-catenin pathway does not directly regulate NF-κB transcription in human astrocytes.

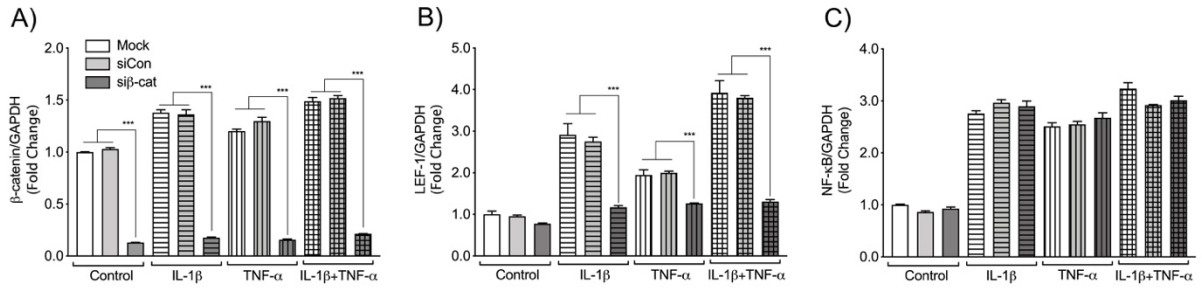

Figure 4. 2 β-catenin knockdown in human astrocytes decreased levels of LEF-1 but not NF-κB during HAND-relevant stimulation.

Human astrocytes were transfected without siRNA (mock) or with non-targeting, scrambled siRNA (siCon) or β-catenin specific siRNA (siβ-cat) by nucleofection and were allowed to recover for 24 hours. Cells were then treated with either IL-1β (20 ng/ml) or TNF-α (50 ng/ml) alone and in combination. Total RNA was isolated eight hours post-treatment, and ***(A)*** *β-catenin,* ***(B)*** *LEF-1, and* ***(C)*** *NF-κB mRNA levels were determined by real-time PCR. GAPDH was used as a normalizing control. Data shown are average mRNA fold changes +/- SD and are representative of experiments in three individual astrocyte donors. Statistical significance was determined by one-way ANOVA with Tukey's post hoc-test for multiple comparisons (***p <0.001).*

4.2. β-catenin negatively regulates astrocyte IL-6 expression:

To determine if β-catenin regulated IL-1β and TNF-α - induced neuroinflammation, human astrocytes were treated with HAND-relevant stimuli, and levels of CXCL8, CCL2 and IL-6 were measured at both mRNA and protein levels. IL-1β and TNF-α treatment significantly increased CXCL8 and CCL2 expression both at RNA (data not shown) and protein levels (Fig 4.3 A & B). Treatment with IL-1β and TNF-α also significantly increased IL-6 mRNA and protein levels (Fig 4.4 A & B). IL-1β treatment increased IL-6 to a greater magnitude than TNF-α and no synergistic effect of the combination treatment was apparent. β-catenin knockdown did not affect the levels of either cytokine CXCL8 or CCL2. However, it exacerbated HIV-associated IL-6 expression. This indicates Wnt/β-catenin pathway may negatively regulate IL-6 expression in human astrocytes during inflammation.

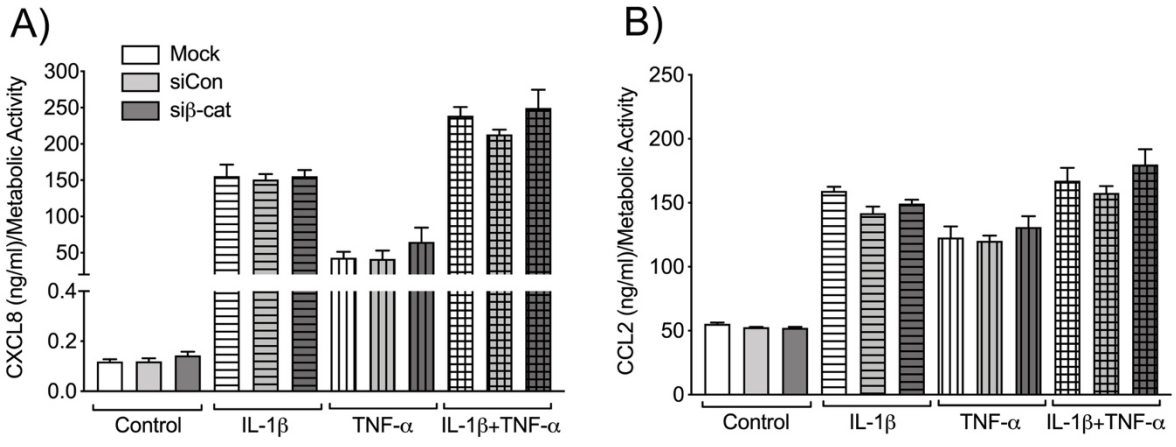

Figure 4. 3 β-catenin knockdown did not alter CXCL8 or CCL2 expression by astrocytes in response to inflammatory stimuli.

Human astrocytes were transfected without siRNA (mock), with siCon or siβ-catenin by nucleofection and were allowed to recover for 24 hours. Cells were then treated with either IL-1β (20 ng/ml) or TNF-α (50 ng/ml) alone or in combination for 24 hours. Culture supernatants were

*then collected and **(A)** CXCL8 and **(B)** CCL2 levels were measured by ELISA. Data are average protein levels +/- SD and are representative of two experiments in individual astrocyte donors. Statistical significance was determined by one-way ANOVA with Tukey's post hoc-test for multiple comparisons (***p <0.001).*

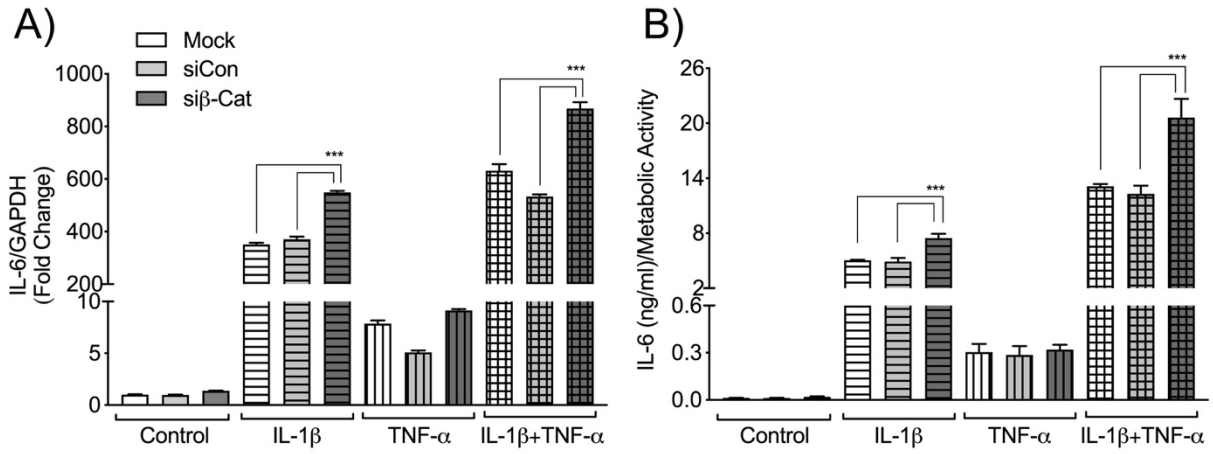

Figure 4. 4 β-catenin knockdown increased astrocyte IL-6 expression in response to inflammatory stimuli.

*Human astrocytes were transfected without siRNA (mock), or siCon or siβ-catenin by nucleofection and allowed to recover for 24 hours. Cells were then treated with IL-1β (20 ng/ml) or TNF-α (50 ng/ml) alone and in combination. Total RNA was isolated eight hours post-treatment, and **(A)** IL-6 mRNA levels were determined by real-time PCR using GAPDH as a normalizing control. Culture supernatants were collected 24 hours post-treatment, and levels of **(B)** IL-6 were measured by ELISA. Data are average mRNA fold change or protein levels +/- SD and are representative of experiments in three individual astrocyte donors. Statistical significance was determined by one-way ANOVA with Tukey's post hoc-test for multiple comparisons (***p <0.001).*

4.3. Activation of β-catenin diminishes the IL-6 expression by human astrocytes:

Since β-catenin knockdown during HAND-relevant stimuli exacerbated the expression of IL-6 by astrocytes, the effects of β-catenin activation were also evaluated. Human astrocytes were pre-treated with 6-bromoindirubin-3'-oxime (BIO), GSK3-β inhibitor that prevents proteasomal-mediated degradation of β-catenin and making it readily available to translocate into the nucleus and activate the pathway. Pre-treated or untreated astrocytes were stimulated with HAND-relevant stimuli, and supernatants were assayed for IL-6 expression by ELISA (Fig 4.5). While TNF-α minimally increased IL-6 levels, β-catenin stabilization did not affect TNF-α - induced IL-6 expression. However, in the context of IL-1β alone and in combination with TNF-α, β-catenin stabilization significantly decreased IL-6 secretion (Fig 4.5, ***p <0.001). Together the data indicate that β-catenin negatively regulates IL-6 expression by human astrocytes during treatment with IL-1β alone and in combination with TNF-α.

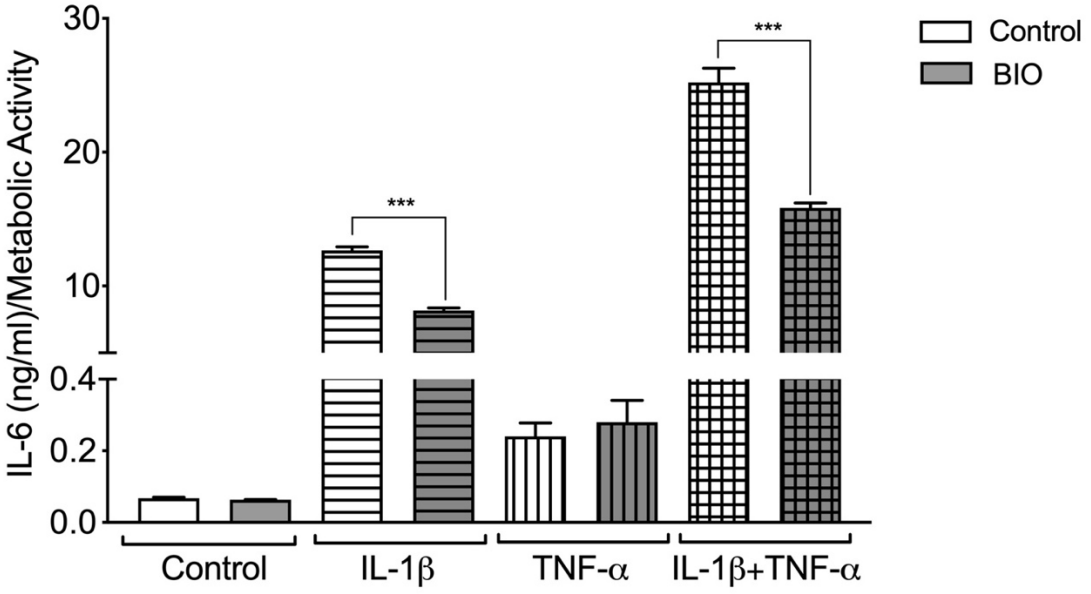

Figure 4. 5 β-catenin stabilization significantly reduced IL-6 expression by human astrocytes during HIV-associated inflammation.

*Human astrocytes +/- pretreated with BIO (500 nM) for one hour were then exposed to IL-1β (20 ng/ml) or TNF-α (50 ng/ml) alone or in combination for 24 hours. Culture supernatants were collected, and IL-6 levels were measured by ELISA. Data are average protein levels +/- SD and are representative of two experiments in individual astrocyte donors. Statistical significance was determined by one-way ANOVA with Tukey's post hoc-test for multiple comparisons (***p <0.001).*

4.4. Activation of Wnt/β-catenin signaling pathway increases the translocation of β-catenin and NF-κB into nucleus:

To determine if activation of the Wnt/β-catenin signaling pathway regulates the nuclear localization of NF-κB, cells were treated with BIO, cytosolic, and nuclear fractions of cell lysates were analyzed for β-catenin and NF-κB levels using simple WES (Protein simple, San Jose, CA). β-catenin stabilization slightly decreased cytosolic levels of both β-catenin and NF-κB (Fig 4.6 A & B), which was coupled to increased translocation of both proteins into the nucleus (Fig 4.6 C & D). Together our data indicate that activating the canonical Wnt/β-catenin signaling pathway significantly increased nuclear translocation of NF-κB in human astrocytes.

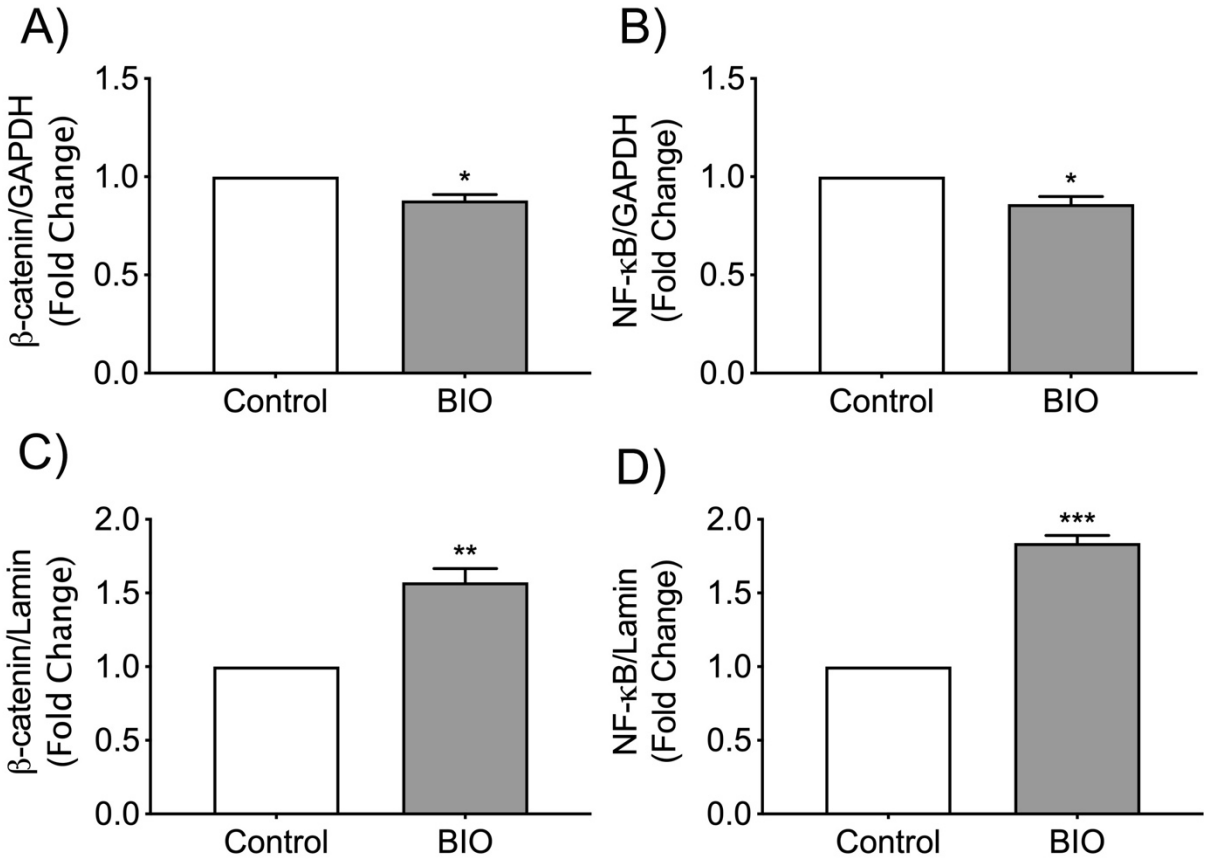

Figure 4. 6 β-catenin stabilization significantly increased NF-κB nuclear localization.

*Human astrocytes were incubated with or without BIO (500 nM) for 24 hours and levels of β-catenin and NF-κB in cytosolic and nuclear fractions were evaluated by WES protein analysis. Fraction specific markers lamin A/C for nucleus and GAPDH for cytosol were used as loading controls. Data are average protein levels +/- SEM from three individual astrocyte donors. Statistical significance was determined by one-way ANOVA with Tukey's post hoc-test for multiple comparisons (*p <0.05, **p <0.01, ***p <0.001).*

4.5 Canonical Wnt/β-catenin signaling negatively regulates NF-κB-mediated IL-6 production by astrocytes.

Altogether as we summarized in **figure 4.7**, our data indicates that HAND-relevant stimuli IL-1β and TNF-α upregulated Wnt/β-catenin signaling and further downstream transcription

factors such as LEF-1 in human astrocytes (Fig 4.1 & 4.2). In parallel, HAND-relevant stimuli also upregulated NF-κB signaling (Fig 4.1 & 4.2) leading to reactive astrogliosis phenotype by secreting inflammatory cytokines such as CXCL8, CCL2 and IL-6 (Fig 4.3 & 4.4). Activation of β-catenin by inhibiting GSK3-β facilitated the translocation of both β-catenin and NF-κB into the nucleus from cytosol (Fig 4.6). Also, β-catenin signaling negatively regulated NF-κB-mediated IL-6 production in astrocytes (Fig 4.4 & 4.5). However, it did not change expression of other inflammatory cytokines CXCL8 and CCL2 (Fig 3). This upregulation of Wnt/β-catenin signaling and its negative regulation of IL-6 production during the HIV-relevant inflammatory stimuli indicates that Wnt/β-catenin signaling is trying to mitigate the inflammatory burden in the CNS mediated by astrocytes.

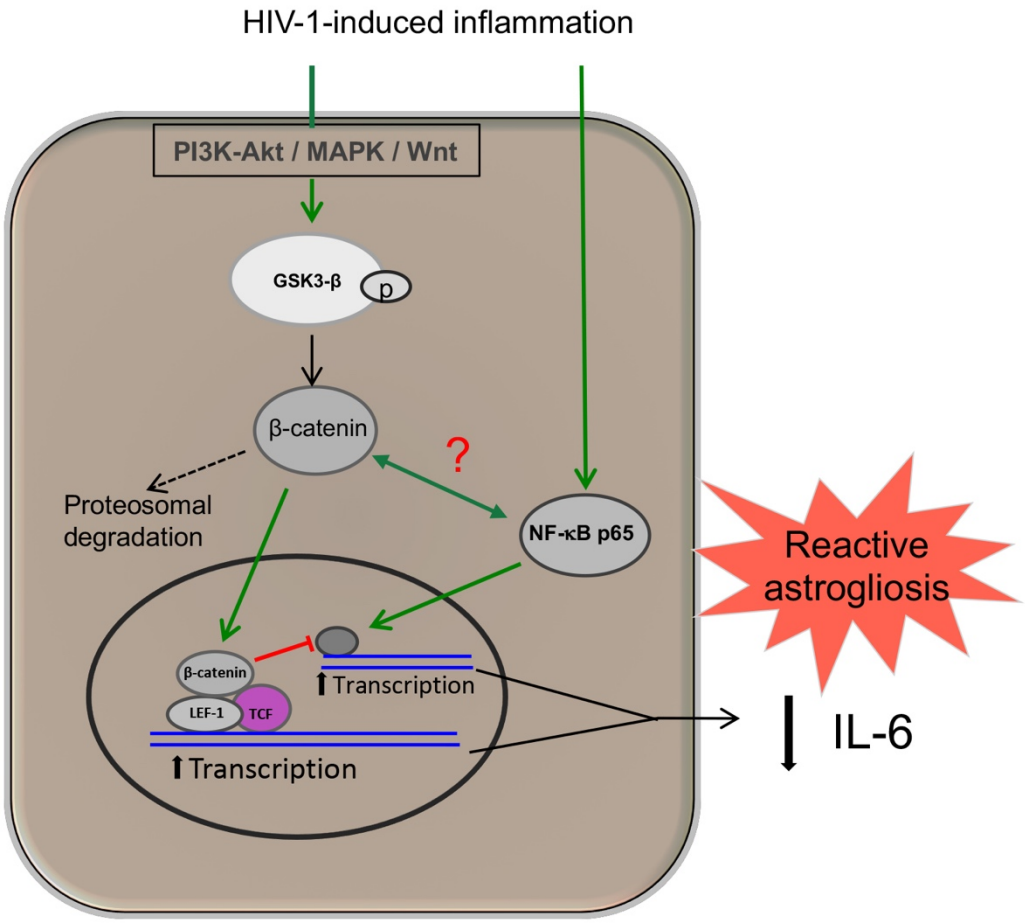

Figure 4. 7 Crosstalk between Wnt/β-catenin and NF-κB signaling during HIV-associated inflammation.

HIV-associated inflammatory stimuli IL-1β and TNF-α upregulated both Wnt/β-catenin and NF-κB signaling in human astrocytes. Activation of β-catenin significantly improved translocation of both β-catenin and NF-κB into nucleus. Simultaneously, it decreased IL-1β-mediated expression of IL-6 by astrocytes. In spite of the regulatory overlap between Wnt/β-catenin and NF-κB signaling during HIV-associated inflammation, the mechanism of interaction between these two pathways is yet to be decoded in human astrocytes. It could be either an inhibitory interaction between the active β-catenin and NF-κB or downstream regulators of β-catenin pathway affecting the NF-κB signaling.

CHAPTER 5

DISCUSSION

PORTIONS FORMATTED AND PUBLISHED AS:

Insights into the Gene Expression Profiles of Active and Restricted Red/Green-HIV^{+} Human Astrocytes: Implications for Shock or Lock Therapies in the Brain

Journal of Virology. 2020. February 28. e01563-19

https://jvi.asm.org/content/94/6/e01563-19.long

5.1 Discussion:

Astrocytes are the non-neuronal cells in the brain that support health and homeostasis of CNS by performing critical functions. Microarray and transcriptome studies established that HIV-1 infection or treatment with viral coat protein gp120 profoundly alters gene expression of astrocytes that ultimately affects cellular functions and contributes to neurotoxicity and dysfunction (114-116). Most of these studies looked at infected astrocytes as a homogenous population and did not differentiate whether it was an active or latent/restricted infection or how this affects astrocyte biology. In this study a pseudotyped doubly labelled fluorescent reporter R/G-HIV-1 was used to identify and enrich active and latently infected populations of HIV+ astrocytes that helped us in understanding the effects of integrated HIV virus and the viral promoter activity on astrocyte function.

HIV-1 latency is established early during the infection and is the result of progressive epigenetic silencing of active infection. The possible epigenetic mechanisms include factors such as location and orientation of the provirus in the host genome, HIV-1 LTR chromatin structure and modifications such as acetylation and methylation, activation state of the host cell, transcription factor pool, and threshold levels of the viral Tat (117). Class 1 HDAC and histone methyl transferases have been shown to epigenetically silence HIV-1 LTR activity in primary human progenitor-derived astrocytes, astrocytoma cell lines and other cell types such as resting CD4 T cells, microglia, T cell lines, and HeLa cells (118, 119).

Apart from the above-mentioned cellular mechanisms driving the establishment of latency, the cellular activity state and activity of other transcription factors during/prior to infection played an important role in the establishment of productive *vs* non-productive infections. In Jurkat cells, R/G-HIV-1 infection leads to non-productive infection in the majority of cells, and this was inversely correlated to cellular activity state, specifically NF-κB activity (120). Our transcriptome analyses indicated significant upregulation of NF-κB subunits 1 and 2 in the R+/G+ population two weeks post-infection. Further investigations into the regulation of HIV infection by prior NF-κB activation may help understand establishment of HIV latency in astrocytes in the context of chronic, low grade neuroinflammation associated with HIV CNS infection. As one of the highly abundant cell types in CNS, astrocytes come in different types and shapes as mentioned earlier. Like neurons astrocytes interact with various cell types and have various functionality, which makes their subpopulations more diverse. Further infection during different cell-cycle stages may also regulate the activity of HIV-1 infection in astrocytes. Further studies would be needed to discern various cellular mechanisms that may drive establishment of active vs restricted HIV-1 infection in human astrocytes.

Studies into the reactivation of latently infected HIV+ astrocytes with LRAs, including HDACi, PKC agonists and proinflammatory mediators have been enigmatic. Some have shown failure to reactivate HIV in astrocytes even in cells with prolonged viral gene expression (121, 122), while others demonstrated HIV reactivation in various types of astrocytes (118, 123). Our data also indicated significant activation in un-sorted HIV+ astrocyte populations by vorinostat alone and in combination with IL-1β. However, we extended upon these studies to show that purified populations with integrated, silent/restricted viral promoters were resistant to these reactivators. While IL-1β and vorinostat marginally increased HIV-1 p24 levels in R+/G-

astrocytes, they did not attain expression levels equal to R+/G+ astrocytes and did not shift from single to double reporter positive. In parallel, astrocytes with active viral promoters were highly inducible. This suggests that reactivation efforts to identify latently infected astrocytes may fail and only promote the expression of neurotoxic viral proteins from active populations.

Barat *et al*. also detected a sub population of latent HIV+ astrocyte expressed HIV p24 and hypothesized that these R+/G- populations were either deeply latent or defective (122). In our study, expression of viral transcripts was detected in the transcriptome of both populations of R/G-HIV-1-infected astrocytes; however, transcription was significantly restricted in R+/G- astrocytes compared to R+/G+ astrocytes in all R/G-HIV transcripts but the CMV-driven mCherry reporter. While the single end 75 base sequencing method used is not an ideal technique to differentiate the spliced *vs* unspliced variants of HIV transcripts; HIV gene mapping indicated very little to no alignment of reads to the 5' or 3' LTR/UTR regions of R/G-HIV-1 in either population. This may indicate that neither R/+G-HIV-1 population is expressing full length RNA transcripts at detectable levels. This effect may be mediated by the R/G-HIV construct that lacks both *nef* and *env* genes, known regulators of viral infection and neurotoxicity in astrocytes (46, 124). Since Barat *et al*. have demonstrated long term productive infection in non-sorted NL4.3 eGFP-IRES-Crimson HIV+ astrocytes, which harbor the complete proviral genome (122), further investigations would be needed to determine if the silent/repressed population identified in our studies is truly capable of infecting other cells. Productive infection of HIV astrocytes shown *in vitro* may be driven by these active HIV LTR populations, while the latent/restricted populations could remain functionally altered yet non-infectious.

While we expected astrocytes with active and silent/repressed viral promoters to be distinctly different, latent/restricted HIV+ astrocytes resembled active HIV+ astrocytes more than

cells without proviral incorporation (D116A). R/G-HIV-1 infection significantly impaired cell proliferation capacity of human astrocytes, regardless of promoter activity. Viral proteins, especially Vpr, are known to induce cell-cycle arrest during G2 phase (125, 126). Complementing these studies, our transcriptome analyses demonstrated downregulation of key transcription factors that regulate S/G2 phases of cell cycle, such as CDK1, Cyclin A & B and E2F, during R/G-HIV-1 infection. Further, Gi Le *et al*., determined that triggering events for G2 phase arrest occurred in the S phase of the cell cycle in response to HIV-1 Vpr overexpression (127). In addition, typical antiviral responses and neuroinflammatory pathways such as interferon signaling, death receptor signaling, and activation of pattern recognition receptors were upregulated in both transcriptome profiles. This corroborates previous gene expression studies using several different approaches, treatment with whole HIV-1, gp120, or productive infection using VSVG pseudotyped HIV-1 in astrocytes (114, 128) and *ex vivo* brain tissues (111, 112). Upregulation of approximately 15 interferon signaling genes by HIV-1 indicates induction of type-1 antiviral response, similar to those observed during typical viral infections. However, the active viral promoter in HIV+ astrocytes and subsequent enhanced transcription of the viral genome lead to induction of more robust and unique gene expression changes.

Upregulated pathways such as iNOS signaling and the role of RIG-1 like receptors in antiviral innate immunity were unique to actively infected astrocytes. RIG-1, a pattern recognition receptor (PRR) and part of the innate immune system, elicits antiviral responses upon recognition of non-self RNA, viral genomes or viral transcripts (129). Upregulation of this pathway only in yellow (R+/G+) cells is a clear indication of active viral genome transcription. Previous studies have shown the dysregulation of iNOS expression during HIV-1 infection contributing to neurological damage. Human astrocytes were a major source of iNOS/NO following coculture

with HIV-1-infected-monocyte derived macrophages (MDM) (130). Further, astrocyte-derived NO also exerted an antiviral response by inhibiting viral replication in infected MDM (130). Treatment with recombinant Tat protein or transfection with Tat encoding plasmid induced expression of iNOS and production of NO in human astrocytes (131). While NO is a known modulator of neuronal firing and excitability, excess NO could be detrimental. In our study actively infected astrocytes were a significant source of viral proteins and use of LRAs significantly increased their expression. The coupling of viral transcript expression and detection by RIG-1 may contribute to iNOS upregulation in actively infected astrocytes and contribute to astrocyte-associated neuronal dysfunction in HIV.

In contrast certain canonical pathways such as endocannabinoid neuronal synapse pathway, nucleotide excision repair (NER) pathway, and ataxia telangiectasia protein (ATM) pathway selectively downregulated in astrocytes harboring an active viral promoter. Esposito *et al.* have shown evidence for the regulation of endocannabinoid pathway by HIV-1 Tat. In their study treatment of C6 cells (rat glioma cells) with recombinant Tat significantly reduced the expression of CB1 receptors at transcriptional level. At the same time, cannabinoid agonists were shown to reduce Tat-induced iNOS production in these cells in a concentration dependent manner (132). In this study, higher Tat levels in actively HIV+ astrocytes could have suppressed the endocannabinoid pathway. Therefore, one could propose that cannabinoids could also protect neurons from HIV-1 Tat induced damage by inhibiting iNOS protein expression and NO overproduction. DNA damage response (DDR) pathways, such as ATM and NER, are typically upregulated during HIV-1 infection; however, selected studies have shown the inverse effect. In a study by Piekna-Przybylska *et al*., two latently infected Jurkat-derived cell lines, CA5 and EF7, had impaired DNA damage responses and increased susceptibility to DNA damaging agents (133).

HIV-1 Tat downregulates expression of DNA-dependent protein kinases (DNA-PKs), which are important in repairing double strand DNA breaks (DSBs) and maintaining telomeres (134). Although DDR pathways were not downregulated in latent/restricted HIV+ astrocytes, actively infected astrocytes showed strong downregulation of both ATM and NER pathways, suggesting that they may also play a role in regulating astrocyte resilience during HIV infection.

Endogenous antiviral mechanisms targeting reverse transcription were differentially regulated in active *vs* latent/restricted HIV+ astrocyte populations. Direct analysis of our transcriptome data indicated a 5.6-fold decrease in apolipoprotein B editing complex 3 (APOBEC3) in actively infected astrocytes. APOBEC3 family proteins exert their antiviral response by inhibiting viral reverse transcription as well as cytidine deamination of viral cDNA. Inhibition of HIV-1 replication by APOBEC3G in CD4 T cells and neural cells has been previously reported (135, 136). HIV-1 viral protein Vif promotes viral replication by downregulating cell-encoded APOBEC3 family proteins. Similarly, in our dataset, only actively infected astrocytes downregulated APOBEC3B, suggesting that ongoing viral expression may be mediating this response. Meanwhile, sterile alpha motif and HD domain-containing protein 1 (SAMHD1), a HIV-1 restriction factor, was significantly increased in both active and latent HIV+ astrocytes, indicating regulation of SAMHD1 may be independent viral protein expression. SAMHD1 depletes the intracellular deoxy nucleoside triphosphates (dNTPs) to impair reverse transcription of viral RNA (137, 138). SIV infection also increased SAMHD1 expression in rhesus adult primary astrocytes, and exogenous IFNβ helped sustain these levels post infection (139). Our transcriptome data have shown significant upregulation of interferon signaling pathway in both populations of R/G-HIV-1-infected astrocytes. Strategies to upregulate APOBEC3 family proteins

and SAMHD1 during CNS HIV-1 infection along with conventional therapies may prevent further spread of newly produced virus and reduce neurotoxicity.

Several gene expression studies have tried to identify HIV-1 associated markers of glial cells or glial changes that are associated with development of HAND. At the onset of our studies, we too were in search of a plasma membrane biomarker capable of differentiating between active and latently infected astrocytes. The sole selective biomarker for latent HIV+ astrocytes was PLVAP, which is typically expressed on endothelial cells and regulates the permeability of the BBB (140). It has not previously been directly implicated in HIV in the CNS. Many of the other biomarkers were directly linked to interferon and viral defense responses. Antigen presentation *via* MHC-1 is often upregulated during viral infections. Other studies have suggested strong upregulation of the HLA-C specific allele during HIV-1 infection (141), which serves as an inhibitory signal to natural killer cells, while also promoting recognition by cytotoxic T cells. Upregulation of ICAM1 in astrocytes in response to HIV Tat, has been suggested to play a significant role in trafficking inflammatory cells into the CNS (142). However, none of these upregulated transcripts were specific to astrocytes or the brain, and in such, are unlikely to serve as targetable biomarkers of HIV-1-infected astrocytes.

Comparison analysis suggested that there were great phenotypic similarities between the transcriptome data from pure *in vitro* red and yellow HIV+ astrocyte cultures and *in vivo* samples from multiple brain regions of HIV-1-infected individuals. Similar canonical pathways included, interferon signaling, neuroinflammatory signaling, role of pattern recognition receptors in recognition of bacteria and viruses, IL-1 signaling, iNOS signaling, type1 diabetes mellitus signaling, and retinoic acid-mediated apoptosis signaling. The comparisons were made based on the altered canonical pathways and upstream regulators. Upregulation of upstream regulators or

transcription factors such as STAT-1/2, NF-κB and IFN-γ in astrocytes significantly drives the expression of inflammatory cytokines and chemokines. Particularly NF-κB transduction and transcription factor system is a central regulator of inflammation in numerous cell types.

While astrocytes are restrictively infected during CNS HIV-1 infection, HIV-1 predominantly replicates in microglia and macrophages. These infected macrophages and microglia are the major source of cytokines such as IL-1β, TNF-α and IFN-γ. Apart from the intrinsic upregulation of NF-κB transcription during HIV-1 infection, macrophage derived inflammatory cytokines both IL-1β and TNF-α are known to further activate NF-κB signaling and induce reactive astrogliosis phenotype in uninfected astrocytes (143, 144). Reactive astrocytes release a wide variety of inflammatory mediators such as cytokines and chemokines that are both neuroprotective (cytokines such as IL-1β and TGF-β) and neurotoxic (such as IL-1β, IL-8, CCL2 and TNF-α) in nature (39). IL-1β is also known to activate phosphoinositide 3-kinase (PI3K)/Akt/GSK-3β pathway in several cell types, such as hepatocytes, epithelial cells, airway and colonic smooth muscle cells (145, 146). Inhibitory serine-phosphorylation is the most frequent mechanism that regulates the activity of GSK3-β. Activated Akt, the product of PI3K pathway inactivates GSK3-β through phosphorylation, which leads to activation of canonical Wnt/β-catenin signaling. Our studies also showed that HIV-associated inflammatory stimuli IL-1β and TNF-α significantly upregulated Wnt/β-catenin signaling and its downstream regulators in uninfected human astrocytes. This activation could be due to IL-1β and TNF-α-mediated phosphorylation of GSK3-β.

Crosstalk between NF-κB signaling and canonical Wnt/β-catenin signaling during inflammation was extensively studied in periphery. A few examples include modulation of

inflammatory responses *via* interaction of Wnt/β-catenin signaling with NF-κB in murine hepatocytes (147), positive regulation of NF-κB activity by β-catenin in human bronchial epithelial cells, during lipopolysaccharide (LPS)-induced activation of NF-κB and proinflammatory cytokines, including IL-6, CXCL8, IL-1β, TNF-α and CCL2 expression (148), and NF-κB promoter regulation by β-catenin in colorectal cancer cells (149). Wnt/β-catenin signaling regulates NF-κB-mediated inflammation both positively and negatively. For instance, inhibition of GSK3-β by lithium or siRNA, potentiated TNF-induced expression of IL-6 and CCL2 in human microvascular endothelial cells (150). Whereas in our study inhibition of GSK3-β by BIO decreased levels of IL-1β-induced IL-6 expression and vice versa. IL-1β and TNF- activates PKC, which plays a primary role in the stimulation of IL-6 gene expression in human astrocytes (151). HIV-1 viral proteins such as gp120 treatment lead to IL-6 expression in human astrocytes, which is mediated by NF-κB pathway (152). The major bacterial pathogen, LPS is also known to induce IL-6 expression by astrocytes in CNS (153).

IL-6 plays a key role in the CNS during health and disease. Under normal physiology, IL-6 functions include induction of neurogenesis from neural stem cells (NScs), neuronal differentiation of PC12 cells (154, 155) as well as production of neural growth factor neurotrophin from astrocytes (156). Meanwhile, CNS IL-6 is upregulated during injury, inflammation and infections such as meningitis and encephalitis. As a prototypic cytokine with role in inflammation, IL-6 was implicated in several neuroinflammatory diseases such as Alzheimer's disease, multiple sclerosis, Parkinson's and Huntington's disease (157-159). Simultaneously IL-6 enhances neuronal damage by beta amyloid peptide in cultures of rat cortical neurons and also causes neuronal loss in developing cerebellar granular neuron cultures (160). Elevated levels of IL-6 was found in HAND patient's CSF confirming its role in neuroinflammation during HIV-1 infection

(161). IL-6 was reported to increase HIV-1 replication in several cell types such as PBMC, MDM, and U1 latently infected cells derived from U937 cells (162, 163).This pro-inflammatory cytokine is known to induce B cell differentiation into immunoglobulin producing cells and also co-activates various subsets of T cells. This could help in producing antibodies against HIV-1 in CNS. Based on literature it is evident that IL-6 has both neuroprotective as well as neurotoxic effects on CNS during various neurodegenerative diseases. Activation of Wnt/β-catenin signaling, specifically transcription factors LEF-1/4 are known restrictive factors of HIV-1 replication and transcription in astrocytes (164). Negative regulation of NF-κB-mediated IL-6 secretion by astrocytes during CNS HIV-1 infection might be another form of mitigating the HIV-1-associated neuroinflammation.

Many effects of IL-6 in the CNS are caused not only by its cell surface receptors (IL-R) on the target cells but also by a complex of IL-6 and s/IL-6R (soluble-IL-6R) binding to the cell surface gp130 (s/gp130). So not only the mechanisms modulating IL-6 expression, the s/IL-R and s/gp130 would also be invaluable targets during disease state. Since, IL-6 is known to be both detrimental and beneficial, cure strategies involving manipulation of IL-6 should be proceeded with caution.

5.2 Limitations and alternative plans:

Despite being able to differentiate between active and restrictedly infected astrocytes by using R/G-HIV-1 reporter virus, the VSVG-mediated infection is a single round replication-deficient infection due to Δ-*env* mutation. In addition, open reading frames of key neurotoxic proteins and virulence factors such as *gp120,* and *Nef* were defective in this reporter virus. Irrespective of lack of these viral factors, we showed significant changes in gene expression and functional profiles. However, it is important to study these outcomes under full disease relevance

with a reporter virus that expresses all viral proteins and regulatory factors intact. To overcome these limitations Barat *et al.* designed a replication-competent dual fluorescent reporter construct NL4.3 eGFP-Crimson, which encodes for all viral proteins. In their study, they also used a mutated form of the X4-tropic HIV-1 NDK *env* called m7NDK, that permitted the infection through CD4-independent and CXCR4-dependent pathway (122). The infection resulted in astrocytes with sustained virus production over a period of time. However, the number of virus-infected cells was critically low.

Even though gene expression patterns of both astrocyte populations were significantly changed due to the HIV-1 infection and difference in the viral promoter activity, our sequencing studies did not yield any astrocyte specific cell surface markers that would help to target HIV+ astrocytes without reactivating them. Future sequencing studies involving more reads as well as investigating the splice variants of the transcripts might help in finding astrocyte specific biomarkers of HIV-1 infection. Further, in our sequencing studies, mapping of HIV-1 transcripts to the reference R/G-HIV-1 genome resulted in a very little to no alignment of reads to the 3' and 5' regions of the viral promoter. This indicates that neither R/G-HIV-1-infected astrocyte population is expressing full length RNA transcripts at detectable levels. Once again, this effect may be mediated by the R/G-HIV construct that lacks both *Nef* and *env* genes, known regulators of viral infection and neurotoxicity in astrocytes. In order to overcome these limitations in the model, infection of astrocytes with VSVG pseudotyped NL4.3 eGFP-Crimson reporter virus that encodes for all viral proteins would be ideal to obtain higher yields of HIV-1-infected astrocytes for functional and gene expression studies. Additionally, performing a 150 base paired-end sequencing would allow us to identify the spliced versus unspliced forms of the viral transcripts,

which will help us to determine whether the restrictive infection in human astrocytes is whether completely silent or not.

Despite using VSVG coat and polybrene during spinoculation to improve transduction efficiencies, the yields of active and restrictively infected astrocytes were still limited. This greatly limited our choice of reactivating agents to classic HDACi vorinostat and neuroinflammatory cytokine IL-1β. Future reactivation studies with different classes of reactivating agents must be conducted to assess if any other mechanisms of cellular activation would reactivate restrictively infected astrocytes to achieve active phenotype.

5.3 Summary and future directions:

Taken together these studies demonstrated that the majority of R/G-HIV-1 infections of human fetal astrocytes resulted in latent infection, with silent/restricted viral promoters that were resistant to reactivation. However, a considerable percentage of astrocytes remained actively infected and were inducible by inflammatory (IL-1β) and pharmacological (vorinostat) reactivating agents. So, strategies such as "Shock and Kill" that reactivate latent reservoirs for clearance by cytotoxic immune cells will be challenging since astrocyte latent reservoirs were resilient to reactivation and actively infected cells were inducible leading to augmented production of neurotoxic viral proteins. This could exacerbate the neurocognitive impairment of PLWH.

Surprisingly, gene expression profiles of the active and latent/restricted HIV+ astrocytes were similar; however, the range and magnitude of changes were larger in actively infected cells. Despite silent/restricted HIV LTR activity, latently infected astrocytes underwent significant changes in cellular gene expression altering their function by elevated neuroinflammatory cytokine expression and decreased cell proliferation rates. This suggests more recent strategies such as

"Block and Lock" that repress HIV-1 transcription to obtain a functional cure may pose a great challenge towards addressing astrocyte reservoirs.

Simultaneously, our functional studies demonstrated that R/G-HIV-1-infected astrocytes were dysfunctional with loss of critical functions such as glutamate clearance which leads to excitotoxicity and neuronal death, as well loss of cell proliferative capabilities which is a key characteristic of astrogliosis during injury and inflammation. Further, HIV-1 infection of astrocytes promoted expression of several neuroinflammatory factors such as CXCL8, CCL2, IL-6, CCL5 and ICAM1, which leads to recruitment and activation of other immune cells into the CNS. Considering their pivotal role in maintaining homeostasis and their abundancy in the CNS, HIV-1 infection of astrocytes whether an active or latent infection would be devastating to the CNS health and could clearly augment the pathogenesis of HAND.

As mentioned earlier, the state of cellular activity and transcription factors during/prior to infection can play important roles in the establishment of productive *vs* non-productive infections. To understand why the majority of R/G-HIV-1 infection in astrocytes leads to silent/restricted infection, it is necessary to conduct experiments involving pre-stimulation of astrocytes with PMA or other HIV-relevant stimuli that are present during chronic neuroinflammation in CNS HIV-1 infection. Assessing this phenomenon in astrocytes would further our knowledge of latency establishment mechanisms, and better replicate the *in vivo* milieu of the brains of PLWH.

Future investigations should examine several critical mechanisms that are likely to influence outcomes in understanding HIV-mediated pathogenesis of harboring proviral genome as well as the transcriptional status of the virus. First, confirmation studies of our *in vitro* findings *in vivo* is necessary. Since they are not susceptible to HIV-1 infection, there is a great lack in HIV-1 rodent models to study HAND pathogenesis. The simian (S)IV infection model in non-human

primates comes with the caveats of rapid progression to AIDS, severity of CNS inflammation due to augmented immune response, and related but distinct viruses. Brain autopsy samples of individuals known to suffer from HAND are a great alternative to carry *ex vivo* studies. Our IPA analysis demonstrated several phenotypic similarities in transcriptome profiles between R/G-HIV+ astrocytes and whole brain tissue samples from individuals suffering from HAND. However, in these studies, RNA was isolated from whole brain rather than astrocytes alone. Alternatively, astrocytes could be cultured from postmortem tissues and used for sequencing studies to isolate changes in their specific transcriptomes.

Even though the majority of infection in astrocytes resulted in restrictive infection, a considerable amount of the viral promoters were active. This enhanced transcription of the viral genome lead to the induction of more robust and unique gene expression changes such as upregulation of iNOS signaling and downregulation of endocannabinoid pathway. Our data corroborate previous studies that showed similar effects by overexpressing Tat in primary astrocytes or cell lines (132). Future confirmation studies examining these outcomes in Tat transgenic mice are warranted.

Active viral transcription significantly decreased glutamate clearance ability of astrocytes. However, we did not observe any changes in the RNA levels of EAAT2 in our RNA-sequencing studies. EAAT2 undergoes several post-translational modifications such as proteasomal degradation and SUMOylation. Increased expression of astrocyte elevated gene-1 (AEG-1) is also negatively correlated to EAAT2 surface expression in glioma, and HIV-1 Tat is known to upregulate AEG-1 expression in astrocytes *via* phospho-inositol-3-kinase (PI3K) signaling (165). Our studies indicate higher levels of Tat expression in actively infected astrocytes. In such, evaluating different posttranslational modifications and AEG-1-mediated regulation of astrocyte

EAAT2 surface expression during active viral infection will help us in further enhancing our understanding of viral protein-mediated neurotoxicity.

Our studies indicate endogenous antiviral protein APOBEC3B that target reverse transcription and integration of viral genome was differentially regulated in active *vs* latent/restricted HIV+ astrocyte populations. APOBEC3B levels in actively infected astrocytes were significantly lower than restrictively infected. This could be due to Vif-mediated proteasomal degradation of APOBEC3B in actively infected cells. Intervention with small molecules that potentially block the viral protein Vif may result in sustained levels of APOBEC3 family members thereby inhibiting viral replication.

Our studies demonstrated that astrocyte proviral reservoirs, whether active or latent, will enhance HAND pathogenesis and they stand out as an unconventional body of proviral reservoirs. Together understanding these mechanisms that contribute to HAND pathogenesis will help in developing therapeutic strategies. These strategies could either inhibit viral protein-mediated toxicity or improve astrocyte function thereby potentially reducing the burden of HAND in PLWH. However, either "Shock and Kill" or "Block and Lock" strategies to address astrocyte HIV-1 reservoirs may be rendered useless or lead to detrimental CNS outcomes in PLWH. Thus, there is a great need to investigate therapeutic avenues, such as CRISPR/Cas9, to excise the HIV-1 genome in an effort to restore astrocyte function and alleviate HIV-associated neurocognitive impairment without reactivating these reservoirs.

REFERENCES

1. **Motomura K, Chen J, Hu WS.** 2008. Genetic recombination between human immunodeficiency virus type 1 (HIV-1) and HIV-2, two distinct human lentiviruses. J Virol **82:**1923-1933.
2. **Galea S.** 2019. The Global Burden of HIV/AIDS.
3. **Control CfD.** HIV in the United States and Dependent Areas.
4. **Cohen MS, Shaw GM, McMichael AJ, Haynes BF.** 2011. Acute HIV-1 Infection. N Engl J Med **364:**1943-1954.
5. **Vanhamel J, Bruggemans A, Debyser Z.** 2019. Establishment of latent HIV-1 reservoirs: what do we really know? J Virus Erad **5:**3-9.
6. **Coffin J, Swanstrom R.** 2013. HIV pathogenesis: dynamics and genetics of viral populations and infected cells. Cold Spring Harb Perspect Med **3:**a012526.
7. **Kulpa DA, Chomont N.** 2015. HIV persistence in the setting of antiretroviral therapy: when, where and how does HIV hide? J Virus Erad **1:**59-66.
8. **Wong JK, Yukl SA.** 2016. Tissue reservoirs of HIV. Curr Opin HIV AIDS **11:**362-370.
9. **Barton K, Winckelmann A, Palmer S.** 2016. HIV-1 Reservoirs During Suppressive Therapy. Trends Microbiol **24:**345-355.
10. **Henderson LJ, Reoma LB, Kovacs JA, Nath A.** 2019. Advances towards curing HIV-1 infection from tissue reservoirs. J Virol doi:10.1128/jvi.00375-19.
11. **Joseph SB, Kincer LP, Bowman NM, Evans C, Vinikoor MJ, Lippincott CK, Gisslen M, Spudich S, Menezes P, Robertson K, Archin N, Kashuba A, Eron JJ, Price RW, Swanstrom R.** 2019. Human Immunodeficiency Virus Type 1 RNA Detected in the Central Nervous System (CNS) After Years of Suppressive Antiretroviral Therapy Can

Originate from a Replicating CNS Reservoir or Clonally Expanded Cells. Clin Infect Dis **69:**1345-1352.

12. **Fiala M, Looney DJ, Stins M, Way DD, Zhang L, Gan X, Chiappelli F, Schweitzer ES, Shapshak P, Weinand M, Graves MC, Witte M, Kim KS.** 1997. TNF-alpha opens a paracellular route for HIV-1 invasion across the blood-brain barrier. Mol Med **3:**553-564.

13. **Koenig S, Gendelman HE, Orenstein JM, Dal Canto MC, Pezeshkpour GH, Yungbluth M, Janotta F, Aksamit A, Martin MA, Fauci AS.** 1986. Detection of AIDS virus in macrophages in brain tissue from AIDS patients with encephalopathy. Science **233:**1089-1093.

14. **Gartner S.** 2000. HIV infection and dementia. Science **287:**602-604.

15. **Churchill MJ, Gorry PR, Cowley D, Lal L, Sonza S, Purcell DF, Thompson KA, Gabuzda D, McArthur JC, Pardo CA, Wesselingh SL.** 2006. Use of laser capture microdissection to detect integrated HIV-1 DNA in macrophages and astrocytes from autopsy brain tissues. J Neurovirol **12:**146-152.

16. **Fois AF, Brew BJ.** 2015. The Potential of the CNS as a Reservoir for HIV-1 Infection: Implications for HIV Eradication. Curr HIV/AIDS Rep **12:**299-303.

17. **KFF.** 2019. U.S. Federal Funding for HIV/AIDS: Trends Over Time.

18. **Elbirt D, Mahlab-Guri K, Bezalel-Rosenberg S, Gill H, Attali M, Asher I.** 2015. HIV-associated neurocognitive disorders (HAND). Isr Med Assoc J **17:**54-59.

19. **Ragin AB, Wu Y, Gao Y, Keating S, Du H, Sammet C, Kettering CS, Epstein LG.** 2015. Brain alterations within the first 100 days of HIV infection. Annals of Clinical and Translational Neurology **2:**12-21.

20. **Heaton RK, Franklin DR, Ellis RJ, McCutchan JA, Letendre SL, Leblanc S, Corkran SH, Duarte NA, Clifford DB, Woods SP, Collier AC, Marra CM, Morgello S, Mindt MR, Taylor MJ, Marcotte TD, Atkinson JH, Wolfson T, Gelman BB, McArthur JC, Simpson DM, Abramson I, Gamst A, Fennema-Notestine C, Jernigan TL, Wong J, Grant I.** 2011. HIV-associated neurocognitive disorders before and during the era of combination antiretroviral therapy: differences in rates, nature, and predictors. Journal of neurovirology **17:**3-16.

21. **Paddick S-M, Flatt A, Eaton P, Kellet-Wright J, Duijinmaijer A, Urasa S, Kisoli A, Yarwood V, Thornton J, McCartney J, Irwin C, Dotchin C, Gray WK, Dekker M, Howlett W, Muaketova-Ladinska E, Walker R.** 2017. 16 Prevalence and risk factors for hiv-associated neurocognitive impairment (hand) amongst adults aged 50 and over attending a hiv clinic in northern tanzania. Journal of Neurology, Neurosurgery & Psychiatry **88:**A19-A19.

22. **Heaton RK, Clifford DB, Franklin DR, Jr., Woods SP, Ake C, Vaida F, Ellis RJ, Letendre SL, Marcotte TD, Atkinson JH, Rivera-Mindt M, Vigil OR, Taylor MJ, Collier AC, Marra CM, Gelman BB, McArthur JC, Morgello S, Simpson DM, McCutchan JA, Abramson I, Gamst A, Fennema-Notestine C, Jernigan TL, Wong J, Grant I.** 2010. HIV-associated neurocognitive disorders persist in the era of potent antiretroviral therapy: CHARTER Study. Neurology **75:**2087-2096.

23. **Saylor D, Dickens AM, Sacktor N, Haughey N, Slusher B, Pletnikov M, Mankowski JL, Brown A, Volsky DJ, McArthur JC.** 2016. HIV-associated neurocognitive disorder--pathogenesis and prospects for treatment. Nat Rev Neurol **12:**234-248.

24. **Grant I, Franklin DR, Jr., Deutsch R, Woods SP, Vaida F, Ellis RJ, Letendre SL, Marcotte TD, Atkinson JH, Collier AC, Marra CM, Clifford DB, Gelman BB, McArthur JC, Morgello S, Simpson DM, McCutchan JA, Abramson I, Gamst A, Fennema-Notestine C, Smith DM, Heaton RK, Group C.** 2014. Asymptomatic HIV-associated neurocognitive impairment increases risk for symptomatic decline. Neurology **82:**2055-2062.

25. **Antinori A, Arendt G, Becker JT, Brew BJ, Byrd DA, Cherner M, Clifford DB, Cinque P, Epstein LG, Goodkin K, Gisslen M, Grant I, Heaton RK, Joseph J, Marder K, Marra CM, McArthur JC, Nunn M, Price RW, Pulliam L, Robertson KR, Sacktor N, Valcour V, Wojna VE.** 2007. Updated research nosology for HIV-associated neurocognitive disorders. Neurology **69:**1789-1799.

26. **Kaul M, Garden GA, Lipton SA.** 2001. Pathways to neuronal injury and apoptosis in HIV-associated dementia. Nature **410:**988-994.

27. **Lipton SA, Gendelman HE.** 1995. Dementia associated with the acquired immunodeficiency syndrome. N Engl J Med **332:**934-940.

28. **Giulian D, Wendt E, Vaca K, Noonan CA.** 1993. The envelope glycoprotein of human immunodeficiency virus type 1 stimulates release of neurotoxins from monocytes. Proc Natl Acad Sci U S A **90:**2769-2773.

29. **Brew B, Corbeil J, Pemberton L, Evans L, Saito K, Penny R, Cooper D, Heyes M.** 1995. Quinolinic acid production is related to macrophage tropic isolates of HIV-1. J Neurovirol **1:**369-374.

30. **Zink WE, Zheng J, Persidsky Y, Poluektova L, Gendelman HE.** 1999. The neuropathogenesis of HIV-1 infection. FEMS Immunol Med Microbiol **26:**233-241.

31. **Kaul M, Zheng J, Okamoto S, Gendelman HE, Lipton SA.** 2005. HIV-1 infection and AIDS: consequences for the central nervous system. Cell Death Differ **12 Suppl 1:**878-892.

32. **Rutka JT, Apodaca G, Stern R, Rosenblum M.** 1988. The extracellular matrix of the central and peripheral nervous systems: structure and function. J Neurosurg **69:**155-170.

33. **Ramon Y CS.** 1909. Histologie du systeme nerveux de l'homme et des vertebres. Maloine, Paris.

34. **Charles AC, Merrill JE, Dirksen ER, Sanderson MJ.** 1991. Intercellular signaling in glial cells: calcium waves and oscillations in response to mechanical stimulation and glutamate. Neuron **6:**983-992.

35. **Oberheim NA, Takano T, Han X, He W, Lin JH, Wang F, Xu Q, Wyatt JD, Pilcher W, Ojemann JG, Ransom BR, Goldman SA, Nedergaard M.** 2009. Uniquely hominid features of adult human astrocytes. J Neurosci **29:**3276-3287.

36. **Jessen NA, Munk AS, Lundgaard I, Nedergaard M.** 2015. The Glymphatic System: A Beginner's Guide. Neurochem Res **40:**2583-2599.

37. **Koehler RC, Roman RJ, Harder DR.** 2009. Astrocytes and the regulation of cerebral blood flow. Trends Neurosci **32:**160-169.

38. **Rothstein JD, Dykes-Hoberg M, Pardo CA, Bristol LA, Jin L, Kuncl RW, Kanai Y, Hediger MA, Wang Y, Schielke JP, Welty DF.** 1996. Knockout of glutamate transporters reveals a major role for astroglial transport in excitotoxicity and clearance of glutamate. Neuron **16:**675-686.

39. **Sofroniew MV.** 2009. Molecular dissection of reactive astrogliosis and glial scar formation. Trends Neurosci **32:**638-647.

40. **Hoxie JA, LaBranche CC, Endres MJ, Turner JD, Berson JF, Doms RW, Matthews TJ.** 1998. CD4-independent utilization of the CXCR4 chemokine receptor by HIV-1 and HIV-2. J Reprod Immunol **41:**197-211.

41. **Edinger AL, Blanpain C, Kunstman KJ, Wolinsky SM, Parmentier M, Doms RW.** 1999. Functional dissection of CCR5 coreceptor function through the use of CD4-independent simian immunodeficiency virus strains. J Virol **73:**4062-4073.

42. **Lee YK, Kwak DH, Oh KW, Nam SY, Lee BJ, Yun YW, Kim YB, Han SB, Hong JT.** 2009. CCR5 deficiency induces astrocyte activation, Abeta deposit and impaired memory function. Neurobiol Learn Mem **92:**356-363.

43. **Li GH, Henderson L, Nath A.** 2016. Astrocytes as an HIV Reservoir: Mechanism of HIV Infection. Curr HIV Res **14:**373-381.

44. **Clarke JN, Lake JA, Burrell CJ, Wesselingh SL, Gorry PR, Li P.** 2006. Novel pathway of human immunodeficiency virus type 1 uptake and release in astrocytes. Virology **348:**141-155.

45. **Nath A, Hartloper V, Furer M, Fowke KR.** 1995. Infection of human fetal astrocytes with HIV-1: viral tropism and the role of cell to cell contact in viral transmission. J Neuropathol Exp Neurol **54:**320-330.

46. **Luo X, He JJ.** 2015. Cell-cell contact viral transfer contributes to HIV infection and persistence in astrocytes. J Neurovirol **21:**66-80.

47. **Chauhan A, Mehla R, Vijayakumar TS, Handy I.** 2014. Endocytosis-mediated HIV-1 entry and its significance in the elusive behavior of the virus in astrocytes. Virology **456-457:**1-19.

48. **Boutet A, Salim H, Taoufik Y, Lledo PM, Vincent JD, Delfraissy JF, Tardieu M.** 2001. Isolated human astrocytes are not susceptible to infection by M- and T-tropic HIV-1 strains despite functional expression of the chemokine receptors CCR5 and CXCR4. Glia **34:**165-177.

49. **Sabri F, Tresoldi E, Di Stefano M, Polo S, Monaco MC, Verani A, Fiore JR, Lusso P, Major E, Chiodi F, Scarlatti G.** 1999. Nonproductive human immunodeficiency virus type 1 infection of human fetal astrocytes: independence from CD4 and major chemokine receptors. Virology **264:**370-384.

50. **Trillo-Pazos G, Diamanturos A, Rislove L, Menza T, Chao W, Belem P, Sadiq S, Morgello S, Sharer L, Volsky DJ.** 2003. Detection of HIV-1 DNA in microglia/macrophages, astrocytes and neurons isolated from brain tissue with HIV-1 encephalitis by laser capture microdissection. Brain Pathol **13:**144-154.

51. **Takahashi K, Wesselingh SL, Griffin DE, McArthur JC, Johnson RT, Glass JD.** 1996. Localization of HIV-1 in human brain using polymerase chain reaction/in situ hybridization and immunocytochemistry. Ann Neurol **39:**705-711.

52. **Bagasra O, Lavi E, Bobroski L, Khalili K, Pestaner JP, Tawadros R, Pomerantz RJ.** 1996. Cellular reservoirs of HIV-1 in the central nervous system of infected individuals: identification by the combination of in situ polymerase chain reaction and immunohistochemistry. Aids **10:**573-585.

53. **Hudson L, Liu J, Nath A, Jones M, Raghavan R, Narayan O, Male D, Everall I.** 2000. Detection of the human immunodeficiency virus regulatory protein tat in CNS tissues. Journal of neurovirology **6:**145.

54. **Nath A.** 2015. Eradication of human immunodeficiency virus from brain reservoirs. J Neurovirol **21:**227-234.

55. **Neumann M, Felber BK, Kleinschmidt A, Froese B, Erfle V, Pavlakis GN, Brack-Werner R.** 1995. Restriction of human immunodeficiency virus type 1 production in a human astrocytoma cell line is associated with a cellular block in Rev function. J Virol **69:**2159-2167.

56. **Tornatore C, Meyers K, Atwood W, Conant K, Major E.** 1994. Temporal patterns of human immunodeficiency virus type 1 transcripts in human fetal astrocytes. J Virol **68:**93-102.

57. **Ma M, Geiger JD, Nath A.** 1994. Characterization of a novel binding site for the human immunodeficiency virus type 1 envelope protein gp120 on human fetal astrocytes. J Virol **68:**6824-6828.

58. **Willey SJ, Reeves JD, Hudson R, Miyake K, Dejucq N, Schols D, De Clercq E, Bell J, McKnight A, Clapham PR.** 2003. Identification of a subset of human immunodeficiency virus type 1 (HIV-1), HIV-2, and simian immunodeficiency virus strains able to exploit an alternative coreceptor on untransformed human brain and lymphoid cells. J Virol **77:**6138-6152.

59. **MacDonald BT, Tamai K, He X.** 2009. Wnt/beta-catenin signaling: components, mechanisms, and diseases. Dev Cell **17:**9-26.

60. **Narasipura SD, Henderson LJ, Fu SW, Chen L, Kashanchi F, Al-Harthi L.** 2012. Role of beta-catenin and TCF/LEF family members in transcriptional activity of HIV in astrocytes. J Virol **86:**1911-1921.

61. **Wortman B, Darbinian N, Sawaya BE, Khalili K, Amini S.** 2002. Evidence for regulation of long terminal repeat transcription by Wnt transcription factor TCF-4 in human astrocytic cells. J Virol **76:**11159-11165.

62. **Halleskog C, Mulder J, Dahlstrom J, Mackie K, Hortobagyi T, Tanila H, Kumar Puli L, Farber K, Harkany T, Schulte G.** 2011. WNT signaling in activated microglia is proinflammatory. Glia **59:**119-131.

63. **L'Episcopo F, Tirolo C, Testa N, Caniglia S, Morale MC, Cossetti C, D'Adamo P, Zardini E, Andreoni L, Ihekwaba AE, Serra PA, Franciotta D, Martino G, Pluchino S, Marchetti B.** 2011. Reactive astrocytes and Wnt/beta-catenin signaling link nigrostriatal injury to repair in 1-methyl-4-phenyl-1,2,3,6-tetrahydropyridine model of Parkinson's disease. Neurobiol Dis **41:**508-527.

64. **Libro R, Bramanti P, Mazzon E.** 2016. The role of the Wnt canonical signaling in neurodegenerative diseases. Life Sci **158:**78-88.

65. **Bharti AC, Aggarwal BB.** 2002. Nuclear factor-kappa B and cancer: its role in prevention and therapy. Biochem Pharmacol **64:**883-888.

66. **Gilmore TD.** 2006. Introduction to NF-kappaB: players, pathways, perspectives. Oncogene **25:**6680-6684.

67. **Choi SS, Lee HJ, Lim I, Satoh J, Kim SU.** 2014. Human astrocytes: secretome profiles of cytokines and chemokines. PLoS One **9:**e92325.

68. **Van Wagoner NJ, Benveniste EN.** 1999. Interleukin-6 expression and regulation in astrocytes. J Neuroimmunol **100:**124-139.

69. **Ma B, van Blitterswijk CA, Karperien M.** 2012. A Wnt/beta-catenin negative feedback loop inhibits interleukin-1-induced matrix metalloproteinase expression in human articular chondrocytes. Arthritis Rheum **64:**2589-2600.

70. **Ma B, Hottiger MO.** 2016. Crosstalk between Wnt/beta-Catenin and NF-kappaB Signaling Pathway during Inflammation. Front Immunol **7:**378.

71. **Pu H, Tian J, Flora G, Lee Y, Nath A, Hennig B, Toborek M.** 2003. HIV-1 Tat protein upregulates inflammatory mediators and induces monocyte invasion into the brain. Molecular and cellular neurosciences **24:**224.

72. **van Marle G, Henry S, Todoruk T, Sullivan A, Silva C, Rourke SB, Holden J, McArthur JC, Gill MJ, Power C.** 2004. Human immunodeficiency virus type 1 Nef protein mediates neural cell death: a neurotoxic role for IP-10. Virology **329:**302-318.

73. **Shrikant P, Benos DJ, Tang LP, Benveniste EN.** 1996. HIV glycoprotein 120 enhances intercellular adhesion molecule-1 gene expression in glial cells. Involvement of Janus kinase/signal transducer and activator of transcription and protein kinase C signaling pathways. J Immunol **156:**1307-1314.

74. **Youn GS, Kwon DJ, Ju SM, Rhim H, Bae YS, Choi SY, Park J.** 2014. Celastrol ameliorates HIV-1 Tat-induced inflammatory responses via NF-kappaB and AP-1 inhibition and heme oxygenase-1 induction in astrocytes. Toxicol Appl Pharmacol **280:**42-52.

75. **Vartak-Sharma N, Gelman BB, Joshi C, Borgamann K, Ghorpade A.** 2014. Astrocyte elevated gene-1 is a novel modulator of HIV-1-associated neuroinflammation via regulation of nuclear factor-kappaB signaling and excitatory amino acid transporter-2 repression. J Biol Chem **289:**19599-19612.

76. **Eugenin EA, Berman JW.** 2007. Gap junctions mediate human immunodeficiency virus-bystander killing in astrocytes. J Neurosci **27:**12844-12850.

77. **Ton H, Xiong H.** 2013. Astrocyte Dysfunctions and HIV-1 Neurotoxicity. J AIDS Clin Res **4:**255.

78. **Gupta RK, Abdul-Jawad S, McCoy LE, Mok HP, Peppa D, Salgado M, Martinez-Picado J, Nijhuis M, Wensing AMJ, Lee H, Grant P, Nastouli E, Lambert J, Pace M, Salasc F, Monit C, Innes AJ, Muir L, Waters L, Frater J, Lever AML, Edwards SG, Gabriel IH, Olavarria E.** 2019. HIV-1 remission following CCR5Delta32/Delta32 haematopoietic stem-cell transplantation. Nature **568:**244-248.

79. **Thorlund K, Horwitz MS, Fife BT, Lester R, Cameron DW.** 2017. Landscape review of current HIV 'kick and kill' cure research - some kicking, not enough killing. BMC Infect Dis **17:**595.

80. **Kessing CF, Nixon CC, Li C, Tsai P, Takata H, Mousseau G, Ho PT, Honeycutt JB, Fallahi M, Trautmann L, Garcia JV, Valente ST.** 2017. In Vivo Suppression of HIV Rebound by Didehydro-Cortistatin A, a "Block-and-Lock" Strategy for HIV-1 Treatment. Cell Rep **21:**600-611.

81. **Allers K, Hutter G, Hofmann J, Loddenkemper C, Rieger K, Thiel E, Schneider T.** 2011. Evidence for the cure of HIV infection by CCR5Delta32/Delta32 stem cell transplantation. Blood **117:**2791-2799.

82. **Laurichesse JJ, Persoz A, Theodorou I, Rouzioux C, Delfraissy JF, Meyer L.** 2007. Improved virological response to highly active antiretroviral therapy in HIV-1-infected patients carrying the CCR5 Delta32 deletion. HIV Med **8:**213-219.

83. **Tebas P, Stein D, Tang WW, Frank I, Wang SQ, Lee G, Spratt SK, Surosky RT, Giedlin MA, Nichol G, Holmes MC, Gregory PD, Ando DG, Kalos M, Collman RG, Binder-Scholl G, Plesa G, Hwang WT, Levine BL, June CH.** 2014. Gene editing of CCR5 in autologous CD4 T cells of persons infected with HIV. N Engl J Med **370:**901-910.

84. **McArthur JC, Brew BJ, Nath A.** 2005. Neurological complications of HIV infection. Lancet Neurol **4:**543-555.

85. **Bruce-Keller AJ, Chauhan A, Dimayuga FO, Gee J, Keller JN, Nath A.** 2003. Synaptic transport of human immunodeficiency virus-Tat protein causes neurotoxicity and gliosis in rat brain. J Neurosci **23:**8417-8422.

86. **Kim BO, Liu Y, Ruan Y, Xu ZC, Schantz L, He JJ.** 2003. Neuropathologies in transgenic mice expressing human immunodeficiency virus type 1 Tat protein under the regulation of the astrocyte-specific glial fibrillary acidic protein promoter and doxycycline. The American Journal of Pathology **162:**1693-1707.

87. **Hong S, Banks WA.** 2015. Role of the immune system in HIV-associated neuroinflammation and neurocognitive implications. Brain Behav Immun **45:**1-12.

88. **Deshpande M, Zheng J, Borgmann K, Persidsky R, Wu L, Schellpeper C, Ghorpade A.** 2005. Role of activated astrocytes in neuronal damage: potential links to HIV-1-associated dementia. Neurotox Res **7:**183-192.

89. **Al-Harti L, Joseph J, Nath A.** 2018. Astrocytes as an HIV CNS reservoir: highlights and reflections of an NIMH-sponsored symposium. J Neurovirol **24:**665-669.

90. **Atwood WJ, Tornatore CS, Meyers K, Major EO.** 1993. HIV-1 mRNA transcripts from persistently infected human fetal astrocytes. Ann N Y Acad Sci **693:**324-325.

91. **Atwood WJ, Tornatore CS, Traub R, Conant K, Drew PD, Major EO.** 1994. Stimulation of HIV type 1 gene expression and induction of NF-kappa B (p50/p65)-binding activity in tumor necrosis factor alpha-treated human fetal glial cells. AIDS Res Hum Retroviruses **10:**1207-1211.

92. **Tornatore C, Nath A, Amemiya K, Major EO.** 1991. Persistent human immunodeficiency virus type 1 infection in human fetal glial cells reactivated by T-cell factor(s) or by the cytokines tumor necrosis factor alpha and interleukin-1 beta. J Virol **65:**6094-6100.

93. **Dahabieh MS, Ooms M, Simon V, Sadowski I.** 2013. A doubly fluorescent HIV-1 reporter shows that the majority of integrated HIV-1 is latent shortly after infection. J Virol **87:**4716-4727.

94. **Borjabad A, Brooks AI, Volsky DJ.** 2010. Gene expression profiles of HIV-1-infected glia and brain: toward better understanding of the role of astrocytes in HIV-1-associated neurocognitive disorders. J Neuroimmune Pharmacol **5:**44-62.

95. **Wang Z, Trillo-Pazos G, Kim SY, Canki M, Morgello S, Sharer LR, Gelbard HA, Su ZZ, Kang DC, Brooks AI, Fisher PB, Volsky DJ.** 2004. Effects of human immunodeficiency virus type 1 on astrocyte gene expression and function: potential role in neuropathogenesis. J Neurovirol **10 Suppl 1:**25-32.

96. **Gardner J, Ghorpade A.** 2003. Tissue inhibitor of metalloproteinase (TIMP)-1: the TIMPed balance of matrix metalloproteinases in the central nervous system. Journal of Neuroscience Research **74:**801-806.

97. **Suzuki Y, Misawa N, Sato C, Ebina H, Masuda T, Yamamoto N, Koyanagi Y.** 2003. Quantitative analysis of human immunodeficiency virus type 1 DNA dynamics by real-

time PCR: integration efficiency in stimulated and unstimulated peripheral blood mononuclear cells. Virus Genes **27:**177-188.

98. **Manthorpe M, Fagnani R, Skaper SD, Varon S.** 1986. An automated colorimetric microassay for neuronotrophic factors. Brain Res **390:**191-198.

99. **Andrews S.** 2010. FastQC: a quality control tool for high throughput sequence data., http://www.bioinformatics.babraham.ac.uk/projects/fastqc/.

100. **Steven W.** 2011. FastQ Screen: quality control tool to screen a library of sequences in FastQ format against a set of sequence databases, http://www.bioinformatics.babraham.ac.uk/projects/fastq_screen/.

101. **Aronesty E.** 2011. ea-utils : Command-line tools for processing biological sequencing data, https://github.com/ExpressionAnalysis/ea-utils.

102. **Kim D, Pertea G, Trapnell C, Pimentel H, Kelley R, Salzberg SL.** 2013. TopHat2: accurate alignment of transcriptomes in the presence of insertions, deletions and gene fusions. Genome Biol **14:**R36.

103. **Liao Y, Smyth GK, Shi W.** 2014. featureCounts: an efficient general purpose program for assigning sequence reads to genomic features. Bioinformatics **30:**923-930.

104. **Robinson MD, McCarthy DJ, Smyth GK.** 2010. edgeR: a Bioconductor package for differential expression analysis of digital gene expression data. Bioinformatics **26:**139-140.

105. **Bolger AM, Lohse M, Usadel B.** 2014. Trimmomatic: a flexible trimmer for Illumina sequence data. Bioinformatics **30:**2114-2120.

106. **Li H, Durbin R.** 2009. Fast and accurate short read alignment with Burrows-Wheeler transform. Bioinformatics **25:**1754-1760.

107. **Li H, Handsaker B, Wysoker A, Fennell T, Ruan J, Homer N, Marth G, Abecasis G, Durbin R.** 2009. The Sequence Alignment/Map format and SAMtools. Bioinformatics **25:**2078-2079.

108. **Oshlack MDRA.** 2010. A scaling normalization method for differential expression analysis of RNA-seq data. Genome Biol **11:**R25.

109. **Herbein G, Gras G, Khan KA, Abbas W.** 2010. Macrophage signaling in HIV-1 infection. Retrovirology **7:**34.

110. **Sama MA, Mathis DM, Furman JL, Abdul HM, Artiushin IA, Kraner SD, Norris CM.** 2008. Interleukin-1beta-dependent signaling between astrocytes and neurons depends critically on astrocytic calcineurin/NFAT activity. J Biol Chem **283:**21953-21964.

111. **Borjabad A, Morgello S, Chao W, Kim SY, Brooks AI, Murray J, Potash MJ, Volsky DJ.** 2011. Significant effects of antiretroviral therapy on global gene expression in brain tissues of patients with HIV-1-associated neurocognitive disorders. PLoS Pathog **7:**e1002213.

112. **Gelman BB, Chen T, Lisinicchia JG, Soukup VM, Carmical JR, Starkey JM, Masliah E, Commins DL, Brandt D, Grant I, Singer EJ, Levine AJ, Miller J, Winkler JM, Fox HS, Luxon BA, Morgello S.** 2012. The National NeuroAIDS Tissue Consortium brain gene array: two types of HIV-associated neurocognitive impairment. PLoS One **7:**e46178.

113. **Brabers NA, Nottet HS.** 2006. Role of the pro-inflammatory cytokines TNF-alpha and IL-1beta in HIV-associated dementia. Eur J Clin Invest **36:**447-458.

114. **Galey D, Becker K, Haughey N, Kalehua A, Taub D, Woodward J, Mattson MP, Nath A.** 2003. Differential transcriptional regulation by human immunodeficiency virus type 1 and gp120 in human astrocytes. J Neurovirol **9:**358-371.

115. **Su ZZ, Kang DC, Chen Y, Pekarskaya O, Chao W, Volsky DJ, Fisher PB.** 2002. Identification and cloning of human astrocyte genes displaying elevated expression after infection with HIV-1 or exposure to HIV-1 envelope glycoprotein by rapid subtraction hybridization, RaSH. Oncogene **21:**3592-3602.

116. **Wang Z, Pekarskaya O, Bencheikh M, Chao W, Gelbard HA, Ghorpade A, Rothstein JD, Volsky DJ.** 2003. Reduced expression of glutamate transporter EAAT2 and impaired glutamate transport in human primary astrocytes exposed to HIV-1 or gp120. Virology **312:**60-73.

117. **Colin L, Van Lint C.** 2009. Molecular control of HIV-1 postintegration latency: implications for the development of new therapeutic strategies. Retrovirology **6:**111.

118. **Narasipura SD, Kim S, Al-Harthi L.** 2014. Epigenetic regulation of HIV-1 latency in astrocytes. J Virol **88:**3031-3038.

119. **Archin NM, Keedy KS, Espeseth A, Dang H, Hazuda DJ, Margolis DM.** 2009. Expression of latent human immunodeficiency type 1 is induced by novel and selective histone deacetylase inhibitors. Aids **23:**1799-1806.

120. **Dahabieh MS, Ooms M, Brumme C, Taylor J, Harrigan PR, Simon V, Sadowski I.** 2014. Direct non-productive HIV-1 infection in a T-cell line is driven by cellular activation state and NFkappaB. Retrovirology **11:**17.

121. **Chauhan A.** 2015. Enigma of HIV-1 latent infection in astrocytes: an in-vitro study using protein kinase C agonist as a latency reversing agent. Microbes Infect **17:**651-659.

122. **Barat C, Proust A, Deshiere A, Leboeuf M, Drouin J, Tremblay MJ.** 2018. Astrocytes sustain long-term productive HIV-1 infection without establishment of reactivable viral latency. Glia **66:**1363-1381.

123. **Diaz L, Martinez-Bonet M, Sanchez J, Fernandez-Pineda A, Jimenez JL, Munoz E, Moreno S, Alvarez S, Munoz-Fernandez MA.** 2015. Bryostatin activates HIV-1 latent expression in human astrocytes through a PKC and NF-kB-dependent mechanism. Sci Rep **5:**12442.

124. **Sami Saribas A, Cicalese S, Ahooyi TM, Khalili K, Amini S, Sariyer IK.** 2017. HIV-1 Nef is released in extracellular vesicles derived from astrocytes: evidence for Nef-mediated neurotoxicity. Cell Death Dis **8:**e2542.

125. **Groschel B, Bushman F.** 2005. Cell cycle arrest in G2/M promotes early steps of infection by human immunodeficiency virus. J Virol **79:**5695-5704.

126. **Andersen JL, Le Rouzic E, Planelles V.** 2008. HIV-1 Vpr: mechanisms of G2 arrest and apoptosis. Exp Mol Pathol **85:**2-10.

127. **Li G, Park HU, Liang D, Zhao RY.** 2010. Cell cycle G2/M arrest through an S phase-dependent mechanism by HIV-1 viral protein R. Retrovirology **7:**59.

128. **Kim SY, Li J, Bentsman G, Brooks AI, Volsky DJ.** 2004. Microarray analysis of changes in cellular gene expression induced by productive infection of primary human astrocytes: implications for HAD. J Neuroimmunol **157:**17-26.

129. **Yoneyama M, Fujita T.** 2007. Function of RIG-I-like receptors in antiviral innate immunity. J Biol Chem **282:**15315-15318.

130. **Hori K, Burd PR, Furuke K, Kutza J, Weih KA, Clouse KA.** 1999. Human immunodeficiency virus-1-infected macrophages induce inducible nitric oxide synthase and nitric oxide (NO) production in astrocytes: astrocytic NO as a possible mediator of neural damage in acquired immunodeficiency syndrome. Blood **93:**1843-1850.

131. **Liu X, Jana M, Dasgupta S, Koka S, He J, Wood C, Pahan K.** 2002. Human immunodeficiency virus type 1 (HIV-1) tat induces nitric-oxide synthase in human astroglia. J Biol Chem **277:**39312-39319.

132. **Esposito G, Ligresti A, Izzo AA, Bisogno T, Ruvo M, Di Rosa M, Di Marzo V, Iuvone T.** 2002. The endocannabinoid system protects rat glioma cells against HIV-1 Tat protein-induced cytotoxicity. Mechanism and regulation. J Biol Chem **277:**50348-50354.

133. **Piekna-Przybylska D, Sharma G, Maggirwar SB, Bambara RA.** 2017. Deficiency in DNA damage response, a new characteristic of cells infected with latent HIV-1. Cell Cycle **16:**968-978.

134. **Sun Y, Huang YC, Xu QZ, Wang HP, Bai B, Sui JL, Zhou PK.** 2006. HIV-1 Tat depresses DNA-PK(CS) expression and DNA repair, and sensitizes cells to ionizing radiation. Int J Radiat Oncol Biol Phys **65:**842-850.

135. **Gillick K, Pollpeter D, Phalora P, Kim EY, Wolinsky SM, Malim MH.** 2013. Suppression of HIV-1 infection by APOBEC3 proteins in primary human CD4(+) T cells is associated with inhibition of processive reverse transcription as well as excessive cytidine deamination. J Virol **87:**1508-1517.

136. **Wang YJ, Wang X, Zhang H, Zhou L, Liu S, Kolson DL, Song L, Ye L, Ho WZ.** 2009. Expression and regulation of antiviral protein APOBEC3G in human neuronal cells. J Neuroimmunol **206:**14-21.

137. **Lahouassa H, Daddacha W, Hofmann H, Ayinde D, Logue EC, Dragin L, Bloch N, Maudet C, Bertrand M, Gramberg T, Pancino G, Priet S, Canard B, Laguette N, Benkirane M, Transy C, Landau NR, Kim B, Margottin-Goguet F.** 2012. SAMHD1

restricts the replication of human immunodeficiency virus type 1 by depleting the intracellular pool of deoxynucleoside triphosphates. Nat Immunol **13:**223-228.

138. **Gramberg T, Kahle T, Bloch N, Wittmann S, Mullers E, Daddacha W, Hofmann H, Kim B, Lindemann D, Landau NR.** 2013. Restriction of diverse retroviruses by SAMHD1. Retrovirology **10:**26.

139. **Buchanan EL, Espinoza DA, McAlexander MA, Myers SL, Moyer A, Witwer KW.** 2016. SAMHD1 transcript upregulation during SIV infection of the central nervous system does not associate with reduced viral load. Scientific reports **6:**22629-22629.

140. **Bosma EK, van Noorden CJF, Schlingemann RO, Klaassen I.** 2018. The role of plasmalemma vesicle-associated protein in pathological breakdown of blood-brain and blood-retinal barriers: potential novel therapeutic target for cerebral edema and diabetic macular edema. Fluids Barriers CNS **15:**24.

141. **Zipeto D, Beretta A.** 2012. HLA-C and HIV-1: friends or foes? Retrovirology **9:**39.

142. **Woodman SE, Benveniste EN, Nath A, Berman JW.** 1999. Human immunodeficiency virus type 1 TAT protein induces adhesion molecule expression in astrocytes. J Neurovirol **5:**678-684.

143. **Han Y, He T, Huang DR, Pardo CA, Ransohoff RM.** 2001. TNF-alpha mediates SDF-1 alpha-induced NF-kappa B activation and cytotoxic effects in primary astrocytes. J Clin Invest **108:**425-435.

144. **Zhao ML, Kim MO, Morgello S, Lee SC.** 2001. Expression of inducible nitric oxide synthase, interleukin-1 and caspase-1 in HIV-1 encephalitis. J Neuroimmunol **115:**182-191.

145. **Dragon S, Rahman MS, Yang J, Unruh H, Halayko AJ, Gounni AS.** 2007. IL-17 enhances IL-1beta-mediated CXCL-8 release from human airway smooth muscle cells. Am J Physiol Lung Cell Mol Physiol **292:**L1023-1029.

146. **Hu W, Li F, Mahavadi S, Murthy KS.** 2009. Upregulation of RGS4 expression by IL-1beta in colonic smooth muscle is enhanced by ERK1/2 and p38 MAPK and inhibited by the PI3K/Akt/GSK3beta pathway. Am J Physiol Cell Physiol **296:**C1310-1320.

147. **Nejak-Bowen K, Kikuchi A, Monga SP.** 2013. Beta-catenin-NF-kappaB interactions in murine hepatocytes: a complex to die for. Hepatology **57:**763-774.

148. **Jang J, Ha JH, Chung SI, Yoon Y.** 2014. Beta-catenin regulates NF-kappaB activity and inflammatory cytokine expression in bronchial epithelial cells treated with lipopolysaccharide. Int J Mol Med **34:**632-638.

149. **Schon S, Flierman I, Ofner A, Stahringer A, Holdt LM, Kolligs FT, Herbst A.** 2014. beta-catenin regulates NF-kappaB activity via TNFRSF19 in colorectal cancer cells. Int J Cancer **135:**1800-1811.

150. **Vines A, Cahoon S, Goldberg I, Saxena U, Pillarisetti S.** 2006. Novel anti-inflammatory role for glycogen synthase kinase-3beta in the inhibition of tumor necrosis factor-alpha- and interleukin-1beta-induced inflammatory gene expression. J Biol Chem **281:**16985-16990.

151. **Norris JG, Tang LP, Sparacio SM, Benveniste EN.** 1994. Signal transduction pathways mediating astrocyte IL-6 induction by IL-1 beta and tumor necrosis factor-alpha. J Immunol **152:**841-850.

152. **Shah A, Verma AS, Patel KH, Noel R, Rivera-Amill V, Silverstein PS, Chaudhary S, Bhat HK, Stamatatos L, Singh DP, Buch S, Kumar A.** 2011. HIV-1 gp120 induces

expression of IL-6 through a nuclear factor-kappa B-dependent mechanism: suppression by gp120 specific small interfering RNA. PLoS One **6:**e21261.

153. **Lee SC, Liu W, Dickson DW, Brosnan CF, Berman JW.** 1993. Cytokine production by human fetal microglia and astrocytes. Differential induction by lipopolysaccharide and IL-1 beta. J Immunol **150:**2659-2667.

154. **Altman J, Das GD.** 1965. Autoradiographic and histological evidence of postnatal hippocampal neurogenesis in rats. J Comp Neurol **124:**319-335.

155. **Satoh T, Nakamura S, Taga T, Matsuda T, Hirano T, Kishimoto T, Kaziro Y.** 1988. Induction of neuronal differentiation in PC12 cells by B-cell stimulatory factor 2/interleukin 6. Mol Cell Biol **8:**3546-3549.

156. **Frei K, Malipiero UV, Leist TP, Zinkernagel RM, Schwab ME, Fontana A.** 1989. On the cellular source and function of interleukin 6 produced in the central nervous system in viral diseases. Eur J Immunol **19:**689-694.

157. **Maimone D, Guazzi GC, Annunziata P.** 1997. IL-6 detection in multiple sclerosis brain. J Neurol Sci **146:**59-65.

158. **Nagatsu T, Sawada M.** 2007. Biochemistry of postmortem brains in Parkinson's disease: historical overview and future prospects. J Neural Transm Suppl doi:10.1007/978-3-211-73574-9_14**:**113-120.

159. **Bjorkqvist M, Wild EJ, Thiele J, Silvestroni A, Andre R, Lahiri N, Raibon E, Lee RV, Benn CL, Soulet D, Magnusson A, Woodman B, Landles C, Pouladi MA, Hayden MR, Khalili-Shirazi A, Lowdell MW, Brundin P, Bates GP, Leavitt BR, Moller T, Tabrizi SJ.** 2008. A novel pathogenic pathway of immune activation detectable before clinical onset in Huntington's disease. J Exp Med **205:**1869-1877.

160. **Conroy SM, Nguyen V, Quina LA, Blakely-Gonzales P, Ur C, Netzeband JG, Prieto AL, Gruol DL.** 2004. Interleukin-6 produces neuronal loss in developing cerebellar granule neuron cultures. J Neuroimmunol **155:**43-54.

161. **Airoldi M, Bandera A, Trabattoni D, Tagliabue B, Arosio B, Soria A, Rainone V, Lapadula G, Annoni G, Clerici M, Gori A.** 2012. Neurocognitive impairment in HIV-infected naive patients with advanced disease: the role of virus and intrathecal immune activation. Clin Dev Immunol **2012:**467154.

162. **Poli G, Bressler P, Kinter A, Duh E, Timmer WC, Rabson A, Justement JS, Stanley S, Fauci AS.** 1990. Interleukin 6 induces human immunodeficiency virus expression in infected monocytic cells alone and in synergy with tumor necrosis factor alpha by transcriptional and post-transcriptional mechanisms. J Exp Med **172:**151-158.

163. **Poli G, Fauci AS.** 1992. The effect of cytokines and pharmacologic agents on chronic HIV infection. AIDS Res Hum Retroviruses **8:**191-197.

164. **Narasipura SD, Henderson LJ, Fu SW, Chen L, Kashanchi F, Al-Harthi L.** 2012. Role of beta-Catenin and TCF/LEF Family Members in Transcriptional Activity of HIV in Astrocytes. Journal of virology **86:**1911-1921.

165. **Ye X, Zhang Y, Xu Q, Zheng H, Wu X, Qiu J, Zhang Z, Wang W, Shao Y, Xing HQ.** 2017. HIV-1 Tat inhibits EAAT-2 through AEG-1 upregulation in models of HIV-associated neurocognitive disorder. Oncotarget **8:**39922-39934.